Oblique wave transmission through rough impermeable rubble mound submerged breakwaters

Valérie Vanlishout

Promotor: prof. dr. ir. Peter Troch
Begeleider: ir. H.J. Verhagen (TU Delft)

Scriptie ingediend tot het behalen van de academische graad van
Burgerlijk bouwkundig ingenieur

Vakgroep Civiele techniek
Voorzitter: prof. dr. ir. Julien De Rouck
Faculteit Ingenieurswetenschappen
Academiejaar 2007-2008

UNIVERSITEIT
GENT

Oblique wave transmission through rough impermeable rubble mound submerged breakwaters

Valérie Vanlishout

Promotor: prof. dr. ir. Peter Troch
Begeleider: ir. H.J. Verhagen (TU Delft)

Scriptie ingediend tot het behalen van de academische graad van
Burgerlijk bouwkundig ingenieur

Vakgroep Civiele techniek
Voorzitter: prof. dr. ir. Julien De Rouck
Faculteit Ingenieurswetenschappen
Academiejaar 2007-2008

UNIVERSITEIT
GENT

Preface

This dissertation is submitted in partial fulfilment of the requirements for the diploma of the Second Cycle in Civil Engineering at the University of Ghent (Master in Civil Engineering). The work for this dissertation is carried out in cooperation with the Delft University of Technology, at the faculty of Hydraulic Engineering of the department of Civil Engineering and Geosciences. The main research objective is to investigate oblique wave transmission through rough impermeable rubble mound submerged breakwaters by means of a 3D physical model.

I would like to thank prof. dr. ir. J. De Rouck and prof. dr. ir. P. Troch for giving me the opportunity to participate with the Erasmus programme at the Delft University of Technology. I am very grateful for the weekly guidance and supervision of ir. H.J. Verhagen. I would also like to thank dr. ir. W.S.J. Uijttewaal for allowing me to use the large facilities of the laboratory. Further, I am very appreciative for the assistance from the laboratory staff members during the experimental months, especially from Sander de Vree and Jaap van Duin for their daily support. Finally, I would like to thank all others who contributed to my dissertation.

Graduation committee:

- prof. dr. ir. P. Troch (University of Ghent)
- prof. dr. ir. M.J.F. Stive (Delft University of Technology)
- dr. ir. W.S.J. Uijttewaal (Delft University of Technology)
- ir. H.J. Verhagen (Delft University of Technology)

Valérie Vanlishout

Delft, May 2008

Oblique wave transmission through rough impermeable rubble mound submerged breakwaters

by

Valérie Vanlishout

Dissertation submitted in partial fulfilment of the requirements for the diploma of the Second Cycle in Civil Engineering

Head supervisor: prof. dr. ir. P. Troch
Supervisor: ir. H.J. Verhagen (TU Delft)

Department of Civil Engineering
Chairman: prof. dr. ir. J. De Rouck
Faculty of Engineering
University of Ghent
Academic year 2007-2008

Abstract

Low crested structures are primarily designed as a coastal defence mechanism, making the prediction of the energy in the lee of the structure of utmost importance. As wave transmission is a measure for the energy that passes the breakwater, experiments on oblique wave transmission have previously been performed by the European project DELOS (2002b) (Environmental Design of Low Crested Coastal Defence Structures) and analysed further by Van der Meer *et al.* (2005). From these experiments, it is unclear whether it is the roughness or the permeability of the core that determines the behaviour of the structure. Therefore,

the objective of this study is to improve the understanding of **oblique wave transmission through rough impermeable rubble mound submerged breakwaters** by means of a 3D physical model. An experimental study is conducted based on the same set-up of DELOS (2002b) but the permeability of the core of the rough structure will be varied. Finally, by comparing the data of this study with the data of DELOS (2002b) and the formulations of Van der Meer *et al.* (2003), insight should be gained on the matter.

In total, four structures are tested using irregular long crested waves; ranging from a fully permeable to a fully impermeable rough rubble mound breakwater. In order to test for oblique waves, the model is rotated progressively by 15°, ranging from 0° to 60°. Secondary effects due to the physical constraints of the wave basin are minimised by placing an additional mound of rubble between the model and the edge of the basin. This prevents a large scale circulation pattern from occurring and reduces wave diffraction effects.

The directional spectral analysis software DIWASP [Johnson (2007)] is used to calculate the variance density spectra of the data. The wave climate is estimated with the IMLM method (Iterated Maximum Likelihood Method) because it is the most suited to portray the narrow directional spread.

The aim of this study is to analyse the influence of the incident wave direction β_i on the transmitted wave direction β_t, the transmission coefficient K_t and the spectral changes of the transmitted spectrum. An analysis of the data shows that for rough structures there is no significant change in wave direction. The incident wave direction is approximately equal to the transmitted wave direction ($\beta_t = 0.94\beta_i$ for $0° \leq \beta_i \leq 60°$). The data of this study also show a slight increase in the transmission coefficient with increasing incident wave angle. However, when considering a combined data set, which includes the data of this study and the rough permeable data of DELOS (2002b), the data show that oblique wave attack has a negligible influence on the transmission coefficient for rough structures. The spectral changes of this study support the model proposed by Van der Meer *et al.* (2005). Finally, it is concluded that it is the roughness of the structure rather than the permeability of the core that determines the behaviour of the breakwater with respect to the incident wave direction.

Key words:

- Oblique wave transmission
- Submerged rubble mound breakwaters
- Physical 3D model

OBLIQUE WAVE TRANSMISSION THROUGH ROUGH IMPERMEABLE RUBBLE MOUND SUBMERGED BREAKWATERS

Valérie Vanlishout

Supervisor(s): prof. dr. ir. P. Troch, ir. H. J. Verhagen

Abstract— **This article discusses the 3D experimental study on the influence of oblique wave attack on the transmission through rough rubble mound submerged breakwaters.**

Keywords—**oblique wave transmission, submerged rubble mound breakwaters, physical 3D model**

I. INTRODUCTION

The importance of oblique wave attack has led to the investigation of Van der Meer *et al.* (2003) under the European project DELOS (2002b), where the behaviour of rough permeable rubble mound structures was found to be significantly different from that of the smooth impermeable low crested structures. It is unclear whether it is the roughness or the permeability of the core that determines the behaviour of the structure. Therefore, the objective of this study is to improve the understanding of oblique wave transmission through rough impermeable rubble mound submerged breakwaters. An experimental study is conducted based on the same set-up of DELOS (2002b) but the permeability of the core of the rough structure will be varied. By comparing the data of this study with the data of DELOS (2002b) and the formulations of Van der Meer *et al.* (2003), insight should be gained on the matter. The findings of the previous study [Van der Meer *et al.* (2003)] are recapitulated briefly:

Rough permeable rubble mound breakwaters:

- The incident wave direction β_i reduces 20% after encountering the structure ($\beta_t = 0.8\beta_i$).
- The transmission coefficient K_t decreases slightly with increasing angles of wave attack ($0° \leq \beta_i \leq 60°$). The effect is considered insignificant.

Smooth impermeable low crested structures:

- There is no change in wave direction for incident wave angles $\beta_i < 45°$. For incident wave directions larger than $45°$, the transmitted wave direction remains at $45°$.
- The transmission coefficient K_t decreases significantly with an increasing incident wave angle.

II. EXPERIMENTAL SET-UP

The experimental set-up of DELOS (2002b) is the basis for the experimental set-up at the Fluid Mechanics Laboratory at the Technical University of Delft (figure 1). The physical model has a fixed armour layer with a constant roughness. The variable core is made up of an impermeable wooden box available in three different heights so that in total four different structures can be simulated; ranging from a fully permeable to a fully impermeable rough rubble mound breakwater.

Three wave generators are synchronized to produce irregular long crested waves (JONSWAP spectrum), making the wave generation perpendicular to the wave boards. Two wave climates are generated per test set-up ($H_i = 0.07m$, $T_p = 1.5s | H_i = 0.09m$, $T_p = 1.3s$).

The total length of the breakwater is five meters and is rotated progressively by $15°$, ranging from $0°$ to $60°$, to generate oblique waves. Secondary effects due to the physical constraints of the wave basin are minimised by placing an additional mound of rubble between the model and the edge of the basin. This prevents a large scale circulation pattern from occurring and reduces wave diffraction effects.

Two sets of five resistive wave gauges are used to acquire the necessary surface elevation data at a sampling frequency of $100Hz$; one set before the breakwater, the other in the lee of the structure. The relative location of the wave gauges is based on an asymmetrical cross sequence to enable directional data retrieval.

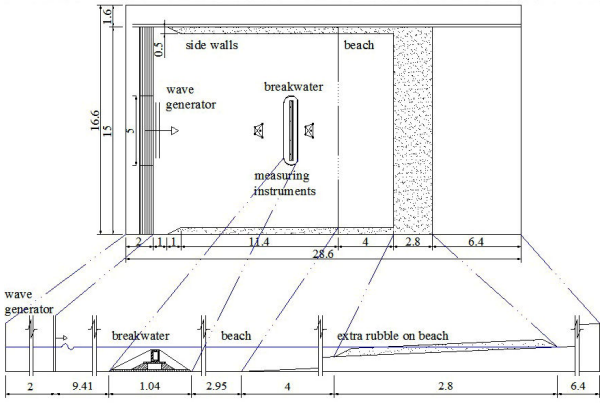

Fig. 1. Wave basin

III. DATA PROCESSING

The directional spectral analysis software DIWASP [Johnson (2007)] is used to calculate the variance density spectra of the data. The wave climate is estimated with the IMLM method (Iterated Maximum Likelihood Method) because it is the most suited to portray the narrow directional spread. The method is proven sufficiently accurate with a known synthetic signal.

IV. RESULTS

First, the study data is analysed with respect to the influence of oblique wave attack. Thereafter, similarities and discrepancies with the previous studies will allow further insight into the reason for the behavioural difference found by Van der Meer *et al.* (2003) for rough permeable and smooth impermeable structures.

Figure 2 shows the transmitted wave angle β_t with respect to the incident wave angle β_i for the data of this study. The

data of DELOS (2002b) and the formulations of Van der Meer *et al.* (2003) are included for comparison. As there were several variables changed during the testing procedure, the effects of these parameters are analysed qualitatively.

- The incident wave direction remains unchanged or increases by 10% after encountering the low crested structure.
- The permeability of the core shows no significant influence on the change in wave direction with oblique wave attack.
- The wave climate has no influence on the observed correlation between the incident angle of wave attack and the transmitted wave direction.
- The additional rubble mound does not influence the change in wave direction.

Some of these findings differ from those of Van der Meer *et al.* (2003), where its rough permeable rubble mound structure shows a reduction of the incident angle of wave attack. The results of this study compare well with the smooth impermeable structure [Van der Meer *et al.* (2003)] [DELOS (2002b)] until an incident wave angle of $45°$. At higher incident angles of wave attack, the β_t remains at $45°$ which contrasts with the findings of this study. Most important, the data of this study originating from the fully permeable rough rubble mound breakwater do not lie within the scatter of the data originating from the previous study for the analogous permeable rough structure.

The transmission coefficient K_t with respect to the incident wave angle β_i is shown in figure 3, along with only the relevant data originating from the submerged models of DELOS (2002b).

- The transmission coefficient remains unchanged or increases slightly with increasing incident angle of wave attack.
- Within the range of the scatter, the permeability of the core has a negligible influence on the transmission coefficient.
- The incident wave climate with the relatively longer waves and lower spectral energy results in relatively higher transmission coefficients.
- The additional rubble mound leads to overall higher transmission coefficients.

These finding differ from the trend found for smooth impermeable breakwaters [Van der Meer *et al.* (2003)]. On the other hand, the data of this study do lie in the scatter of the data originating from the rough permeable rubble mound of DELOS (2002b).

Qualitatively, the findings of this study seem to conflict with the findings of Van der Meer *et al.* (2003). However, of the few parameters varied during this study, the range of the variation was also very limited. Therefore, a linear regression analysis is performed on the individual and grouped data sets, leading to more objective results. The change in wave direction can be formulated as (figure 2):

Rough structures	β_t	$=$	$0.94\beta_i$	for $\beta_i \leq 60°$
Smooth structures	β_t	$=$	$0.94\beta_i$	for $\beta_i \leq 45°$
	β_t	$=$	$45°$	for $\beta_i > 45°$

Smooth structures are highly influenced by oblique wave attack; the transmission coefficient decreases with increasing angle of wave attack. The transmission coefficient of rough structures, on the other hand, is not dependent on the incident wave direction. Therefore it is recommended to keep the empirical formulations of Van der Meer *et al.* (2003).

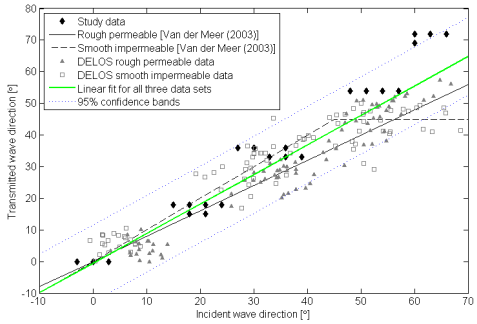

Fig. 2. β_t with respect to β_i

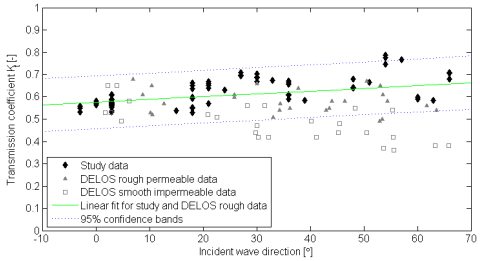

Fig. 3. K_t with respect to β_i

V. Conclusions

When considering the experimental results in comparison with the results formulated by Van der Meer *et al.* (2003) and DELOS (2002b), one finds one essential aspect. The influence of oblique wave attack on the behaviour of the physical model does not alter when the permeability of the core is varied. The fully permeable rough rubble mound behaves analogous to the fully impermeable rough rubble mound. This suggests that the behavioural difference found by Van der Meer *et al.* (2003) may have its roots in the roughness of the structure instead of the permeability.

Acknowledgments

I would like to thank my supervisors prof. dr. ir. P. Troch and ir. H.J. Verhagen for guiding me. I am grateful for the assistance from the laboratory staff members.

References

DELOS. 2002b. *Wave basin transmission tests: Internal report*. http:// www.delos.unibo.it/ Docs/ Deliverables/ D31.pdf. EU Fith Framework Programme 1998-2002 (Contract EVK3-CT-2000-00041).

Johnson, D. 2007. *DIWASP: DIrectional WAve SPectra toolbox version 1.3*. http:// www.metocean.co.nz/ software. MetOcean Solutions Ltd., New Zealand.

Van der Meer, J. W., Wang, B., Wolters, A., Zanuttigh, B., & Kramer, M. 2003. Oblique wave transmission over low-crested structures. *Proceedings Coastal Structures 2003*.

Contents

Symbols and abbreviations

B	Crest width	$[m]$
B_k	Blockiness coefficient	$[-]$
D_{n15}	Nominal diameter of the 15% value of the sieve curve	$[m]$
D_{n50}	Median nominal diameter of the armour layer material	$[m]$
D_{n85}	Nominal diameter of the 85% value of the sieve curve	$[m]$
E	Energy of the wave climate	$[N/m]$
$E_{JONSWAP}(f)$	Unidirectional variance density spectrum	$[m^2s]$
f	Frequency	$[Hz]$
f_p	Peak frequency	$[Hz]$
g	Gravitational acceleration	$[m/s^2]$
$G(\theta\|f)$	Wave directional spreading function	$[1/rad]$
h_c	Breakwater height	$[m]$
H_i	Significant wave height of the incident wave climate	$[m]$
H_{m_0}	Significant wave height calculated spectrally	$[m]$
H_s	Significant wave height	$[m]$
H_t	Significant wave height of the transmitted wave climate	$[m]$
K_t	Transmission coefficient	$[-]$
m_0	Zeroth-order moment of the variance density spectrum	$[m^2]$
Re	Reynolds number	$[-]$
R_c	Crest freeboard	$[m]$
R_c/H_i	Relative crest height (Dimensionless freeboard)	$[-]$

$S(f, \theta)$	Multidirectional wave spectrum	$[m^2 s/rad]$
s_{op}	Wave steepness	$[-]$
$T_{p,i}$	Peak period of the incident wave climate	$[s]$
T_p	Peak period	$[s]$
$T_{p,t}$	Peak period of the transmitted wave climate	$[s]$
W_{15}	Weight of the 15% value of the sieve curve	$[kg]$
W_{50}	Median weight of the armour layer material	$[kg]$
W_{85}	Nominal weight of the 85% value of the sieve curve	$[kg]$
$tan(\alpha)$	Seaward slope of the structure	$[-]$
β	Wave direction (Angle of wave attack)	$[^\circ]$
β_i	Wave direction of the incident wave climate	$[^\circ]$
β_t	Wave direction of the transmitted wave climate	$[^\circ]$
ξ_{op}	Surf similarity parameter	$[-]$
θ	Direction	$[rad]$
ρ	Density of the water fluid	$[kg/m^3]$

BDM	Bayesian Direct Method
DELOS	Environmental Design of Low Crested Coastal Defence Structures
DFTM	Direct Fourier Transform Method
DIWASP	DIrectional WAve SPectra toolbox
EMEP	Extended Maximum Entropy Principle
EMLM	Extended Maximum Likelihood Method
EP	Estimation parameters
ID	Instrument Data
IMLM	Iterated Maximum Likelihood Method
SM	Spectral Matrix

Trademarks

"The use of trademarks in any publication of the University of Ghent and of the Delft University of Technology does not imply any endorsement or disapproval of this product by the Universities."

Registered Trademarks:

Accropode	Sogreah Consultants, France
Core-loc	US Army Corps of Engineers
DasyLab	National Instruments, Ireland
Delft-Auke	WL | Delft Hydraulics
Elastocoast	Elastogran GmbH, Lemförde, Germany (subsidiary of BASF)
Matlab	The MathWorks Inc.

List of Figures

List of Tables

Chapter 1

Introduction

1.1 Introduction

Many breakwaters are known to have their crest high above the water surface. However, in many cases of breakwater design, a considerable amount of overtopping is deemed acceptable. This leads to the use of low crested structures such as rubble mound breakwaters. The main feature of these breakwaters is that the overtopping is dominant. The crest may be near the water surface, submerged, emerged or alternatively both.

Low crested structures are mostly built in shallow areas as detached breakwaters. They are primarily designed to act as a coastal defence mechanism by reducing the wave action on the lee side. These structures are usually parallel to the shoreline with wave attack perpendicular to the structure. However, breakwaters are also used for harbours where the structure is no longer parallel to the shoreline and oblique wave attack occurs. These breakwaters are designed to reduce the wave loads on ships along navigation channels and to provide relatively calm water conditions in harbours. During high water normative conditions, these breakwaters may become low crested, broadening the definition scope of low crested breakwaters. On the whole, low crested breakwaters serve to reduce the wave energy in the lee side of the area with respect to the open sea.

There is an increasing interest for **submerged rubble mound breakwaters**. The visual intrusion is reduced; resulting in a more natural landscape. This is often considered as an aesthetic advantage of safeguarding the landscape. Often, submerged breakwaters allow for a simple rehabilitation of existing protective structures by reducing the incident wave conditions. In areas of high sediment transportation, the submerged breakwater has the advantage that this transport will not be completely blocked; the area can remain open and sheltered simultaneously. Finally, a submerged breakwater is environmentally friendly

because they facilitate the protected areas with suitable amounts of water; the quality of the coastal environment is preserved.

1.2 Conventional rubble mound breakwater

A definition sketch of a conventional rubble mound breakwater, along with the related transmission parameters, can be found in figure 1.1. The main parameters related to wave transmission are the rubble mound characteristics (such as the structural geometry, the porosity, the permeability, the crest width, the slope angle and the surface roughness), the hydraulic wave parameters (such as the wave height, the wave period, the wave steepness and the water depth) and the combined parameters (such as the crest freeboard and the relative water depth).

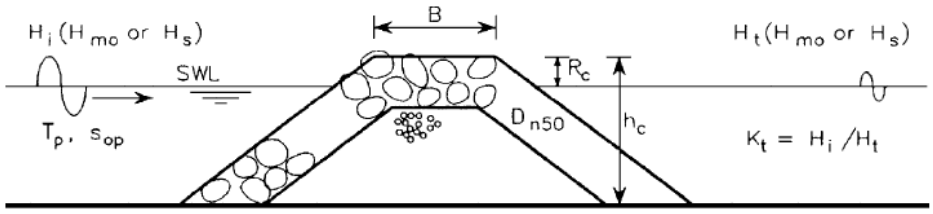

Figure 1.1: A definition sketch of a conventional rubble mound breakwater and the related transmission parameters [Van der Meer *et al.* (2005)]

List of parameters:

- H_i: Incident significant wave height, preferably $H_{m_0,i}$, at the toe of the structure
- H_t: Transmitted significant wave height, preferably $H_{m_0,t}$
- T_p: Peak period
- s_{op}: Wave steepness
- R_c: Crest freeboard
- B: Crest width
- D_{n50}: Nominal diameter of the armour rock
- K_t: Transmission coefficient
- ξ_{op}: Surf similarity parameter
- $tan(\alpha)$: Seaward slope of the structure

- h_c: Breakwater height

The incident and transmitted wave heights are spectrally calculated, linking the wave heights directly to the energy state of the waves through the zeroth-order moment of the variance density spectrum m_0:

$$\begin{aligned} E &= \frac{1}{16}\rho g \cdot H_{m_0}^2 \qquad (1.1) \\ &= \rho g \cdot m_0 \\ H_{m_0} &= 4\sqrt{m_0} \qquad (1.2) \end{aligned}$$

The transmission coefficient is defined as the ratio:

$$K_t = \frac{H_t}{H_i} \qquad (1.3)$$

, where the incident wave height does not include the reflected waves from the breakwater. When a wave encounters a low crested rubble mound breakwater, three wave transformation processes on and inside the structure will take place: wave reflection, wave transmission and wave dissipation. Wave transmission is a measure for the energy that passes the breakwater. It indicates the effectiveness of the breakwater in preventing the energy (via reflection and dissipation) of the open sea from passing the breakwater to the lee area. Part of the transmission originates from the wave passing the breakwater above the crest; called overtopping. Another part occurs via wave penetration through the openings of the core of the structure. The entire phenomenon results in a reduction of the wave energy in the lee of the structure; the wave action is reduced and the area is more protected.
Since the interaction between the wave and the structure is very complex, its modelling has proved to be difficult and the derivation of an acceptable formula an iterative process. Research has led to various proposed formulae, each with its own limitations.

1.3 Experimental research: 2D

There are a large variety of breakwaters available in practice, ranging from asphalt grouted breakwaters, groynes, caisson type breakwaters, breakwaters with concrete structures and so forth. Thus, the rubble mound breakwater is one extreme of the breakwater spectrum, whereas the smooth impermeable breakwater forms the other extreme. Wave transmission over such a smooth breakwater is very different from rubble mound structures and must be investigated independently. Since there is no wave penetration through the impermeable structure, and the smooth slope allows for no energy dissipation via friction, the wave

transmission tends to be larger for the same crest height. Also, these smooth impermeable breakwaters tend to have a more gentle slope, which causes the waves to break, whereas this is not so with the steeper rubble mound breakwater slope. This diversion from the rubble mound breakwaters, allowing for the large variety of breakwater types, has lead to a growth in the research of this branch over the last two decades. The most present research is based on a vast database, consisting of the 'old database' and the 'new database.'

1.3.1 Old database

d'Angremond *et al.* (1996) is considered to be the starting point of the most current research on wave transmission at rubble mound breakwaters. Data were collected from several investigations preceding the nineties and reanalysed to form one whole. Many structures were represented, including rubble mound breakwaters and breakwaters with tetrapod and accropode armour layers. The most important outcome is the well-known figure 1.2, which expresses the transmission coefficient K_t with respect to the relative crest height R_c/H_i.

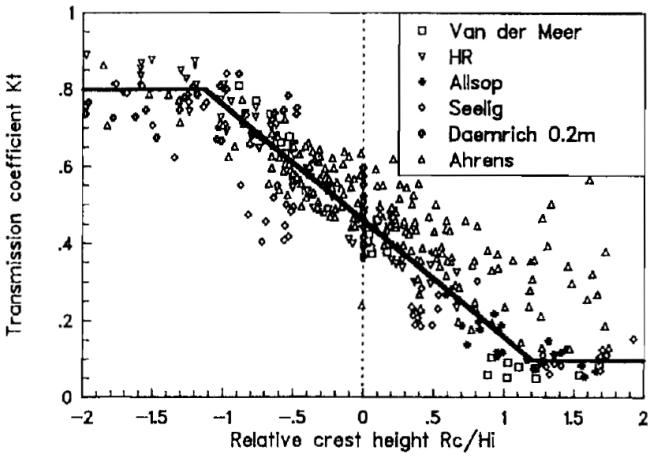

Figure 1.2: The transmission coefficient K_t with respect to the relative crest height R_c/H_i [d'Angremond *et al.* (1996)]

One can observe (figure 1.2) that the transmission coefficient K_t lies between the limits of 0 and 1. Further, it shows that the lower the relative crest height, the larger the transmission. These two facts can be felt intuitively. However, for a breakwater with its crest at the water surface, the transmission coefficient is in the order of one half. This is equivalent to a reduction of half of the initial wave height or in terms of energy, one fourth of the initial energy. Depending on how calm the water of the protected area needs to be, the appropriate crest height can be found for the rubble mound breakwater. However, the large scatter of data indicates that the wave transmission is also dependent upon other factors.

Seabrook & Hall (1998) focused the research primarily on classical rubble mound submerged breakwaters with very wide crests. A similar study was performed by Hirose *et al.* (2002) for submerged breakwaters with Aquareef concrete block armour layers and very wide crests. Melito & Melby (2001) investigated breakwaters with Core-loc armour layers; emerged as well as submerged structures. This collection of research data forms the basis of the present work on the wave transmission coefficient.

1.3.2 New database

The European project DELOS (Environmental Design of Low Crested Coastal Defence Structures) consisted of several research groups, carrying out experiments aimed at extending and completing the existing database. The Polytechnic of Catalonia in Spain performed large scale wave channel tests [Gironella *et al.* (2002)] whilst the University of Cantabria in Spain performed small scale wave channel tests [Garcia *et al.* (2004)]. Both used the classical rubble mound breakwater, varying the hydraulic conditions and the crest widths.
The European project "Low crested and submerged breakwaters in the presence of broken waves" is a second European initiative between the Coastal Research Centre in Hanover in Germany and the University of Naples in Italy [Calabrese *et al.* (2002)]. Large scale tests were conducted on shallow foreshores in the large wave channel in Hanover and the results were analysed in Naples. The aim was to verify the existing formulae at large scale so as to minimize scaling effects. These two European projects form the basis for the most recent knowledge.

1.3.3 Latest research

The old and the new database was gathered to form one vast consistent 2D database consisting of 2337 tests. In the analysis of this database, two different paths were followed; one by Buccino & Calabrese (2007) and the other by Van der Meer *et al.* (2005). Buccino & Calabrese (2007) looked at the physical processes of wave transmission in a theoretical sense, resulting in a nonlinear differential equation, linking the transmission coefficient to the rubble mound breakwater and the wave parameters. The database then served as a calibration and validation tool.
Van der Meer *et al.* (2005) reanalysed the existing formulae for rubble mound low crested structures and reanalysed the existing data for smooth impermeable breakwaters. From this analysis, the wave transmission prediction formulae were improved for the conventional rubble mound breakwater and derived for the smooth breakwater for the full range of relative crest

heights. As the formulae derived by Seabrook & Hall (1998) and Hirose *et al.* (2002) are solely based on submerged structures, they were not reanalysed because they could not serve for the full range of relative crest heights. Furthermore, the change of the spectral shape due to wave transmission was described.

1.4 Experimental research: 3D

Two dimensional research assumes that the wave attack is perpendicular to the low crested breakwater. This is mostly true because such structures are usually built parallel to the shoreline. However, the actual wave field acts in all directions and not all structures are built parallel to the shoreline. One only needs to think of a breakwater protecting a harbour to understand that being able to predict the transmission coefficient for oblique wave attack is of high importance in the engineering design process.
This area of concern was investigated through a series of 3D experiments, which were conducted in the laboratory at the Aalborg University of Denmark, under the European project DELOS. In total, 168 wave transmission tests were performed in a short crested wave basin with the goal of studying the influences of wave obliquities on transmitted wave directions, energy and spectral changes. A short recapitulation of the most important results will be summarized in section 1.4.1, in section 1.4.2 and in section 1.4.3.

1.4.1 Change in wave direction

According to Van der Meer *et al.* (2003), the incident wave direction reduces 20% after encountering the low crested structure for rubble mound structures (figure 1.3a):

$$\text{Rubble mound structures} \qquad \beta_t = 0.8\beta_i \tag{1.4}$$

, where the definition of the β-terms can be found in figure 1.4. It is suggested that the reason lies with the roughness and the porosity of the structure, which causes dissipation of energy in such a way that the waves do not remain in the same direction. Smooth impermeable structures behave differently (figure 1.3b). The transmitted wave angle is equal to the incident wave angle, up to an incident wave angle of 45°. For more oblique wave attack, the transmitted wave angle remains at 45°. It has been suggested that the smooth structure probably works in such a way that for angles larger than 45°, the wave runs along the crest of the structure. Another observed tendency is that, for lower wave transmission, the transmitted wave angle

is slightly smaller than the incident wave angle.

$$\begin{array}{lrcll} \text{Smooth structures} & \beta_t & = & \beta_i & \text{for } \beta_i \leq 45° \\ & \beta_t & = & 45° & \text{for } \beta_i > 45° \end{array} \tag{1.5}$$

It is also interesting to note that the influence of oblique wave attack on the wave direction for smooth impermeable breakwaters is formulated differently in the 'Transmission Internal Report' of DELOS (2002b), which states:

$$\begin{array}{lrcll} \text{Smooth structures} & \beta_t & = & 0.9\beta_i & \text{for } \beta_i < 50° \\ & \beta_t & = & 45° & \text{for } \beta_i \geq 50° \end{array} \tag{1.6}$$

However, the 'Transmission Internal Report' of DELOS (2002b) stresses that there is a physical limit where the structure loses its influence on the incoming waves so that the incoming wave direction remains unchanged. Thus, the above formulation is only applicable where the relative crest height $R_c/H_i > -1$.

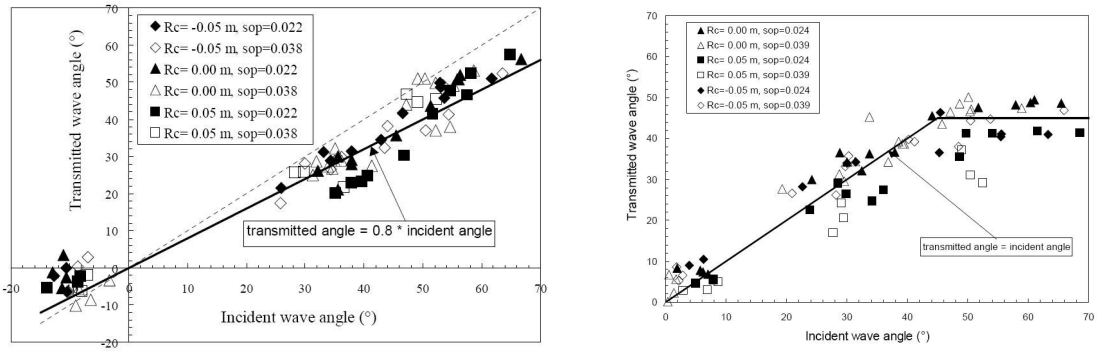

(a) Rubble mound (b) Smooth impermeable

Figure 1.3: The transmitted wave direction β_t with respect to the incident wave direction β_i [Van der Meer *et al.* (2003)]

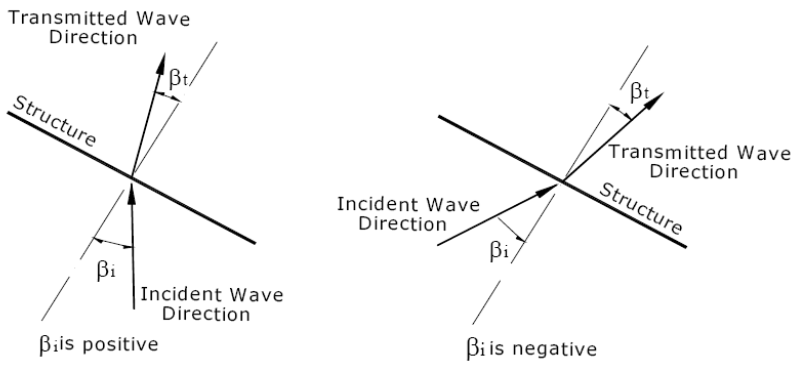

Figure 1.4: The definition of a positive wave direction [DELOS (2002b)]

1.4.2 Transmission

Van der Meer *et al.* (2003) states that there is no influence of the angle of wave attack on the transmission coefficient K_t for the incident wave angles up to 60° for rubble mound breakwaters eventhough a slight trend can be observed in figure 1.5a. There seems to be a slight tendency for the transmission coefficient to decrease with increasing angle of wave attack; the trend being less apparent for the two lowest crest heights. However, it has been suggested that the influence is marginal and this trend insignificant with respect to the scatter of the data. Therefore, it has been concluded that for rubble mound structures, the angle of wave attack has no or minimal influence on the wave transmission coefficient. The prediction formulae for transmission at rubble mound structures are therefore also valid for oblique wave attack, with the restriction of small crest widths and up to an angle of about 60°.

During the research of Seabrook & Hall (1998) on submerged structures, a few 3D experiments were also performed with an incident wave angle of 30°. A similar conclusion as that of Van der Meer *et al.* (2003) was made; there is no substantial influence of the angle of wave attack on the transmission coefficient.

The transmission coefficient of smooth impermeable low crested structures, on the other hand, has been found to be strongly dependent on the angle of wave attack. Van der Meer *et al.* (2003) shows that there is a $cos^{2/3}(\beta_i)$ dependency, suggesting a decrease in the wave transmission with an increase of the incident wave angle (figure 1.5b). The slight scatter is disregarded. This has led to a straightforward adjustment of the prediction formula for the transmission coefficient for smooth structures, within the limitations.

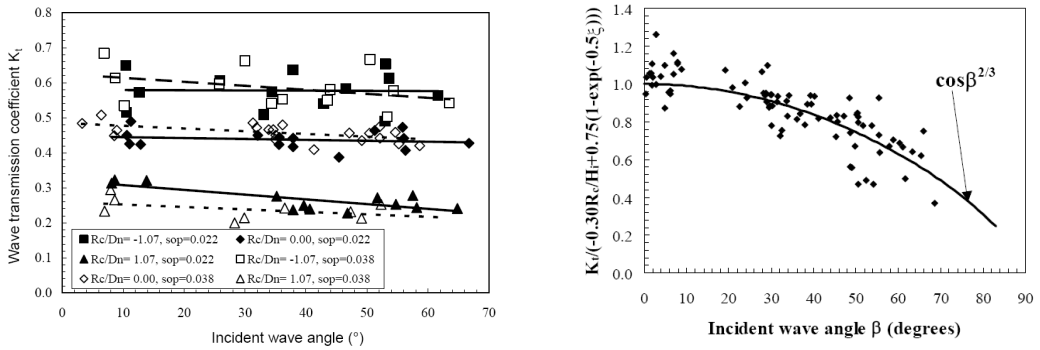

(a) Rubble mound (b) Smooth impermeable

Figure 1.5: The influence of the incident wave angle on the transmission coefficient [Van der Meer *et al.* (2003)]

Formulae for K_t

The most recent transmission coefficient formulae for rubble mound breakwaters that take into account the effects of obliquity are formulated by Van der Meer *et al.* (2005):

$$\text{For } \frac{B}{H_i} < 8: \begin{cases} K_t = -0.4\frac{R_c}{H_i} + 0.64(\frac{B}{H_i})^{-0.31}(1 - e^{-0.5\xi_{op}}) \\ \text{Lower limit: } K_{t,min} = 0.075 \\ \text{Upper limit: } K_{t,max} = 0.8 \end{cases}$$

$$\text{For } \frac{B}{H_i} > 12: \begin{cases} K_t = -0.35\frac{R_c}{H_i} + 0.51(\frac{B}{H_i})^{-0.65}(1 - e^{-0.41\xi_{op}}) \\ \text{Lower limit:} K_{t,min} = 0.05 \\ \text{Upper limit:} K_{t,max} = -0.006\frac{B}{H_i} + 0.93 \end{cases}$$

$$\text{For } 8 \leq \frac{B}{H_i} \leq 12\text{: Linear interpolation} \tag{1.7}$$

The expression for rubble mound structures (equation 1.7) has not been altered significantly as the influence of obliquity is negligible. The initial formulation proposed by d'Angremond *et al.* (1996) has been improved to fit best with the vast 2D database. Also, there is a supplementary restriction of small crest widths and a maximum angle of wave attack of 60°. Van der Meer *et al.* (2005) derived a wave transmission prediction formula for the smooth impermeable low crested structure for a large range of relative crest heights:

$$\text{For } 1 < \xi_{op} < 3;\ 0° \leq \beta \leq 70°;\ 1 < \frac{B}{H_i} < 4: \begin{cases} K_t = [-0.3\frac{R_c}{H_i} + 0.75(1 - e^{-0.5\xi_{op}})]cos^{\frac{2}{3}}(\beta_i) \\ \text{Lower limit: } K_{t,min} = 0.075 \\ \text{Upper limit: } K_{t,max} = 0.8 \end{cases} \tag{1.8}$$

The formulations (equation 1.7) (equation 1.8) are at present being used in the overtopping manual EurOtop (2007).

Theoretically, the transmission through a breakwater should give similar results whether long crested or short crested waves are present for perpendicular wave attack. For smooth impermeable structures, Van der Meer *et al.* (2003) found that this was also true for oblique wave attack. Even though short crested waves did produce lower values ($1 - 2\%$) for rubble mound structures, the same conclusion was given; there is none or only an insignificant difference between long crested and short crested waves.

1.4.3 Spectral changes

When waves encounter a low crested structure, not only will the transmitted wave energy be reduced; the shape of the energy spectrum will change as well. Van der Meer *et al.* (2000) gave a first analysis of this topic and concluded that the peak period of the transmitted spectrum stays similar to the incident peak period. This is in contrast with the change of the mean period, which decreases. An overview of a proposed method for predicting the shape of the transmitted spectrum for submerged structures is shown in figure 1.6.

It has been suggested that in average, 60% of the transmitted energy is present in the area where $f < 1.5f_p$ whereas 40% lies in the area $1.5f_p < f < 3.5f_p$. It is assumed that a negligible amount of transmitted energy lies in the area $f > 3.5f_p$. Furthermore, there was no effect found on the angle of wave attack so that the data were taken together to develop this model.

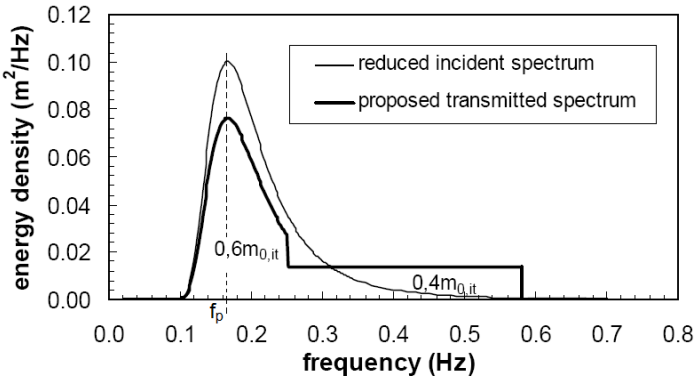

Figure 1.6: The spectral changes observed in the transmitted spectrum [Van der Meer *et al.* (2000)]

Van der Meer *et al.* (2000) warns that this model has been based on a limited number of tests. With the more recent data of DELOS, Van der Meer *et al.* (2005) is able to further support the initial model. However, it has been developed to larger depths because rubble mound structures and smooth impermeable structures do not behave similarly.

Briganti *et al.* (2003) explains that there are two phenomena which will determine the energy shift towards the higher frequencies. Wave breaking will be the dominant reason of spectral change for submerged structures, whereas the overtopping and the flow through the structure will be the main cause of the spectral shift for other structures. If the reduction of the wave energy is mainly due to the dissipation of flow through the structure, then the higher frequencies will be cut. An overview of the model specifications can be found in table 1.1, where Van der Meer *et al.* (2005) compares the newer model to that of Van der Meer *et al.*

(2000).

The model is not valid for emerged rubble mound structures as they show a different trend. Also, these results on the spectral change are not conclusive and further research in this area is recommended by Van der Meer *et al.* (2005).

	Method Van der Meer *et al.* (2000)	Method Van der Meer *et al.* (2005)	
		Rubble mound	Smooth structure
$\frac{f_{max}}{f_p}$	3.5	3.2 (2.1-4.3)	3.8 (2.9-5.6)
$\frac{E_{(1.5f_p \rightarrow f_{max})}}{E_{total}}$	40%	34% (20-52%)	42% (30-60%)

Table 1.1: A measure for the spectral changes observed in the transmitted spectrum [Van der Meer *et al.* (2005)]

1.5 Problem analysis: A discussion on the limitations of the existing formulae

Low crested structures are primarily designed as a coastal defence mechanism, making the prediction of the energy in the lee of the structure of utmost importance. Not only is the transmission useful to predict the reduced wave heights, it plays an important role in the prediction of circulation patterns and in the prediction of the shoreline changes. The spectral shape in the lee of the breakwater is also an important variable for predicting the long-term morphological changes in the area due to these low crested structures. Furthermore, the spectral shape is also necessary in cases where large fetches are present in the lee of the structures, for the prediction of the wave reforming.

Many of the low crested breakwaters are designed parallel to the shoreline, allowing for a dominant perpendicular wave direction. For these cases, the 2D wave transmission coefficient formulae for perpendicular wave attack have been analysed and reanalysed over the past two decades to improve the reliability. However, not only does the wave field act in all directions, but the alignment of low crested structures is not always parallel to the shoreline. Accordingly, there are many more low crested structures, such as groynes, which have a continuous oblique wave attack. During extreme storm surges, harbour breakwaters may also become low crested, thus extending the realm for which oblique wave attack is of utmost importance.

Oblique wave attack was investigated through a series of 3D experiments on two structures (figure 1.7), which were conducted in the laboratory at the Aalborg University of Denmark. The first structure is a rough rubble mound (figure 1.7a) with a thick permeable armour layer A, whereas the second structure is smooth and impermeable (figure 1.7b). In total, 168 wave

transmission tests were performed with the goal of studying the influences of wave obliquities on transmitted wave directions, energy and spectral changes.

The results of Van der Meer *et al.* (2000)(2003)(2005) are very valuable for they are the first which were dedicated to the influence of oblique wave attack. They covered a range of crest heights, wave heights, wave steepness and angles of wave attack (table 1.2). However, one must realize that there are also limitations to the research which will call for further research.

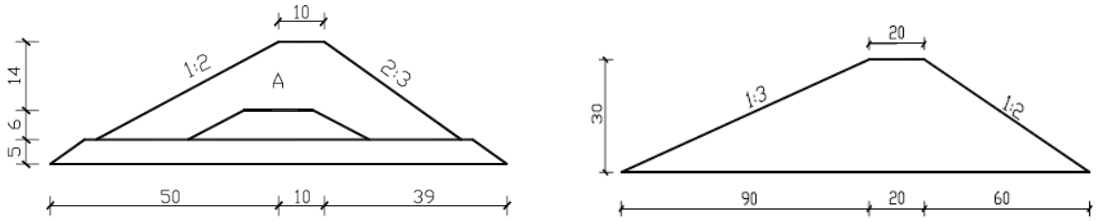

(a) Rubble mound (b) Smooth impermeable

Figure 1.7: The structures used during the experiments of DELOS (2002b), with wave propagation from left to right [Dimensions in cm]

Test per structure	84 (10 long crested, 74 short crested)
Crest freeboard R_c	+0.05m; 0.0m; -0.05m
Dimensionless freeboard $\frac{R_c}{H_s}$	-0.7 to +0.8
Incident wave height H_s	0.07m to 0.14m
Wave steepness s_{op}	0.02 and 0.04
Angles of wave attack β	0°, 20°, 30°, 40°, 50° and 60°

Table 1.2: The experimental programme of DELOS (2002b) [Van der Meer *et al.* (2003)]

In the physical model tests, the structure slope at the seaside was 1:2 for the rubble mound and 1:3 for the smooth impermeable breakwater. The slopes used were different with the reason that in practice, smooth impermeable structures usually have a gentler seaside slope than rubble mound structures. Although this is justifiable, the slope angle may influence the effect of the incident wave angle on the transmission. For example, on a steeper slope, the waves might no longer break on the slope, thus increasing the transmission. Also, an oblique wave attack will no longer increase the travel distance along the slope significantly, decreasing the chance of the wave breaking on the seaside slope. Thus, the steep slope of the rubble mound structure used may be a reason for the lack of influence of the angle of wave attack. Further research could clarify this aspect.

The crest width was $0.1m$ for the rubble mound and $0.2m$ for the smooth breakwater. For

the rubble mound, the lack of influence of the angle of wave attack on the transmission coefficient may be due to the fact that the crest width is relatively short. A wave passing over the smooth breakwater travels twice the distance than if it were passing over the rubble mound, making the comparison troublesome. Thus, more physical tests with variable crest widths could clarify the uncertainty.

Another limiting aspect of the research can be derived from the fact that the structures had a fixed slope and crest width. This allowed for a narrow range of the relative crest width B/H_i between 1 and 4 and of the surf similarity parameter ξ_{op} between 1 and 3 for the smooth structure. It is also the reason why the formula for the respective transmission coefficient is restricted to these ranges. However, because the influence of oblique wave attack was found to be negligible for rubble mound breakwaters, the limiting ranges were not applied for its respective transmission coefficient formulae. This may need further confirmation.

One confusing aspect of the results lies with intuition. The interference of the propagating wave by a low crested structure dissipates a fraction of the incident wave energy, whilst a part is transmitted and another is reflected. One could assume that increasing the incident wave obliqueness results in an increasing energy flux in the parallel direction and a decreasing energy flux in the direction perpendicular to the structure, so that an influence should also be found for the rubble mound structure.

The major conclusion of the research was that for rubble mound structures, there is a negligible influence of the angle of wave attack on the transmission whereas there is a significant influence for smooth structures. The greatest area of doubt within the research lies with the definition of the two structures. The first is a rough permeable rubble mound breakwater whereas the second is a smooth impermeable breakwater. One can consider them the two extremes of all found breakwaters in practice. What is valid for all the other breakwater structures which lie in between these two extremes?

The parameters characterising the two extreme structures are the permeability and the smoothness. Therefore, does the difference in behaviour lie in the fact that the rubble mound is permeable or rough; the smooth structure smooth or impermeable? Assuming that the formulae are reliable for the applicable ranges and restrictions, it is therefore difficult to know for which other structures these formulae could be valid. Are the formulae still valid for rubble mound breakwaters which are impermeable but rough; where the impermeable core reaches larger heights?

A large portion of the low crested structures have the characteristic of being rough but highly impermeable. One only needs to think of a typical harbour breakwater to realise that the

permeable armour layer is kept at a minimum thickness for economic reasons. Furthermore, if the constructed rubble mound breakwater turns out to be more impermeable than designed in an area of dominant oblique wave attack, will the lee area be under more danger because a reduction of the transmission is no longer allowed? There are many doubts as to which breakwater structures the available formulae are applicable to, due to the fact that it is not known whether the observed behaviour is due to the permeability or the roughness of the structure. Further research may clarify this aspect.

1.6 Problem definition

At present, it is known that for permeable rough rubble mound breakwaters, there is a negligible influence of the angle of wave attack on the transmission of the structure. For smooth impermeable breakwaters, the transmission decreases significantly with increasing angle of wave attack. The reason for this difference in behaviour is unclear. For practical engineering circumstances, it is considered desirable to have more insight into the reason of this difference.

1.7 Research objective

The objective of this research is to gain insight into the reason for the large difference in behaviour between rough permeable rubble mound and smooth impermeable breakwaters. The behaviour of rough impermeable rubble mound breakwaters will be investigated under the influence of oblique waves. As there is an increasing interest for submerged rubble mound breakwaters, the investigation will be limited to breakwaters with the crest below the water surface. Within the area of hydraulic influence, the focus will be on the influence of irregular short waves as they occur in fetch limited seas and not on long waves, such as tides, or exceptional events, such as tsunamis. Therefore, the aim of the study is to investigate **oblique wave transmission through rough impermeable rubble mound submerged breakwaters** by means of a 3D physical model.

1.8 Report outline - methodology

As the research is of an experimental nature, the second chapter gives an extensive overview of the experimental set-up. All aspects of the wave basin are described in such a way that the set-up can be reconstructed. The framework of the experimental programme is explained so that a clear overview of the tests is obtained. Chapter three describes the spectral analysis

software used to process the data. Furthermore, the sources of error are identified and justified so that the findings of the analysis can be fully accounted for. The fourth chapter focuses on the results of the experiment. As several parameters are varied during the testing procedure, not only is the data of this study analysed as a whole but the effects of these parameters are also analysed qualitatively. Furthermore, by comparing the data of this study with the data of DELOS (2002b) and the formulations of Van der Meer *et al.* (2003) (2005), insight should be gained into the reason for the behaviour difference between rough permeable and smooth impermeable breakwaters. Finally, a last chapter summarizes the found conclusions; recommendations and future perspectives are touched upon.

Chapter 2

Experimental set-up

The 3D experiments conducted in the laboratory at the Aalborg University of Denmark [DELOS (2002b)] led to a behavioural difference between permeable rough rubble mound and smooth impermeable breakwaters. As the aim of this study is to gain insight into the reason for this behavioural difference, the experimental set-up of DELOS (2002b) will be the basis for the experimental set-up at the Fluid Mechanics Laboratory of the department of Civil Engineering and Geosciences at the Technical University of Delft.
According to Kramer *et al.* (2005), a survey of the 1248 existing low crested breakwaters in the European Union was conducted to identify the typical ranges of the structural geometries. Herewith, the chosen geometries were scaled by 1 : 20; leading to appropriate sizes of the models with respect to the size of the available wave basin at the Aalborg University ($9.0m$ x $12.5m$ x $0.9m$). As the wave basin at the Technical University of Delft has the effective horizontal dimensions of $28.60m$ x $16.60m$ and a maximum depth of $0.60m$, the scaling of 1 : 20 will be maintained. A general overview of the basin layout can be found in figure 2.1, with its different aspects:

- Beach
- Sidewalls
- Wave generator
- Breakwater
- Measuring instruments

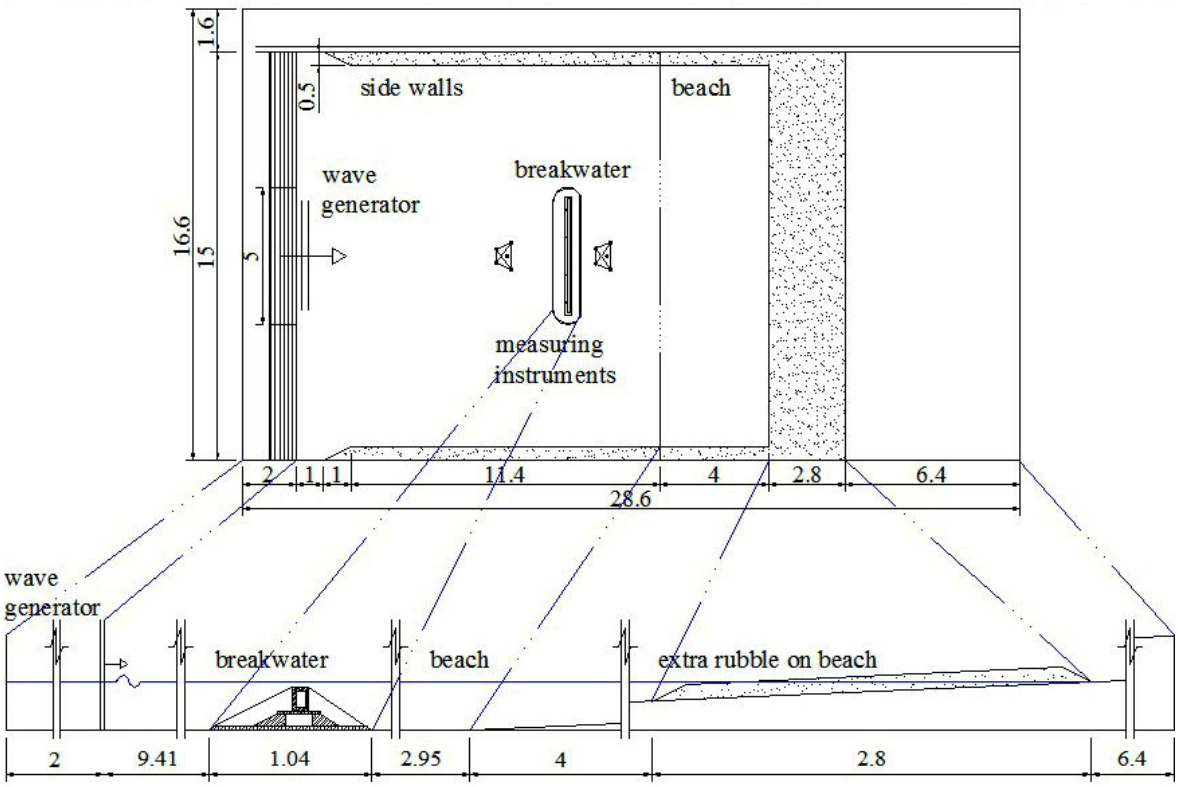

Figure 2.1: Overview of the wave basin [Dimensions in meters]

2.1 Wave basin boundaries (beach and sidewalls)

Since the experiment should not be affected by the physical constraints of the wave basin, it is essential that the waves travelling towards the side walls and beach are not re-reflected back towards the breakwater. In order to dampen the reflection originating from the sidewalls, a sloping layer of coarse rubble is placed. Also, the wave basin has a fixed concrete seabed which remains horizontal until the beach starts; having a slope of 1 : 30. Higher upwards the beach, there is a layer of coarse rubble to further dampen the waves and minimize the reflection back towards the breakwater. The influence of the reflected waves on the wave climate at the lee of the breakwater is hereby minimized.

2.2 Wave generation

2.2.1 Wave generator

There are three hydraulic piston-type wave generators alongside each other, each with a length of five meters; capable of generating irregular waves over the basin width of $15m$. Each generator has one wave board which is driven from one meter above the seabed and has

a maximum stroke of $0.26m$. The three generators are synchronized to produce long crested waves, making the wave generation perpendicular to the wave boards (figure 2.2).

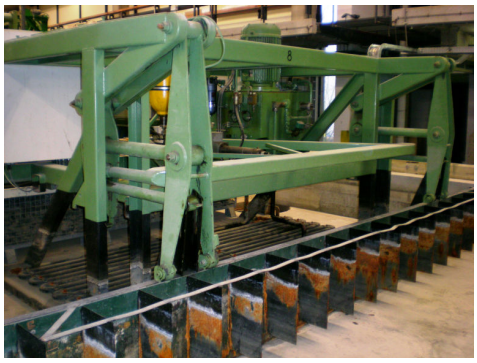

(a) Wave generator

(b) Waves reaching the breakwater, from right to left

Figure 2.2: Generating waves

The drive signal for the wave generator is produced by the programme MultiLin version 7.10, a subsection of the Auke software package. It transforms the desired wave condition in the spectral domain to the necessary steering signal for the generator in the time domain. The duration of the generated time wave signals are $50min$ long, with a time-step of $100Hz$ and repeated cyclically.

The wave generators are not equipped with an active reflection compensator, meaning that the generator is not able to minimise re-reflections from the wave board. The wave generator will send waves to the breakwater, which will reflect part of the wave back towards the wave boards. Upon reaching these wave boards, the wave signal will be re-reflected and sent back towards the breakwater. This, on top of the wave generated directly from the wave generator, will result in a wave climate with higher energies than initially accounted for. There are several risks associated with these re-reflections. The incident wave climate arriving at the breakwater may have higher wave heights than accounted for or the higher waves may break prematurely due to the limited water depth. A third result is the formation of standing waves; where the wave heights will grow during the test as a result of the resonance. As the breakwater takes up maximum $1/3^{rd}$ of the basin width, there is sufficient room for the wave energy to disperse. The chance that the waves will become 'trapped' and resonate between the wave boards and the breakwater is very small. However, these phenomena should be checked so that the target incident wave climate can be simulated correctly. As compensation, the signal sent to the generator is set at 90% capacity.

2.2.2 Wave climate

As the research is based on the low crested structures found in the European Union, the modelled wave climate should correspond herewith. The JONSWAP (JOint North Sea WAve Programme) spectrum represents a wave climate with limited fetch and storm duration, making it realistic for the coastal areas. The variance density spectrum generating the waves of such a young sea state is formulated as [Holthuijsen (2007)]:

$$E_{JONSWAP}(f) = \alpha g^2 (2\pi)^{-4} f^{-5} exp\Big[\frac{-5}{4}\Big(\frac{f}{f_{peak}}\Big)^{-4}\Big]\gamma^{exp\Big[-\frac{1}{2}\Big(\frac{f/f_{peak}-1}{\sigma}\Big)^2\Big]} \tag{2.1}$$

$$\sigma = \begin{cases} 0.07 & \text{if } f \leq f_{peak} \\ 0.09 & \text{if } f > f_{peak} \end{cases} \tag{2.2}$$

, where:

$E_{JONSWAP}(f)$	:	variance density	$[m^2 s]$
f	:	frequency	$[Hz]$
f_{peak}	:	peak frequency	$[Hz]$
g	:	gravitational acceleration	$[m/s^2]$
α	:	an energy scale parameter	$[-]$
$\gamma = 3.3$	:	a peak enhancement factor	$[-]$
σ	:	a peak width parameter	$[-]$

From the variance density spectrum, the n-th order moment of $E_{JONSWAP}(f)$ can be calculated (equation 2.3), where the zeroth-order moment represents the area underneath the spectrum m_0 and which directly relates to the wave climate's energy and significant wave height (equation 1.1) (equation 1.2).

$$m_n = \int_0^\infty f^n E(f) df \quad \text{for } n = \ldots, -2, -1, 0, 1, 2, \ldots \tag{2.3}$$

The standard JONSWAP spectrum (equation 2.1) is used for all the test series. More specifically, the transmission response of each breakwater test set-up is investigated under two target wave climates (table 2.1). This allows for a first wave climate with a lower energy and longer waves. The second wave climate has a higher energy, along with higher, shorter and therefore, steeper waves.

Since the experiments are three dimensional, one cannot only refer to the wave climate according to an unidirectional frequency spectrum $E_{JONWSWAP}(f)$. This calls for the definition of a multidirectional wave spectrum $S(f, \theta)$, describing the wave energy in both frequency and spatial domains [Hashimoto (1997)]:

$$S(f, \theta) = E_{JONSWAP}(f) \cdot G(\theta|f) \tag{2.4}$$

$$\int_{-\pi}^{\pi} S(f,\theta).d\theta = E_{JONSWAP}(f) \quad (2.5)$$

$$\int_{-\pi}^{\pi} G(\theta|f).d\theta = 1 \quad (2.6)$$

, where $G(\theta|f)$ is a wave directional spreading function which describes the distribution of wave energy on their propagation directions from $-\pi$ to π. The form of $G(\theta|f)$ is usually characterized by a cosine power spreading function and can be as simple as [Van Dongeren (2007)]:

$$G(\theta|f) = \frac{1}{\sqrt{\pi}} \cdot \frac{\Gamma(s+1)}{\Gamma(s+0.5)} \cdot cos^{2s}(\theta - \theta_0) \quad (2.7)$$

, where Γ is the standard Gamma function, θ_0 is the main wave propagation direction and s is a spreading parameter. Long crested waves travelling in one direction can be characterized by a high value of s ($s = 75$); allowing the directional spread to be very narrow whereas short crested wind waves have a higher directional spread and a low value of s ($s = 5$).

Even though the wave energy can be distributed in various directions, the total energy of the wave field should remain unchanged. As the wave generator available can only generate waves in one direction (long crested waves), all the wave energy will be concentrated in a very narrow range around $\theta_0 = 0°$. Therefore, the drive signal for the wave generator can still be based on $E_{JONSWAP}(f)$ and the respective target wave climates (table 2.1).

Test name	$H_i[m]$	$T_p[s]$	$s_{op}[-]$	$E[N/m]$
Test02	0.07	1.5	0.020	3
Test03	0.09	1.3	0.034	5

Table 2.1: Target wave climates

2.2.3 Water depth

The water depth is initially set at $0.30m$. However, since some of the highest waves of the Test03 wave climate start to break prematurely before the breakwater, the water depth is changed to $0.31m$. In the analysis, there is a distinction made between these two situations.

2.3 Physical Model

2.3.1 Dimensions

As the insight on the behavioural difference between permeable rough rubble mound and smooth impermeable breakwaters is desired, the aim of the study is to investigate oblique wave transmission through rough impermeable rubble mound submerged breakwaters by

means of a 3D physical model. It is opted for a rubble mound breakwater with constant roughness and a changeable core. The dimensions of the cross-section (figure 2.3a) are based on the rubble mound structure (figure 1.7a) of the DELOS (2002b) experiments.

The aim of the study is to analyse the effect of the permeability of the breakwater core. The outer dimensions and its roughness need to be kept constant. As the breakwater will be moved during the testing programme, it is decided to fix the armour layer because it is not possible to rebuild the breakwater every time with the armour stones in exact the same positions. Furthermore, as the breakwater will be moved on several occasions, it is best to have a fixed physical model to limit the time needed to do this. However, when fixing the stones to each other, it is essential that the permeable armour layer does not become clogged. A polyurethane substance called Elastocoast fulfils these requirements as it forms a thin film around the stones without decreasing the permeability of the armour layer.

The core is made up of an impermeable wooden box available in three different sizes so that in total four different structures (figure 2.3b) can be simulated; ranging from a fully permeable (d) to a fully impermeable (a) (figure 2.5a) rough rubble mound breakwater. The armour stones in the core are not fixed but are consistently used from the same batch and randomly placed in the same manner.

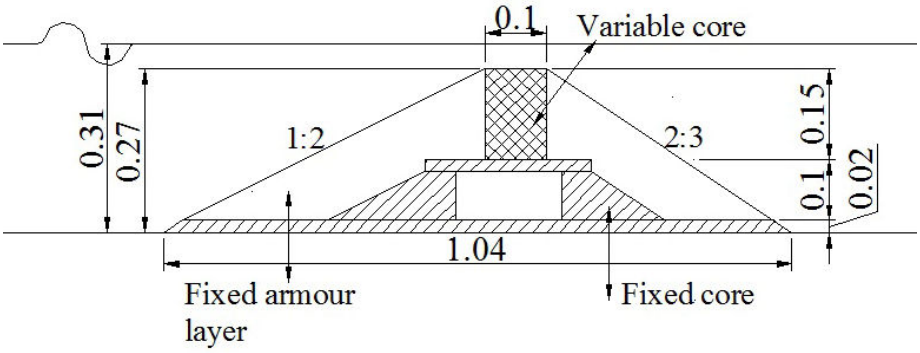

(a) General cross-section

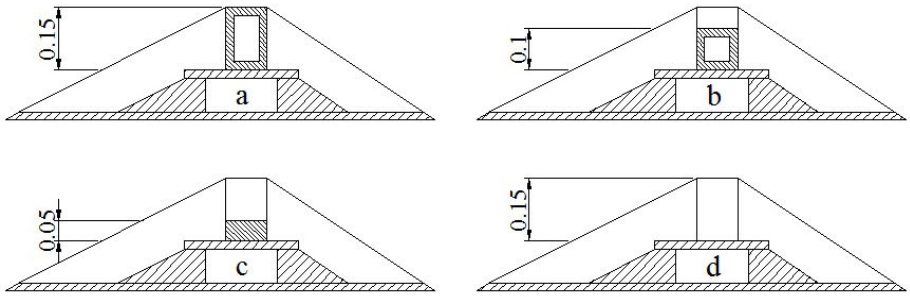

(b) Variable core

Figure 2.3: Cross-section of the physical model [Dimensions in meters]

The total length of the breakwater is five meters but is constructed in two parts (figure 2.4) so that the model can be rotated safely in the basin. Each part has three hoist eyes which can be attached for hoisting with the laboratory crane and removed during testing. The circular roundheads have a variable radius analogous to the cross-section dimensions and prevent the breakwater from ending abruptly.

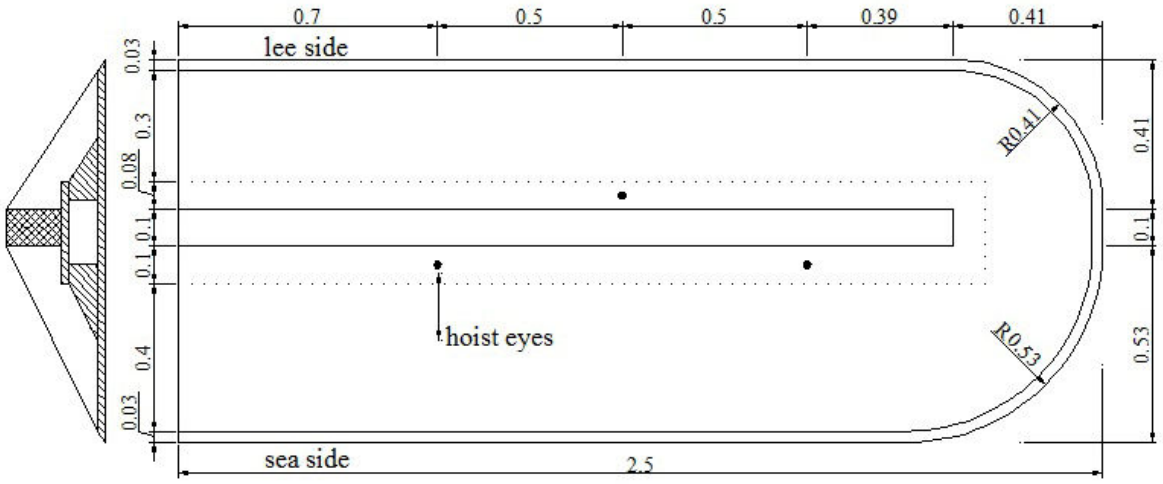

Figure 2.4: Top view of one part of the model [Dimensions in meters]

(a) Cross-section: Fully impermeable

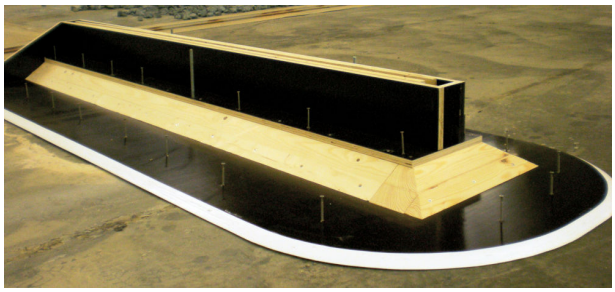

(b) One part of the model before fixation of the armour layer

Figure 2.5: The making of the model

The model is rotated progressively by 15°, ranging from 0° to 60°, about the centre of the crest width in order to simulate oblique waves (figure 2.6). In the extreme orientation of 60°, the breakwater has a remaining perpendicular length of $2.5m$, which is of the same order of magnitude as the longest wave. As it is not the aim to observe the influence of diffraction on the wave climate in the lee of the breakwater, an additional permeable mound of rubble (figure 2.7) is placed alongside the breakwater, consisting of stones originating from the excess supply of armour layer material. Every stance of the breakwater is tested both with and without this extra rubble mound so its effect can be monitered. This allows the data

sets of the different angles to be comparable with each other. The height of this additional rubble mound is $0.07m$ lower than the main physical model. The width is approximately $0.40m$. This is to make sure that the original model stays the dominant source affecting the incident wave climate.

Because of the finite dimensions of the wave basin, the model will suffer from these physical constraints. Especially when the breakwater is rotated to simulate incident oblique waves, there will no longer be a symmetrical flow in the basin. According to Hughes (1993), this will result in longshore currents along the basin sidewalls and in an overall large scale circulation pattern that is more pronounced than what would be in the sea. As long as the testing is limited to the regions unaffected by these sidewall effects, the results can be deemed reliable. When the additional rubble mound is placed alongside the breakwater (figure 2.7), it will interfere and reduce these effects.

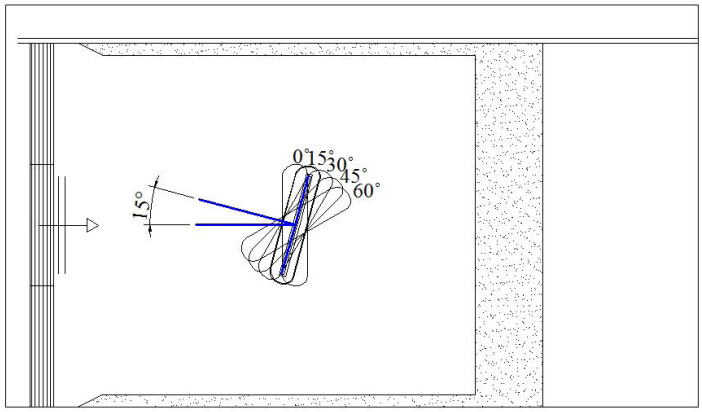

Figure 2.6: Generating oblique waves

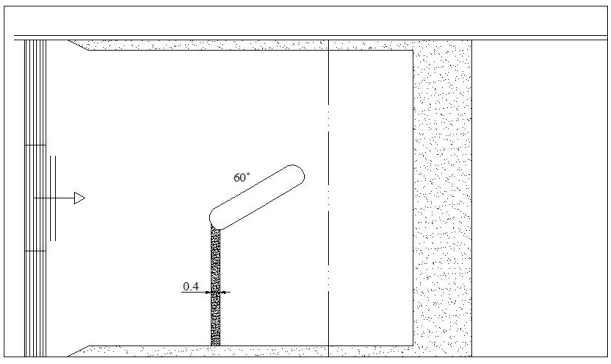

(a) Position of the additional rubble mound

(b) View of the additional rubble mound in the dry wave basin

Figure 2.7: Additional mound of rubble: 60°

2.3.2 Armour layer

The stones of the armour layer originate from Norway and are classified as Norwegian granite railroad ballast. The delivered stones fulfil the $NEN - EN - ISO$ 9001 requirements, from which a selection is made. The very elongated and flat stones are discarded to allow for realistic shapes for the breakwater model. For the characterization of the used armour layer stones, a random sample of 100 stones is selected and weighed. From these 100 stones, a second random sample of ten stones are chosen and measured in more detail so that not only the specific weight and grading (figure 2.8) can be established, but also the average blockiness coefficient. Finally, the D_{n15}, D_{n50} and D_{n85} are also calculated.

The specific weight of the used material is $2705 kg/m^3$, which is heavier than the material used at the Aalborg University. The average dimensionless blockiness coefficient B_k is 0.514, which corresponds with a slightly less elongated and flaky shape as the stones used at the Aalborg University. The D_{n50} is $0.033m$, which is only slightly smaller than the material used at the Aalborg University. The grading has a D_{n85}/D_{n15} of 1.48, which is considered to be a narrow grading. These conditions allow for the armour layer to be highly permeable. An overview of the armour layer specifications can be found in table 2.2.

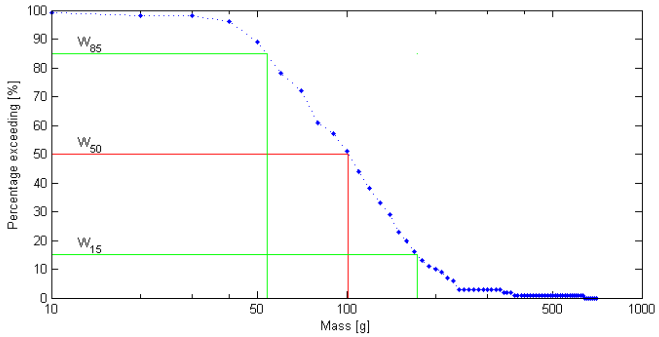

Figure 2.8: Armour stone grading

W_{15} $[kg]$	W_{50} $[kg]$	W_{85} $[kg]$	D_{n15} $[m]$	D_{n50} $[m]$	D_{n85} $[m]$	B_k $[-]$	ρ $[kg/m^3]$
0.173	0.101	0.055	0.040	0.033	0.027	0.514	2705

Table 2.2: Armour layer specifications

2.3.3 Scaling effects

This study is not a model research of a prototype breakwater so one is not interested in which scale (1 : 20) is being used as such. The interest lies in the relative behaviour of

the breakwater under changing conditions. However, because the results of model research are often of use for cases in reality, it is still important to keep to the scaling rules when determining the model dimensions and input parameters. Otherwise, the results will not represent what would happen on prototype level; the results would be useless.

In a hydraulic wave model, where the water depths are greater than $0.02 - 0.03m$, the wave heights greater than $0.02m$ and the wave periods greater than $0.3s$, the viscous damping of the waves is considered to be negligible [DELOS (2002a)] so that it is custom to use Froude scaling. This assures that the waves are reproduced correctly. More specifically for rubble mounds, it is required that the models be geometrically undistorted in length scale and the Froude criteria be used to model the flow hydrodynamics [Hughes (1993)]. However, as the requirements of the Froude scaling and the Reynolds scaling cannot be met at the same time, the effects of viscosity and surface tension will be neglected. If the breakwater material is chosen via the 1 : 20 geometric scale, there will be relatively less wave transmission through the model structure because there will be more frictional losses. The flow in the breakwater will be laminar instead of turbulent because the viscosity forces, and thus also the flow resistance, would be too high (Reynolds number too low). Increasing the diameter of the breakwater material is a common way to correct for this scale effect so that the transmission can still be modelled correctly. More specifically, the flow fields of the prototype and the model should be matched. However, one must remember that when porous flow is being modelled, the scale effects are significant and can never be driven away completely [DELOS (2002a)].

When wave breaking is considered, the scale effects are more favourable. According to Hughes (1993), the entrained air bubbles during wave breaking are larger in the model because of the effects of surface tension. This will result in a different flow process during the wave breaking on the rubble mound model. However, it is stated that the differences in the fine details of the flow process will not affect the overall energy dissipation; the process of energy dissipation will still be in similitude. Thus there is no need to worry about scale effects due to wave breaking on the physical model.

According to Kramer *et al.* (2005), the Reynolds number was sufficiently large (approximately 3.10^4 to 5.10^4) during the experiments at the Aalborg University. This was due to the larger breakwater material used and problems with viscous scale effects were avoided. As the experimental set-up at the Aalborg University was closely followed as the basis for this experiment, one can assume that the results of a scaling analysis will be similar. Also, since the breakwater dimensions and the input parameters are also closely followed and taken over,

it is no longer necessary to check the scaling laws in detail. However, this is a dangerous assumption which must not be forgotten and calls for an estimation of the Reynolds number (equation 2.8) [Hughes (1993)], which is found to be $2.7 \cdot 10^4$. This is slightly lower but still in the same order of magnitude.

$$Re = \left(\frac{W_a}{\rho_a g}\right)^{1/3} \cdot \frac{\sqrt{gh}}{\nu} \tag{2.8}$$

2.3.4 Stability check

Even though the experimental set-up is following the set-up used at the Aalborg University [DELOS (2002b)] and even though the fixed armour layer is held in place by the Elastocoast, it is still recommended to check if the model would be stable on its own. According to the 'Final Structural Design Report for Low Crested Structures' of Tirindelli & Lamberti (2002), it is recommended that a crest width of at least three stones should be chosen. Furthermore, the crest width should also be at least equal to the largest significant wave height. The overall structural stability of low crested structures with low relative crest heights is formulated as:

$$\frac{H_i}{\Delta D_{n50}} = 0.06\left(\frac{R_c}{D_{n50}}\right)^2 - 0.23\frac{R_c}{D_{n50}} + 1.36 \quad \text{for } -3 \leq \frac{R_c}{D_{n50}} < 2 \tag{2.9}$$

With the wave conditions defined (table 2.1), the minimum D_{n50} required is $0.03m$, making the breakwater just stable.

2.4 Measuring devices

2.4.1 Resistive wave gauges

Two sets of five resistive wave gauges are used to acquire the necessary data. The wave gauges consist of two thin poles next to each other so that when the gauge is operational and high frequency alternating voltage is passing through the wires, the water level is found by recording the conductance between them. More specifically, the changes in conductance are linearly related to the changes in surface elevation ($1V : 0.025m$). It is evident that each wave gauge needs to be piercing the water surface to a depth below the lowest wave trough and needs to be calibrated before commencing the test series. The calibration is also performed at several other occasions during the whole test procedure for validation. Furthermore, each gauge has a reference electrode mounted at the lower end of the instrument to avoid influences of the water's conductivity fluctuations. A supplementary measure to insure a stable performance of the wave gauges is for them to remain on at all times during the weeks of testing so that their temperature stays levelled. The measuring range of the wave gauges

is $-10V$ to $10V$, which is equivalent to a water level variation of $0.50m$. This is sufficient for the testing procedure.

The relative location of the measuring instruments (figure 2.9) is based on a non-symmetrical cross sequence so that directional data can be retrieved after signal processing. One set of five wave gauges is placed before the breakwater for the recording of the incident wave conditions while the second set of five wave gauges is placed in the lee of the breakwater for the recording of the transmitted wave conditions. Both sets of wave gauges are mounted on a longer frame (figure 2.10) to minimize the amount of interference from the support legs and to assure that the relative positions of the wave gauges remain constant.

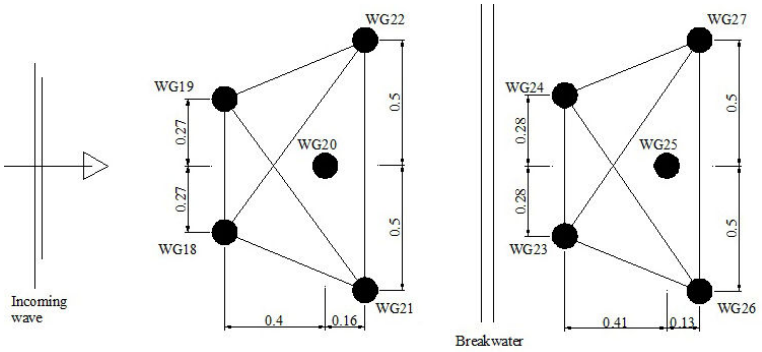

Figure 2.9: Cross configuration of the wave gauges [Dimensions in meters]

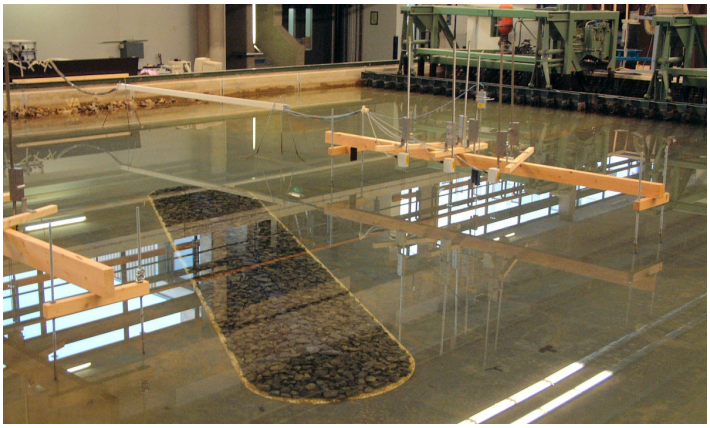

Figure 2.10: Wave gauges mounted on a longer frame

According to Gironella *et al.* (2002), it is recommended to place the measuring instruments at a distance approximately equivalent to six times the crest width ($0.60m$) from the rear toe of the structure. However, in order to measure the wave conditions in the lee of the breakwater solely due to the wave transmission, the wave gauges need to be placed in an area where diffraction is not dominant. For sure the instruments need to be placed in the shadow zone

of the breakwater, where the diffraction is reduced to 50% of the initial wave height [Battjes (2000)]. According to Briggs *et al.* (1995) and the Shore Protection Manual CERC (1984), the area which is at least 80% free from the diffraction effects can roughly be sketched as the area in between the 15° lines (figure 2.11). Also, as the beach starts relatively near the lee of the breakwater, the wave gauges should not be placed too close to the start of the beach. This results in three specifications that determine an area where the measuring instruments may be placed. It is to be noted that with increasing obliquity, these conditions are hard to abide by (figure 2.12). Therefore, the additional permeable mound of rubble (figure 2.7a) placed alongside the breakwater can also serve as a means to decrease the diffraction.

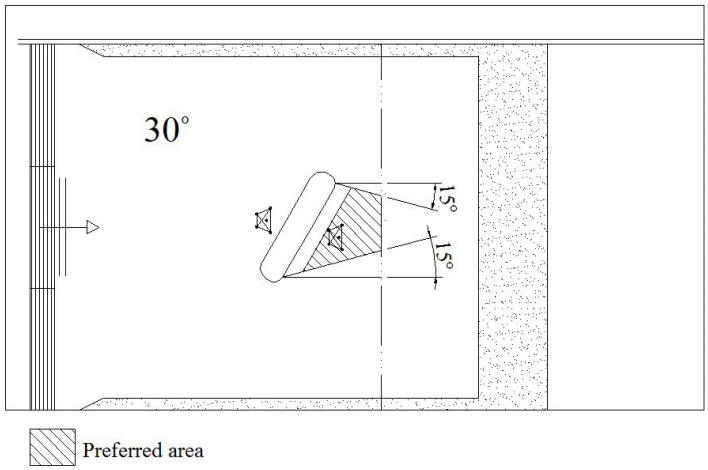

Figure 2.11: Location of the wave gauges: 30°

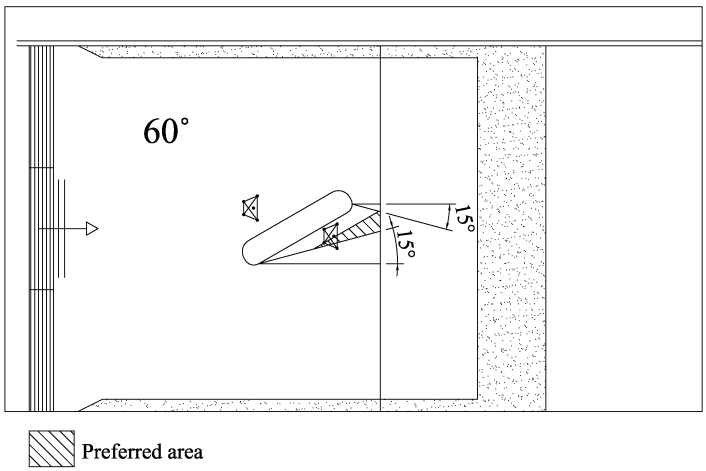

Figure 2.12: Location of the wave gauges: 60°

2.4.2 Visual aid

Many small floating wax spheres with a diameter or approximately $0.05m$ are randomly placed in the basin at least once per experimental set-up so that the surface water currents can be recorded on video from a birdseye view (figure 2.13b). This visual test acts as an aid to understanding the magnitude of the unwanted side effects in the area of the measuring instruments and the influence of the additional rubble mound. During this visual test, the wave gauges are not recording data.

(a) Overall view (b) Birdseye view

Figure 2.13: Visual aid

2.5 Data acquisition

The signals from the wave gauges are sent to the computer simultaneously. The 32-bit software package DasyLab 9.0 (Data Acquisition SYstem LABoratory) is used to record the signals with a sampling frequency of $100Hz$ and creates one ASCI file per test sequence of minimal $50min$. After an overview header, the file consists of columns, of which the first being the time. Thereafter, each wave gauge fills a column with its respective digitised measured voltage data (table 2.3). The order is specified beforehand by the user. All further processing of the data is done by Matlab version $R2007b$, which is a numerical programme based on a high level language for technical computing.

The data from the first ten minutes of testing are discarded, which is sufficient time for the wave climate to become fully developed in the wave basin. The transient behaviour should not be kept as a steady state is desired. Furthermore, the data records are zero-meaned because the average surface elevation should equal the water depth measured at the start of each test. As the data sampling frequency is noted, the time column is of no importance and is also discarded. This leaves a data matrix directly derived from the raw ASCI data files.

DASYLab - V 9.00.00					
WORKSHEET	:	Metingen v1			
Recording Date	:	2/12/2008, 2:56:01 PM			
Block Length	:	64			
Delta	:	0.01 sec			
Number of Channels	:	10			
Elapsed Time[s];	Write 0 [V];	Write 1 [V];	Write 2 [V];	Write 3 [V];	Write 4 [V];
0.00;	-0.004;	-0.010;	0.001;	0.007;	0.006;
0.01;	-0.004;	-0.008;	0.000;	0.008;	0.000;
0.02;	-0.005;	-0.008;	-0.001;	0.005;	0.004;
0.03;	-0.005;	-0.009;	0.003;	0.010;	0.000;

Table 2.3: An example of a data ASCI file, where only the data of the first five wave gauges are shown (Test02a0_1)

The frequency range of the incident wave climate is of the order of $0 - 3Hz$. This results in the frequency range of the transmitted wave climate in the lee of the breakwater to be of the order of $0 - 5Hz$ (table 1.1). According to Massel (1996), the absolute minimum sampling frequency required to properly describe the surface elevation is twice the maximum expected frequency. Therefore, the minimum sampling frequency is $10Hz$.

A sampling frequency of $100Hz$ causes a numerical overflow during further analysis because the amount of data is too high. In order to keep the data manageable, the sampling frequency needs to be as low as possible without allowing the risk of aliasing. It is decided to chose a sampling frequency of $20Hz$ instead of keeping the initial $100Hz$ or the minimum of $10Hz$. Choosing the right sampling frequency ensures that the effect of aliasing will not occur during the analysis of the data. However, in order to assure that the energy in the highest frequencies ($> 100Hz$) will not disturb the analysis by being interpreted as waves occurring at an extremely low frequency, the data need to pass through a low-pass filter. The data collected during the trial tests are analysed with and without the low-pass filter; showing no difference. Therefore, no low-pass filter is needed because the energy of the higher frequencies is negligible and will not affect the analysis.

To reduce the sampling frequency from $100Hz$ to $20Hz$, the average value of every five data points is taken. Hereby, it is implicitly assumed that the surface elevation changes linearly between two data points. This is fair for short time intervals. Another advantage of using the average value method is that the method allows for a supplementary smoothing by reducing the high frequency noise within the frequency range of $20 - 100Hz$. All the data are used to provide a more stable data set.

2.6 Experimental programme

The core of the breakwater, the angle of wave attack (by rotating the breakwater), the wave climate and whether or not an additional mound of rubble is placed alongside the physical model are all independent variables that have to be tested consequently, resulting in a minimum of 80 tests. An overview of these independent variables can be found in table 2.4.

Variable	Range	Number of tests per sequence
Core	a b c d	4
Breakwater layout	0° 15° 30° 45° 60°	5
Wave climate	Test02 Test03	2
Additional rubble mound	yes no	2

Table 2.4: Independent parameters varied during this study

There are a few aspects that need to be considered before commencing the experiments, such as when to change the variables, which are the most time consuming and which can be done single handedly? Changing the wave climate is a matter of changing the settings in the computer that sends the signal to the wave generator. This is the easiest and fastest of the variables to change; in a matter of several minutes, the next test is ready. Changing the core can be done alone (about $30min$ work) whereas changing the breakwater layout requires a lower water level, a crane and two additional pairs of hands. When placing the additional mound of rubble, the basin needs to be empty of water. Furthermore, it is faster to fill the basin with water in comparison to emptying the basin. One can count on having the basin filled in less than half an hour whereas emptying the basin takes at least two to three hours. This leads to a test hierarchy as the basis for the experimental programme (figure 2.14).

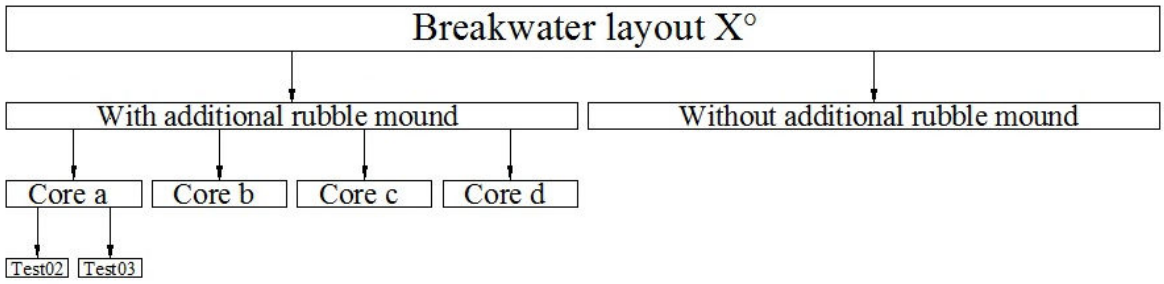

Figure 2.14: Experimental programme hierarchy

Each test will have a specific name, to which its ASCI data file will be named after. The general build up can be deducted from an example; 'Test02b45_3.' The 'Test' refers to the initial data file instead of a processed variant. The '02' applies to the wave climate (table 2.1). The 'b' refers to the core (figure 2.3b) whereas the '45' refers to the breakwater layout in degrees (figure 2.6). Finally, the '3' states that this data file comes from the third trial with the same test specifications. Not only does each test have a specific name, but the following is recorded in a logbook (appendix A) for every test:

- Date
- Test name
- Wave climate
- Breakwater core
- Breakwater layout
- Water depth
- Additional rubble mound used or not
- Notes

In total, there were 77 ASCI data files and ten visual aid films collected. The breakwater layouts of 45° and 60° were not tested without an additional rubble mound because of the large secondary effects. The first layout was run three times to prove the reproducibility of the experiments. Each test formation was only tested once because of the time constraints. Furthermore, two tests were conducted without the breakwater in the basin so that the two sets of measuring instruments could be compared with each other. Finally, one test was performed with still water to check the sensitivity of the wave gauges.

Chapter 3

Data processing

3.1 Spectral analysis software

The DIrectional WAve SPectra toolbox version 1.3 (DIWASP) is used for the spectral analysis of the data through calculation algorithms described by Hashimoto (1997) and Pawka (1983). This open source software package is developed by Johnson (2007) at the Centre for Water Research at the University of Western Australia, Perth and is currently distributed and maintained by MetOcean Solutions Ltd, New Zealand.
The build up of DIWASP is relatively simple; it is made up of a collection of Matlab functions, which calculate the directional wave spectra from field data. Standard wave recorder data types, such as the surface elevation, the pressure or the current velocity components, are supported. Therefore, the data of the two sets of five wave gauges used in this study can be processed by DIWASP. After specifying the required input parameters, the cross power spectra of the discrete time signals are initially calculated. Thereafter, according to the estimation method specified, the data can be translated into a three dimensional variance density spectrum. Herewith, supplementary Matlab functions can be written to calculate the significant wave height, the wave direction and the peak period from the calculated spectrum.

3.1.1 Input parameters for DIWASP

The input parameters are composed of three main data structures:

- The instrument data ID consists of all the available information regarding the measuring instruments.
- The spectral matrix SM is the variance density matrix that DIWASP will generate as output.

- The estimation parameters EP give the information necessary for the chosen calculation method to proceed.

The instrument data contain all the specifications needed concerning the measuring devices. The data matrix is directly taken from the processed ASCI data files and can be used as such; organized in sequential columns with one wave gauge per column. As the DIWASP package is capable of analysing data from many kinds of measuring devices, it is specified that the used sensors give surface elevations. The layout of the measuring instruments needs to be defined in a (x, y, z) coordinate system; the z axis being the vertical axis originating from the seabed. The x axis is chosen to be the direction of the theoretical incident wave; being from the wave generator towards the beach. The y axis follows from the definition of the right handed coordinate system. Furthermore, the water depth and the sampling frequency ($20Hz$) of the wave gauges need to be specified.

The spectral matrix is the final matrix that will contain the variance density spectrum of the wave climate per unit frequency and per unit of direction. The spectral matrix SM needs to be initially specified by two evenly spaced vectors; one of the frequencies and the other of the directions. The direction θ, specified in degrees or radians, is measured positive anticlockwise from the positive x axis. The frequencies can be specified in Hz or as angular frequencies in rad/s. There is also an option to define the direction in a nautical convention but no use will be made of this.

The most important aspect of the DIWASP package is defining the **estimation parameters**. The number of frequency bins and directional bins to be used during the calculation of the frequency spectra needs to be stated. This will determine the frequency and directional resolution. When choosing the number of bins, one needs to make a trade off between a high or coarse resolution. The more bins, the higher the resolution, but the lower the quality of the outcome within each bin. Choosing a resolution that is too high will result in a frequency spectrum with many sharp peaks. When a too low resolution is chosen, the variation of the spectrum with respect to the frequency will be lost and an unrealistic continuum will be observed (figure 3.1). Furthermore, the number of iterations and whether or not one wishes for a smoothing of the output need to be defined. Finally, the estimation method needs to be chosen that is most applicable to the current situation. There are five estimation methods available:

- DFTM: Direct Fourier Transform Method
- EMLM: Extended Maximum Likelihood Method

- IMLM: Iterated Maximum Likelihood Method
- EMEP: Extended Maximum Entropy Principle
- BDM: Bayesian Direct Method

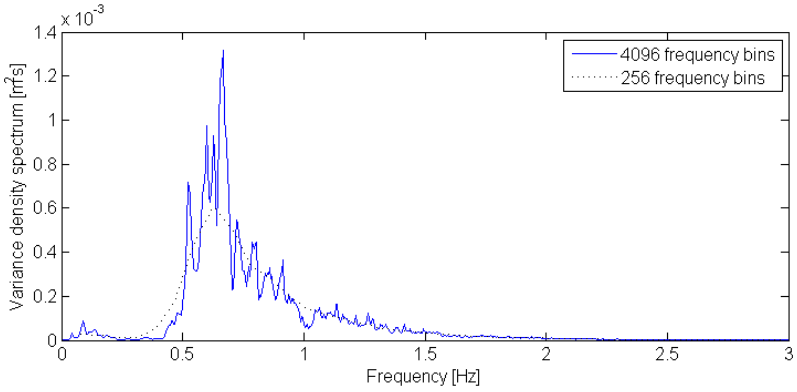

Figure 3.1: Frequency resolution: Comparing a variance density spectra with a high and a low frequency resolution

The basic difference between the various EP methods lies in the definition of the wave directional spreading function $G(\theta|f)$ (equation 2.4). However, an intricate analysis of the different methods lies outside the scope of this study so that the necessary knowledge is sought in previous studies. The data analysis of the transmission experiments conducted at the Aalborg University [DELOS (2002b)] did not use the programme DIWASP but another variant. However, Zanuttigh & Lamberti (2002) used the programme DIWASP when performing three dimensional hydrodynamic tests in a similar test set up (also at the Aalborg University). This allows for feedback on the different estimation methods.
The DFTM method is the fastest, most stable method, which produces a good initial overview of the spectral shape. However, it has poor directional resolution and sometimes gives negative energy distributions, which is not physically possible. The EMLM method works well with spatial arrays of measuring instruments but not for single point instruments. The IMLM method is a refinement of the EMLM method, which improves it iteratively. It can handle regular waves whereas the other methods do not converge in this situation. On the other hand, the accuracy is sensitive to the number of iterations and if the method goes wrong, it will be very obvious to the user. The EMEP method is best used for three quantity measurements and can account for errors in the raw data. Nevertheless, low spectral energies at the low and high frequencies can cause problems because the computation time will increase drastically. The most computationally intensive method is the BDM method, which is only fit for four or more quantity measurements.

3.1.2 Choice of the estimation parameters

Directional wave spectra software analyse data in the assumption that the waves are short crested wind waves with a high directional spread. Due to the available wave generator, the incident wave climate will mainly be long crested. The directional spread should in theory be infinitely narrow as the waves are only travelling in the x direction (0°). The DIWASP software is therefore not intended for such a specific situation. This calls for an initial short comparison of the different EP methods for a random test performed in this study. More importantly, the programme will be validated quantitatively by means of a synthetic signal thereafter.

Comparison of the EP methods for a random test sequence

The data of the first test will be used to find which EP method is the most suitable for the data analysis; Test02a0_1. Both surface plots and polar plots are generated (appendix C), along with a direct comparison of the frequency spectra (figure 3.2) and of the directional spreading (figure 3.3) for both the incident and transmitted wave climates.

The variation of the frequency spectrum with EP method is not great for the incident wave climate; the shape remains relatively similar regardless of the method used. The BDM method portrays the least amount of energy in the positive x direction whereas the EMEP method calculates the highest amount of energy. For the transmitted wave climate, the EMEP method no longer gives the highest amount of energy; the DFTM, EMLM and IMLM methods do. However, it is important to conclude that the shape is similar for all EP methods so that no final conclusion can be taken from comparing the frequency spectra.

The directional spreading shows great differences with respect to the chosen EP method. For both the incident and transmitted wave climate, the IMLM method shows the most narrow spread whereas the BDM gives an even spread for all directions. As long crested waves are generated, it seems that the IMLM method may be the most appropriate method for the analysis of the data. Furthermore, it is interesting to observe that the reflection of waves from the breakwater is being calculated by DIWASP for the EMLM and IMLM methods; only slightly for the DFTM method.

When observing the surface and polar plots, the same conclusions can be drawn regarding the directional spread. The BDM method does not cope with the long crested wave signals and spreads the energy out in all directions. Although the DFTM method shows a clear peak in the x direction, there is still a small amount of energy travelling in all directions. The EMEP method seems to work better but the EMLM and IMLM methods seem to work best.

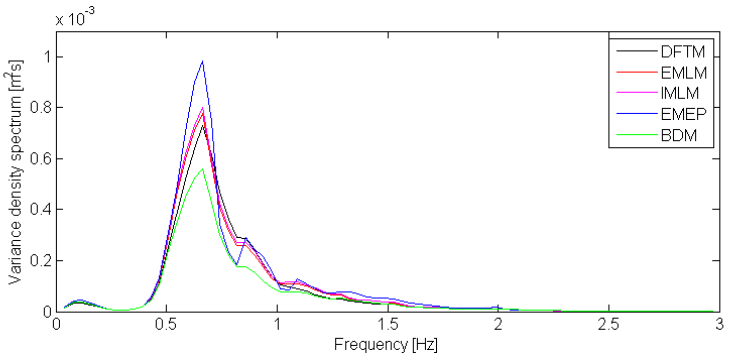

(a) Incident wave climate

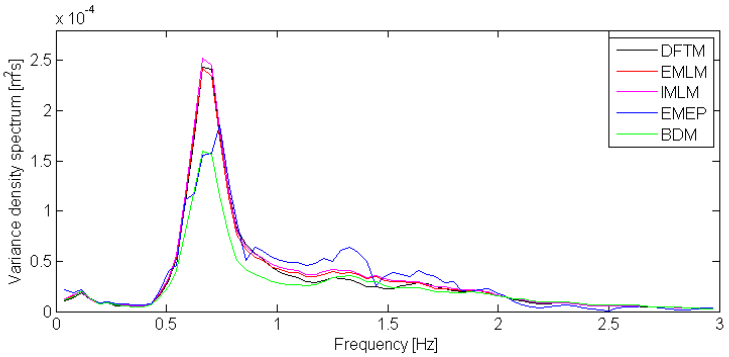

(b) Transmitted wave climate

Figure 3.2: Comparison of EP methods: Frequency spectrum (Test02a0_1)

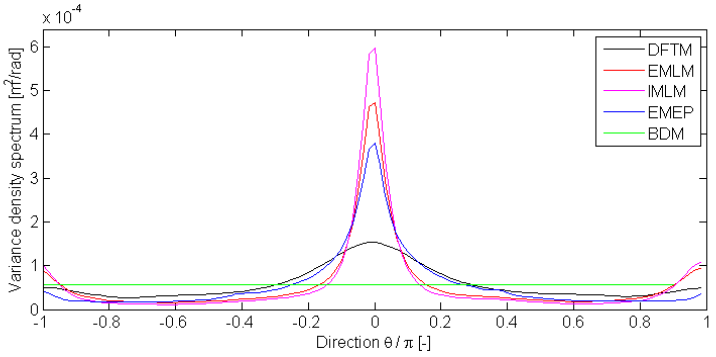

(a) Directional spread: Incident wave climate

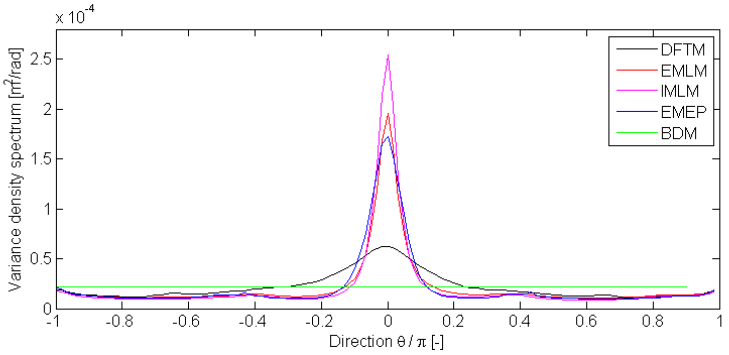

(b) Transmitted wave climate

Figure 3.3: Comparison of EP methods: Directional spread (Test02a0_1)

Comparison with a synthetic signal

Although the IMLM method may seem to be the most appropriate method for the analysis of the data, the method still needs to be proven accurate. The calculated output of DIWASP needs to be proven correct. This can be done by generating data of which the output is already known (a synthetic signal). A target wave climate is simulated (Test02) with a narrow directional spread ($s = 75$) (equation 2.7) in the spectral domain and converted to its respective time domain for the specific instrument layout at hand (figure 2.9). The data are then processed with DIWASP for the different EP methods, frequency resolutions, directional resolutions and number of iterations. The outcome can be compared with the theoretical outcome ($H_s = 0.07m$, $T_p = 1.5s$, $\beta = 0°$) and provide a measure of how accurate DIWASP really is.

When comparing the different EP specifications, several considerations need to be made. First of all, the aim of the study leads to analyzing the influence of the incident wave direction β_i on the transmitted wave direction β_t, the transmission coefficient K_t and the spectral changes of the transmitted spectrum. Therefore, three distinct variables need to be calculated precisely (β, H_s and $f_p = 1/T_p$). Second of all, the unidirectional frequency spectrum and the directional spread need to resemble the respective theoretical plots.

A comparison of the EP methods shows the same trend as with the comparison of the transmitted wave climate of Test02a0_1. The IMLM and EMLM method have the closest frequency spectra (figure 3.4a) as well as the most accurate directional spread (figure 3.4b). A qualitative comparison of the different EP methods (table 3.1) allows one to conclude that the choice of the EP method lies between the EMLM and the IMLM method.

EP method	Frequency spectrum	Directional spread	β	H_s	T_p
DFTM	+	−−	−	+	+
EMLM	++	++	+	++	+
IMLM	++	++	+	++	+
EMEP	−−	+	−	−−	−
BDM	−	−	+	−	+

Table 3.1: A qualitative comparison of the different EP methods

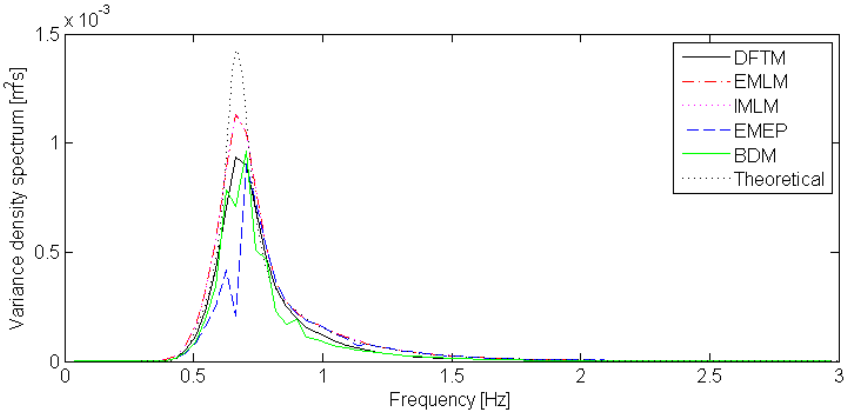

(a) Frequency spectrum

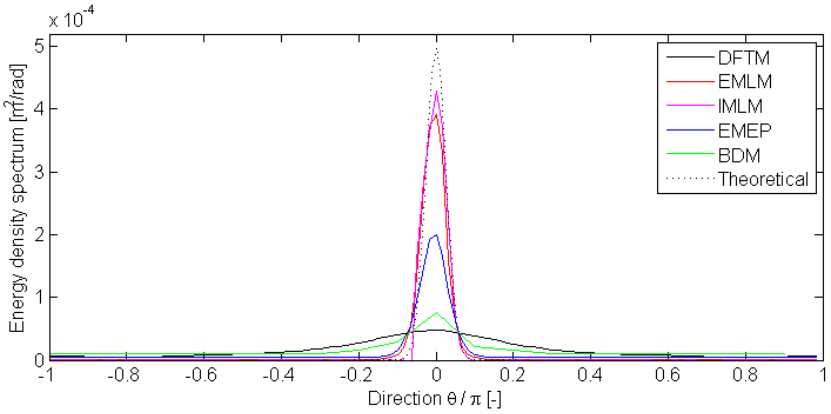

(b) Directional spread

Figure 3.4: Comparison of EP methods: Synthetic signal ($s = 75$)

The EMLM method estimates the directional spectrum $\hat{E}_0(\theta)$ from the study data. According to Pawka (1983), this estimate is a 'smeared' version of the true directional spectrum $E(\theta')$:

$$\hat{E}_0(\theta) = \int_{\theta'} W(\theta, \theta') \cdot E(\theta').d\theta' \tag{3.1}$$

, where the spectral window $W(\theta, \theta')$ is dependant on the cross configuration of the measuring devices. In theory, if an infinite number of measuring devices are placed in the basin, then the spectral window is represented by a Dirac δ function. This allows for the true directional spectrum to be calculated:

$$\begin{aligned} \hat{E}_0(\theta) &= \int_{\theta'} \delta(\theta - \theta') \cdot E(\theta').d\theta' \\ &= E(\theta) \end{aligned} \tag{3.2}$$

As there are only a limited number of measuring devices, the window function is wider and causes smearing. This can be seen as a sort of smoothing transformation. The IMLM method assumes that this smoothing transformation can also be applied to the estimate itself:

$$T_0(\theta) = \int_{\theta'} W(\theta, \theta') \cdot \hat{E}_0(\theta').d\theta' \tag{3.3}$$

The IMLM method modifies the estimated spectrum in an iterative manner until $T_i(\theta)$ is sufficiently close to the original estimate $\hat{E}_0(\theta)$ for all θ:

$$\begin{aligned} T_i(\theta) &= \int_{\theta'} W(\theta,\theta') \cdot \hat{E}_i(\theta').d\theta' \\ &\simeq \hat{E}_0(\theta) \\ \hat{E}_0(\theta) &= \int_{\theta'} W(\theta,\theta') \cdot E(\theta').d\theta' \\ \Rightarrow \hat{E}_i(\theta) &\simeq E(\theta) \end{aligned} \tag{3.4}$$

The closer $T_i(\theta)$ is equal to the original estimate $\hat{E}_0(\theta)$, the closer the improved estimate $\hat{E}_i(\theta)$ will equal the true directional spectrum $E(\theta)$. It should be noted that mathematically, equation 3.4 has an infinite number of solutions. There is no mathematical proof that the final estimate $\hat{E}_i(\theta)$ will equal the true directional spectrum $E(\theta)$. However, according to Pawka (1983), the method has been tested vigorously and shown to produce accurate results. Furthermore, if the calculated solution does not correspond with the true spectrum, then this will become very obvious to the user. Hence, one may assume that the IMLM method allows for a final estimated directional spectrum $\hat{E}_i(\theta)$ that estimates the true spectrum more precisely than the EMLM method. Therefore, the IMLM method is the chosen method, with which the remaining estimation parameters are investigated:

- The number of iterations does not have a visible effect on the frequency spectrum. However, the higher the number of iterations, the more the directional spreading function has the tendency to overshoot; being too high and too narrow. Five iterations compare the best.

- As explained earlier, the greater the number of frequency bins chosen, the higher the frequency resolution, but more sharp peaks will be observed in the spectral plot; 1024 frequency bins compare well to the theoretical spectrum.

- The effect on the directional spread is not significant. The greater the directional resolution, the better the directional plot compares to the theoretical one with respect to the peak energy value. However, the downside is that the greater the directional resolution, the greater the directional plot has the tendency to have a double peak in the main wave direction. Therefore, 180 or 120 directional bins compare best.

The intermediate conclusions regarding the different EP parameters still need to be verified with the respective values for the wave directions, the significant wave heights and the peak periods. After comparing the different possibilities, it is found that using the IMLM method with 5 iterations, 512 frequency bins and 120 directional bins will give the best results.

Herewith, the wave direction is 0°, the significant wave height $0.0702m$ and the peak period $1.5059s$. An overview of the EP parameter specifications can be found in table 3.2 as well as the respective results in table 3.3. The final frequency spectrum and directional spread (figure 3.5) also show a good resemblance to the theoretical result.

EP method	# of iterations	# of frequency bins	# of directional bins	Frequency resolution	Directional resolution
IMLM	5	512	120	$0.04Hz$	3°

Table 3.2: Choice of the estimation parameters

	H_s $[m]$	β [°]	T_p $[s]$
Theoretical	0.07	0	1.50
IMLM	0.0702	0	1.5059

Table 3.3: Results of the synthetic signal using the chosen estimation parameters

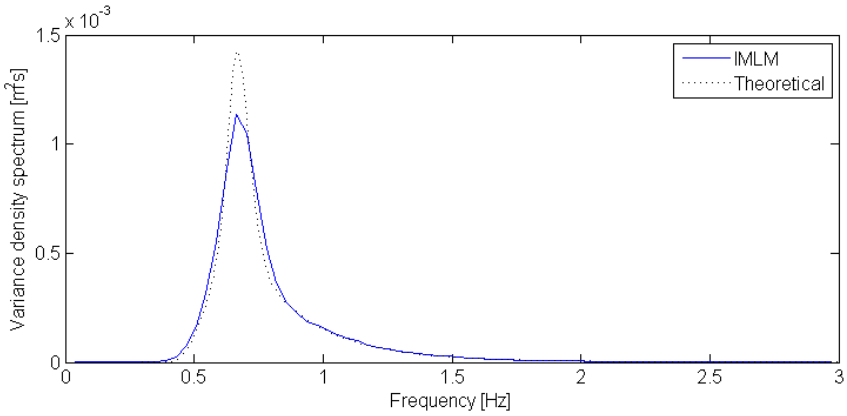

(a) Frequency spectrum

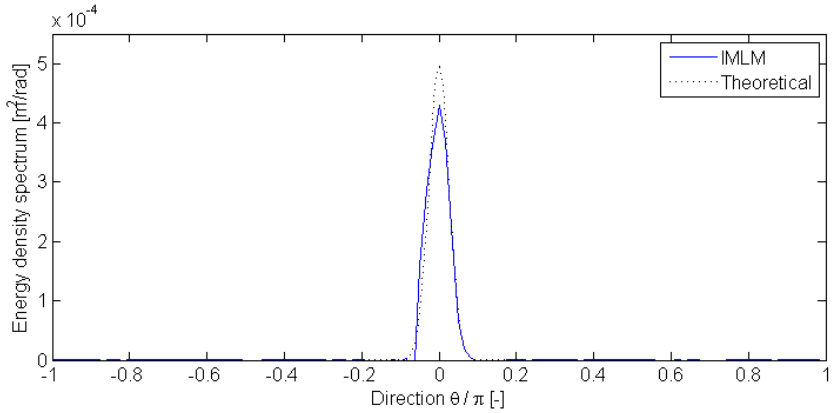

(b) Directional spread

Figure 3.5: Chosen EP method: IMLM

3.2 Sources of error

There are many sources of error during the testing procedure that could influence the results and decrease the reliability of the data. These have to be accounted for and validated before the analysis can commence. Otherwise, the results of any data analysis cannot be justified.

3.2.1 Sampling length

The length of the data sample needs to be long enough for two reasons. First, the incident wave climate should resemble that of the target wave climate (table 2.1). Therefore, each test needs to proceed long enough to be able to generate waves of all the frequencies of the desired spectrum. Second, any spectral calculation from data in the time domain needs a sufficient amount of data to perform properly. A general guideline is that a minimum of 1000 waves should be generated to acquire the full spectral range. With a wave period of $1.5s$, a minimum sampling length of $25min$ is needed. The minimum sampling length during the whole testing procedure of this experiment is $50min$; the maximum $90min$; on average $60min$. Keeping in mind that the first $10min$ are discarded from the data (section 2.5), a minimum of 1600 waves are tested during each test sequence; on average 2400 waves. This is undoubtedly sufficient.

3.2.2 Reproducibility of the experiments

Due to the time constraints, each test is performed only once. However, in order to check the reproducibility of the tests, the first layout is run three times (Test02a0_1, Test02a0_2 and Test02a0_3). The data are analysed by DIWASP and the results can be found in table 3.4. As the sampling length of the tests is sufficiently long, no great deviations are found in the results. The longer the sampling length, the more the results of the same test sequence will converge (figure 3.6).

	H_i $[m]$	H_t $[m]$	β_i $[°]$	β_t $[°]$	$T_{p,i}$ $[s]$	$T_{p,t}$ $[s]$
Test02a0_1	0.0663	0.0404	3	0	1.5059	1.5059
Test02a0_2	0.0667	0.0405	3	0	1.5059	1.5059
Test02a0_3	0.0657	0.0400	3	0	1.5059	1.5059
Average	0.0662	0.0403	3	0	1.5059	1.5059
Deviation [±]	0.0005	0.0003	0	0	0	0

Table 3.4: Reproducibility of the experiments

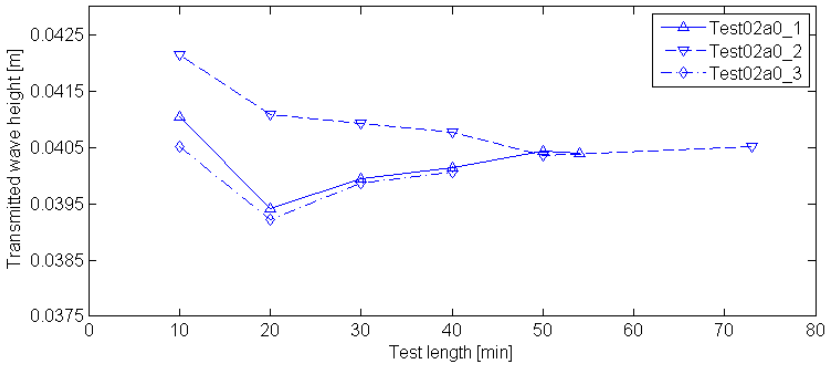

Figure 3.6: Reproducibility of the experiments

3.2.3 Wave gauge error

There are in total ten resistive wave gauges, which are calibrated frequently at different occasions during the testing programme. The differences found in the calibration factors are negligible ($\pm 2 \cdot 10^{-4} m/V$). This allows the average to be sufficient (appendix B). The instruments themselves have a standard error of $\pm 0.001V$, making the recordings sufficiently accurate. A still water measurement without the presence of the physical model was performed to confirm the accuracy. The fact that such a measurement without waves may still have errors (such as a coincidental water ripple) will be disregarded. When looking at two consecutive data recordings, the maximum change of the water surface level is $\pm 1 \cdot 10^{-4} m$. When looking at the data set as a whole, the absolute maximum change in water surface level is $\pm 2 \cdot 10^{-4} m$. This confirms that the individual measuring instruments are sufficiently accurate for this study.

3.2.4 Test sequence without the breakwater

There are two groups of five wave gauges, from which the data will be compared at later stages. Therefore, it is essential to compare the performance of these two groups relative to each other. Two tests are conducted without the breakwater in the basin; one for each target wave climate (table 2.1). The data are analysed by DIWASP and the results can be found in table 3.5. The group of wave gauges placed in the lee side of the breakwater give on average a significant wave height of 8% greater than that from the group of wave gauges measuring the incident wave climate ($H_t/H_i = 1.08$). This will have an immediate effect on the analysis of the transmission coefficient K_t of the data; K_t will be overestimated. The frequency spectra measured resembles that of the target wave climates reasonably well (figure 3.7). However, there is no absolute guarantee that the wave climate reaching the breakwater is exactly equal

to the target wave climate. Therefore, it cannot be deducted if H_t is overestimated or if H_i is underestimated. Only the relative difference is known.

	H_i $[m]$	H_t $[m]$	β_i $[°]$	β_t $[°]$	$T_{p,i}$ $[s]$	$T_{p,t}$ $[s]$
Test02nb0_1	0.0704	0.0759	0	0	1.5059	1.5059
Test03nb0_1	0.0908	0.0969	0	0	1.2800	1.2800

Table 3.5: Essential variables measured during the test without the breakwater

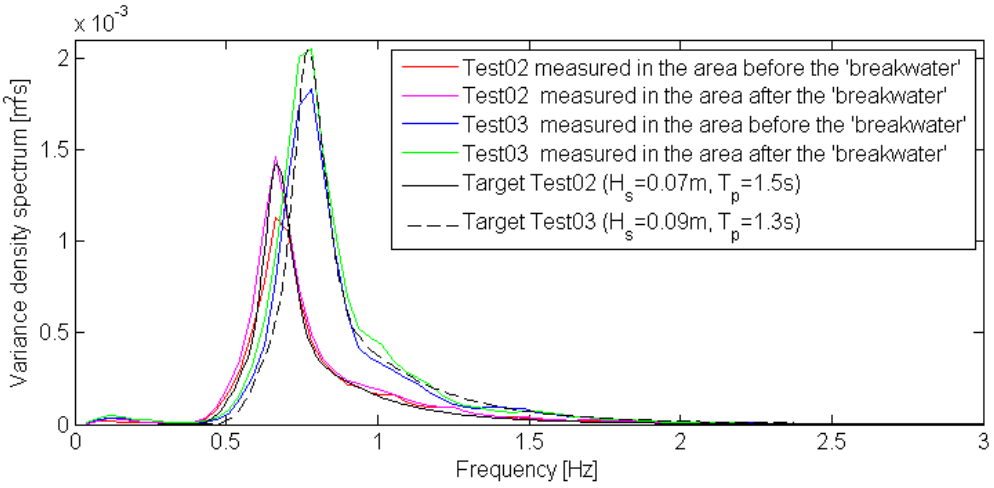

Figure 3.7: Comparison of the frequency spectra measured during the test without the breakwater with the target wave climates

In order to find the reason for this 8% difference, the variance density spectrum is calculated for each wave gauge individually and compared with one another. From this it is found that on average, the transmission coefficient is also overestimated by an average of 6%. This corresponds with 12% more energy in the area at the lee side of the breakwater. This shows that the beach does not fully remove the energy from the waves. As a result, a long standing wave develops in the wave basin and causes a slight energy difference between the two locations. The remaining 2% difference lies with the DIWASP software. The IMLM method is known for slightly overestimating the wave reflection, especially with wave climates with a very narrow directional spread. Therefore, the analysis of the incident wave climate will be slightly less accurate. In conclusion, the overestimation of K_t will not affect the final analysis of the data because this effect will be constant and present in all tests. However, the overestimated transmission coefficient should be reduced during the analysis.

3.2.5 Water depth

The DIWASP software needs the measured water depth to calculate the respective wave numbers. Therefore, the sensitivity of the software to an error in the water depth measurement needs to be checked. The data of the first layout as well as the data from the tests without a breakwater are analysed with deviating water depths ($\pm 0.01m$). DIWASP gives negligible deviation from the original results for the wave direction, the significant wave height and the peak period. As the water depth measurement has a relative error of $\pm 0.001m$, one can assume that DIWASP's sensitivity to the measured water depth is very low. The error in measuring the water depth manually will have no influence on the results of the data analysis.

3.2.6 Experimental layout

The incident and transmitted wave angles calculated in DIWASP are relative to the x direction; from the wave generator to the beach. When simulating oblique waves, the breakwater is rotated. The position of the two groups of wave gauges as a whole are assumed to be such that the x direction defined in the software corresponds to the x direction in the wave basin. This allows for the total incident wave angle to be equal to the incident wave angle calculated with DIWASP plus the layout angle of the breakwater. Analogous, the total transmitted wave angle is equal to the transmitted angle calculated with DIWASP plus the layout angle of the breakwater.

The largest errors will originate from the placing of the instruments and of the physical model in the wave basin. There will be an error due to the rotation of the physical model, the placing of the two groups of wave gauges as a whole and the error in the relative positioning of the wave gauges with respect to one another. The first two sources of error will have an effect on the final wave angles calculated. The third error will also have an effect on the significant wave height values because the relative position of the wave gauges is an important input parameter in DIWASP.

The breakwater is rotated with the help of a crane, one person managing the crane and two people positioning the breakwater. The breakwater is rotated so that the marked ends align with the marked basin floor. This allows for the ends of the breakwater to have a maximum relative error of $\pm 0.05m$; the angle of error being $\pm 1.2°$. The two groups of measuring instruments are also moved by hand. The outer edges of the frame are used as a reference point when measuring the necessary distances. This allows for an angle of error of $\pm 1°$. Therefore, a total angle of error of $\pm 2.2°$ can be accounted for due to the positioning of the breakwater and the instrument groups.

The individual wave gauges are fixed on a frame (figure 2.9) so that the relative position will not vary during the test procedure. The relative distances can be measured with care, allowing for a great maximum relative positioning error of $\pm 1.5cm$. This relative error will become noticable in DIWASP because the cross-correlation of the various signals is highly dependant on the relative positions of the wave gauges. Therefore it is crucial to investigate the sensitivity of the programme to such an error. It is investigated for the first group of measuring instruments. This will be done by comparing the output of DIWASP of the original and of the three alternative layouts (figure 3.8), where each 'moved' wave gauge moves $1.5cm$. The outcome can be found in table 3.6 for the tests Test02a0_1, Test02nb0_1 and Test03nb0_1. The peak period seems unaffected by a slight change in the instrument layout, whereas the wave angle gives a maximum deviation of $\pm 3°$. The significant wave heights change; resulting in an average deviation of ± 0.0005. The effect is greatest for a more skewed layout and least for a symmetrical change.

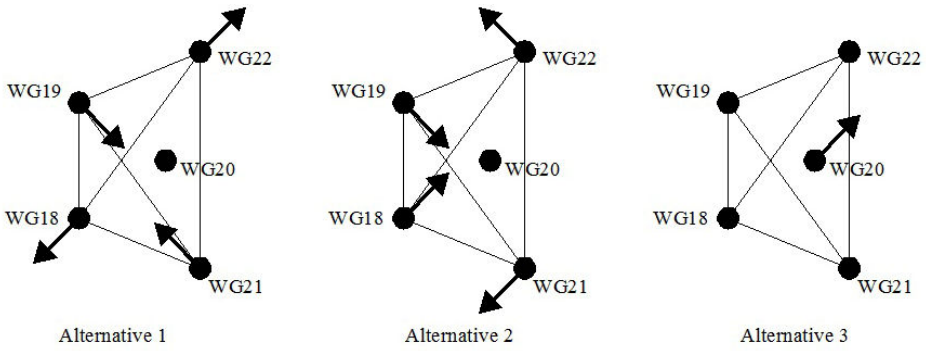

Figure 3.8: Sensitivity of DIWASP to alternative layouts, where the arrows indicate a displacement of $1.5cm$ with respect to the original configuration

	Test02a01			Test02nb1			Test03nb1		
	H_i $[m]$	β_i $[°]$	$T_{p,i}$ $[s]$	H_i $[m]$	β_i $[°]$	$T_{p,i}$ $[s]$	H_i $[m]$	β_i $[°]$	$T_{p,i}$ $[s]$
Original	0.0663	3	1.5059	0.0704	0	1.5059	0.0908	0	1.2800
Alternative 1	0.0665	0	1.5059	0.0697	-3	1.5059	0.0901	-3	1.2800
Alternative 2	0.0670	3	1.5059	0.0710	0	1.5059	0.0915	0	1.2800
Alternative 3	0.0671	3	1.5059	0.0713	0	1.5059	0.0917	0	1.2800

Table 3.6: Sensitivity of DIWASP to alternative layouts

3.2.7 Influence of the additional rubble mound

The additional mound of rubble is placed alongside the physical model for two reasons. First, an overall large scale circulation pattern is feared due to the physical constraints of the basin walls and the asymmetrical flow during the rotated positions of the breakwater. In order to measure the wave conditions in the lee of the breakwater solely due to the wave transmission, the wave gauges need to be placed in an area where diffraction is not dominant. As diffraction effects become more prominent in the lee of the breakwater under the more extreme positions, the additional rubble mound is placed with the intention to reduce these effects. The results of the data analysis can only be deemed reliable as long as these side effects do not significantly affect the area that this study is investigating and the measuring instruments in it.

Many small floating wax spheres are randomly placed in the basin so that the surface water currents can be visualised and recorded on video. This visual aid will help to explain qualitatively the effects of placing the additional mound of rubble. Without the additional rubble mound, one observes a relatively fast circulation around the breakwater in the oblique positions of the breakwater. This effect can already be seen at the smallest tested oblique angle (15°). At an oblique layout of 30°, there are also visible diffraction patterns to be seen entering the lee of the breakwater where the instruments are positioned. When the additional rubble mound is placed alongside the breakwater the circulation pattern can be observed to change. The wax spheres no longer travel in large circles but travel in much smaller circles, concentrated at one side of the breakwater at the outer edge (figure 3.9). The relative speed of the spheres is slower than those during the visual test without the additional rubble mound. It should also be noted that the direction of the current is constant because at the end of each test, a small pile of dirt is accumulated in the centre of the travelled circular path. The diffraction patterns at both ends of the breakwater are no longer very visible (figure 3.10). To sum up, it can be stated that the additional mound of rubble has a positive effect on decreasing the effect of diffraction and breaking the large circulation pattern around the breakwater. Nevertheless, it is dangerous to conclude that these side effects are completely negligible.

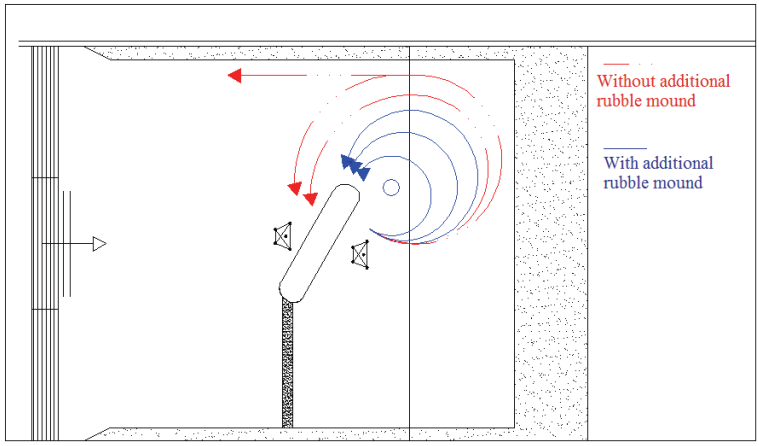

Figure 3.9: Circulation patterns observed in the wave basin

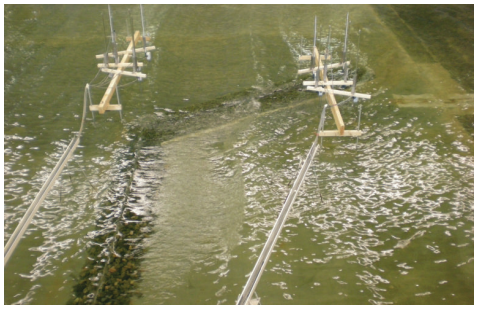

Figure 3.10: Reduced diffraction effects observed due to the additional rubble mound

Chapter 4

Results

The influence of oblique wave attack on the transmitted wave direction, on the transmission coefficient and on the spectral changes of the transmitted spectrum has been found to be different for rough permeable and smooth impermeable breakwaters [Van der Meer *et al.* (2003)]. The objective of this research is to gain insight into the reason for this behavioural difference by experimental means. By varying the permeability of the core and keeping the roughness of the structure constant in this study, these two parameters become uncoupled. Analysing the data of this study allows for the influence of the permeability of the core to be found. When the data of this study is compared with the data of DELOS (2002b) and the formulations of Van der Meer *et al.* (2003)(2005), the observed similarities and discrepancies will allow further insight into this matter.
After initially considering the transmission coefficient K_t with respect to the dimensionless factor R_c/H_i, the focus of the data analysis concerns the following three dependences:

- Change in wave direction: The transmitted wave direction β_t with respect to the incident wave direction β_i
- Transmission: The transmission coefficient K_t with respect to the incident wave direction β_i
- Spectral changes: The percentage of wave energy in the high frequency range ($f \geq 1.5f_p$) of the transmitted spectrum

Each dependency will be analysed in a systematic manner. First, the data will be analysed qualitatively as one set and compared with the data of DELOS (2002b) and the formulations of Van der Meer *et al.* (2003)(2005). Second, as several parameters were varied during the testing procedure (the permeability of the core, the wave climate and the additional rubble mound), the effects of these parameters will be analysed qualitatively. Third, linear

regressions will be performed to obtain a quantitative analysis. Finally, conclusions will be drawn from the found results regarding the influence of the permeability of the core and the roughness of the structure on the behaviour of the breakwater.

4.1 The transmission coefficient K_t with respect to the relative crest height R_c/H_i

The transmission coefficient K_t with respect to the dimensionless factor R_c/H_i is shown in figure 4.1a. The empirical relation of d'Angremond *et al.* (1996), along with the upper and lower limits [d'Angremond & van Roode F.C. (2001)], are also visualized. The relation is valid for rough permeable rubble mound breakwaters whereas the physical model tested in this study varies from rough permeable to rough impermeable rubble mounds. Intuition allows one to understand that the more permeable the breakwater, the more transmission will take place. Therefore, it is reasonable to predict that the transmission coefficient of this study will be equal or lower than the theoretical values. It can be observed that the data have higher K_t values than predicted by d'Angremond *et al.* (1996). However, in (section 3.2.4), it has been noted that the transmission coefficient would consistently be overestimated by 8%. When this constant factor is taken into account, one sees that the data fall into the expected limits (figure 4.1b).

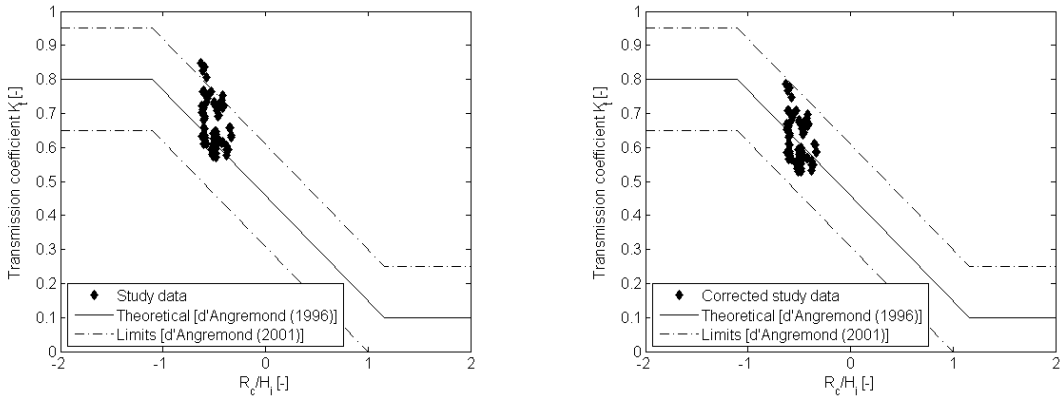

(a) Original study data

(b) Corrected study data

Figure 4.1: The transmission coefficient K_t with respect to the relative crest height R_c/H_i

4.2 Change in wave direction: The transmitted wave direction β_t with respect to the incident wave direction β_i

The transmitted wave direction is shown with respect to the incident wave direction (appendix D) (figure 4.2). Before analysing the figures, two aspects of DIWASP should be noted. The directional resolution of 3° can easily be observed. This causes the data to seem organized and the effect of the different influences hard to plot on one graph because the symbols will overlap and cover one another. However, as the directional error is of the same magnitude as that of the directional resolution, no improvement will be found by increasing the resolution. Furthermore, the spread of the data is greater for the incident wave direction than for the transmitted wave direction. This reinforces the fact that DIWASP performs better for short crested directional wave climates. The software gives a more stable analysis for the wave climate in the lee of the breakwater than for the incident wave climate.

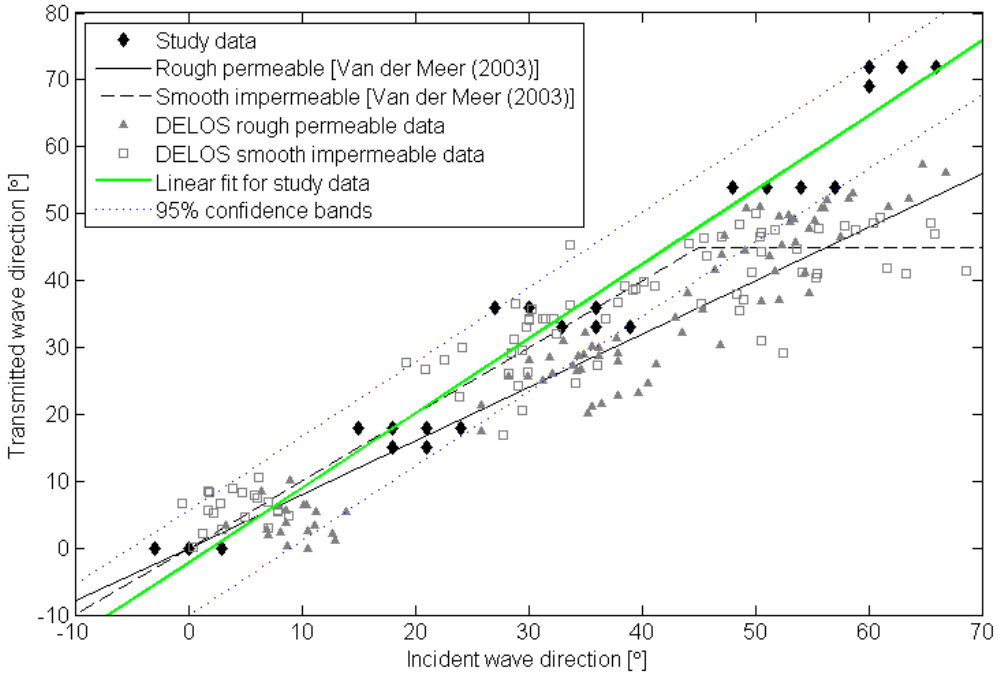

Figure 4.2: The transmitted wave direction β_t with respect to the incident wave direction β_i: Linear fit

Qualitative comparison with Van der Meer* et al. *(2003) and DELOS (2002b)

The data of DELOS (2002b) and the formulations of Van der Meer *et al.* (2003) for both the rough permeable and the smooth impermeable breakwater structures are included for comparison purposes (figure D.1) (figure 4.2). It can be seen that the general trend compares

reasonably well to both of the previous studies. The transmitted wave direction seems to be equal to the incident wave direction, which is similar to the previous findings for the smooth impermeable breakwater up to an incident wave direction of 45°. There is a constant linear relation between the incident and the transmitted wave directions within the range of 0° to 60°, which is analogous to the previous findings for the rough permeable breakwater. However, the gradient is different as the data of this study do not fully lie within the scatter of the data of DELOS (2002b).

Qualitative influence of the parameters varied

The data of this study represent rough rubble mound breakwaters ranging from a fully permeable to a fully impermeable core; allowing four different structures to be tested. When comparing the data of each structure separately, there seems to be no influence of the permeability of the core on the correlation between the incident and transmitted wave direction (figure D.2). One should note that the data representing the tests of the physical model with the fully permeable core should in theory lie completely within the scatter of the data of the rough permeable breakwater of DELOS (2002b). This is not observed.

Two wave climates were simulated with each test set-up (table 2.1). Test02 represents an incident wave climate with relatively longer waves and having a lower energy. Test03 represents an incident wave climate with shorter and steeper waves; having a higher energy. The data of this study are grouped according to the wave climate (figure D.3). However, no significant difference between the two wave climates is measured. The wave climate seems not to be important when considering the influence of the incident angle of wave attack on the transmitted wave angle.

Sorting the data with respect to tests with or without the additional rubble mound show no potential findings (figure D.4). Within the range of the incident wave directions where both set-ups were tested, there does seem to be a greater scatter for the tests performed without the additional rubble mound. However, this spread of data can only be observed when the data is sorted according to both the wave climate and the use of the additional rubble mound (figure D.5). It should be kept in mind that the extent to which this is observed is minimal.

Quantitative analysis: Linear regressions

One way to describe the influences of the different variables in a more concrete manner is to fit the data with a linear regression between the incident and transmitted wave direction. This is done for the data set as a whole and for selections of the data set; according to the

different variables that were altered during the experimental programme. The gradient varies around a mean of 1.1, which, within the scatter of the data, concludes that the data of this study can be fitted as one set. The linear fit can be described as equation 4.1, which is valid for incident wave angles in the range of $0° \leq \beta_i \leq 60°$ (figure 4.2).

$$\beta_t = m \cdot \beta_i + a \begin{cases} \text{Mean values:} & m = 1.11 \\ & a = -2.20 \\ \text{95\% Confidence bands:} & 1.07 \leq m \leq 1.16 \\ & -3.56 \leq a \leq -0.85 \end{cases} \tag{4.1}$$

The linear fit needs to be explained in more detail. First of all, the data is fit by means of the least squares method. The outcome produces a mean gradient m and a constant a. Next, the upper and lower limits for the linear relation is calculated so that if future studies were to be performed, then in 95% of the studies, the estimated parameters would lie between these limits. Finally, the 95% confidence bands are calculated for the data points. This means that if future studies were to be performed, then 95% of the data will lie within the bands. These bands can be seen in the respective figures (example figure 4.2).

It is known that for perpendicular wave attack ($\beta_i = 0°$), there is no change in the wave direction. Therefore, the value of the constant a is a measure for the systematic and statistical error of the tests. One can observe that the values of the constant have the same order of magnitude as the directional error found in section 3.2. For practical use, the constant should be discarded.

A statistical value of how well a regression line approximates the real data points is the R^2 statistic. The closer the value is to 1, the more the two parameters are correlated and the more the fit is a success. A perfect correlation is characterised as $R^2 = 1$ whereas a R^2 value of 0 suggests no correlation at all. The R^2 value here is 0.98, which represents a good fit. However, this may be due to the fact that few parameters were varied during this study. Therefore, the following sets of data are also fitted linearly (figure D.6) (figure D.7):

- Rough permeable data of DELOS (2002b) (84 data points)
- Smooth impermeable data of DELOS (2002b) (54 data points)
- All three data sets ($84 + 54 + 74 = 212$ data points)
- Study data and the rough permeable data of DELOS (2002b) ($84 + 74 = 158$ data points)
- Study data and the smooth impermeable data of DELOS (2002b) ($54 + 74 = 128$ data points)

As the smooth impermeable data of DELOS (2002b) shows a distinct change at $\beta_i = 45°$, only the data corresponding to incident wave angles lower than 45° will be used during the linear regression. The values of the gradient m and the constant a are summarized in table 4.1.

	DELOS rough perm. data	DELOS smooth imperm. data	All three data sets	Study data & DELOS rough	Study data & DELOS smooth
Mean values					
m	0.91	0.92	0.94	0.96	1.07
a	-3.84	2.64	-0.61	-2.39	-0.79
95% Confidence bands					
m_{lower}	0.85	0.84	0.89	0.91	1.03
m_{upper}	0.96	1.01	0.98	1.01	1.11
a_{lower}	-6.14	0.39	-2.05	-4.13	-2.02
a_{upper}	-1.54	4.89	0.83	-0.65	0.43
R^2 [-]	0.93	0.90	0.90	0.93	0.95

Table 4.1: The transmitted wave direction β_t with respect to the incident wave direction β_i: Linear regression

First of all, the linear fits for the individual data sets of DELOS (2002b) do not completely agree with the formulations of Van der Meer *et al.* (2003). The slope for the smooth impermeable data set corresponds more to the initial formulation made by DELOS (2002b) (equation 1.6) and not by Van der Meer *et al.* (2003) (equation 1.5). The reason for this discrepancy is not clear. It is possible that alternative linear regression algorithms were used or that no all data points were used during the analysis. The gradient found for the rough permeable data set (0.91) has a higher value, which makes it comparable to the gradient of the smooth impermeable data set (0.92). The study data does not lie within the 95% confidence bands of both DELOS (2002b) data sets. The greatest deviation lies at incident angles larger than 45°.

Second of all, it is interesting to observe how the data of this study would affect the linear fit of the DELOS (2002b) data sets. As expected, the data of this study increases the slope of the linear relations. However, by including the study data one finds that the quality of the fit improves slightly; the R^2 value increases and the constant a decreases. This is most noticeable with the fit for the study data with the smooth impermeable data of DELOS (2002b).

Finally, when considering all three data sets, the fit proves to be less accurate but the differ-

ence with the previous findings is not large. Therefore, it is fair to conclude that for rough structures there is no significant change in wave direction ($0° \leq \beta_i \leq 60°$). For smooth structures, the transmitted wave direction is approximately equal to the incident wave direction up to an incident wave direction of 45°. For incident wave directions larger than 45°, the transmitted wave direction stays at 45° (equation 4.2). From the findings of this study, it is the roughness of the breakwater that seems to determine how the transmitted wave direction is affected by oblique wave attack.

$$\begin{array}{lrcll} \text{Rough structures} & \beta_t & = & 0.94\beta_i \pm 0.05\beta_i & \text{for } \beta_i \leq 60° \\ & & & & \\ \text{Smooth structures} & \beta_t & = & 0.94\beta_i \pm 0.05\beta_i & \text{for } \beta_i \leq 45° \\ & \beta_t & = & 45° & \text{for } \beta_i > 45° \end{array} \tag{4.2}$$

4.3 Transmission: The transmission coefficient K_t with respect to the incident wave direction β_i

Qualitative comparison with DELOS (2002b)

The transmission coefficient is shown with respect to the incident wave direction (appendix E) (figure 4.3). When comparing the data of this study with the data of DELOS (2002b), only the relevant data originating from the submerged models ($R_c = -0.05$) will be used (figure E.1). When considering the data as one set, one observes a large scatter. The data seem to agree with the scatter of the rough permeable breakwater data of DELOS (2002b), although the values are slightly higher. Even though there seems to be no significant influence of the incident wave direction, one may point out that the transmission coefficient slightly increases with increasing angle of wave attack. Also, at incident wave angles of approximately 60°, the transmission coefficient decreases a bit. These findings contrast with the trend found for smooth impermeable breakwaters; where the transmission coefficient decreases with increasing incident angle of wave attack.

Qualitative influence of the parameters varied

When regarding the data of this study sorted by the permeability of the core, there is no apparent influence observed (figure E.2). However, intuition forces one to look for a trend proving that the more permeable the breakwater, the higher the transmission coefficient. Although this trend is not consistent with every incident angle of wave attack, the average values do support it (table 4.2). When considering the deviation of the data from the average

values, the trend is not important.

The data of this study is sorted and compared with respect to the wave climates simulated (figure E.3). Although the incident wave climate Test02 has about 40% less energy than the incident wave climate Test03, the former still results in relatively more transmission to the lee of the physical model (table 4.3). Furthermore, the data from Test02 show a greater increase in the transmission coefficient with an increasing incident angle of wave attack. Thus, the wave climate with the longer waves and the lower energy results in the higher transmission coefficients and the higher growth in transmission with increasing incident angle of wave attack. These influences are confirmed when the data is fit to a basic linear relation (figure E.4). The gradients are larger for the data originating from tests simulated with the Test02 wave climate. These findings support the fact that low crested structures are more effective at removing energy from relatively shorter waves.

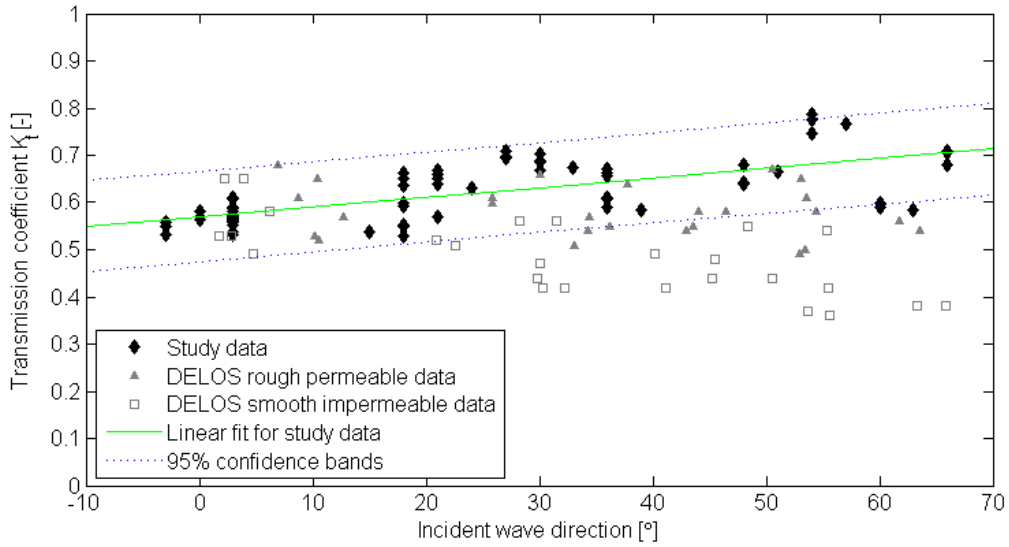

Figure 4.3: The transmission coefficient K_t with respect to the incident wave direction β_i: Linear fit

Sorting the data with respect to tests with or without the additional rubble mound show no systematic deviations (figure E.5). The scatter of the data is similar but the average transmission coefficient values are slightly higher for the data with the additional rubble mound (table 4.3). This may be due to the fact that the large scale circulation is reduced with the placing of the additional rubble mound. The wave can no longer fully travel alongside the breakwater but is forced to go over and through it. When fitting the data to a basic linear relation, one finds that for the tests performed without the additional rubble mound, the increase of the transmission coefficient with an increase in the incident wave direction is

slightly greater (figure E.6). However, one must realize that within the scatter of the data, these findings are disputable.

Data sorted by	Core a	Core b	Core c	Core d
Average K_t [-]	0.605	0.616	0.628	0.634
Deviation [±]	0.113	0.105	0.112	0.118

Table 4.2: Average values measured for the transmission coefficient K_t (part 1)

Data sorted by	Test02	Test03	With add. rubble mound	Without add. rubble mound
Average K_t [-]	0.649	0.590	0.648	0.588
Deviation [±]	0.112	0.075	0.114	0.084

Table 4.3: Average values measured for the transmission coefficient K_t (part 2)

Quantitative analysis: Linear regressions

For a more objective perspective on the influence of oblique wave attack on the transmission coefficient, a linear regression is made for the study data (figure 4.3). The gradient m is a measure of the influence of oblique wave attack on the transmission coefficient whereas the constant a is the transmission coefficient for perpendicular wave attack. The linear relation found (equation 4.3) shows that there is only a slight increase in transmission with increasing incident wave angles (figure 4.3). However the R^2 value is only 0.47, which means that there is a weak correlation between the incident wave direction and the transmission coefficient. The linear regression is not very satisfactory.

$$K_t = m \cdot \beta_i + a \begin{cases} \text{Mean values:} & m = 0.0020 \\ & a = 0.56 \\ \text{95\% Confidence bands:} & 0.0015 \leq m \leq 0.0026 \\ & 0.55 \leq a \leq 0.59 \end{cases} \tag{4.3}$$

When analysing the linear regression for the individual as well as for the grouped data sets, one finds that all combined fits are not satisfactory (figure E.7) (figure E.8) (table 4.4). They result in extremely low correlations (R^2). Only the smooth permeable data of DELOS (2002b) shows that there is an influence of the incident wave angle. The study data does not compare to the smooth impermeable data of DELOS (2002b). The 95% confidence bands for the linear relations are wide and allow for a large range of gradients. Furthermore, there is a discrepancy between the study data and the rough permeable data of DELOS (2002b)

for incident wave angles greater than 45°. Considering all three data sets as one results in a very crude model and is not recommended. In short, one may conclude that for smooth structures, the transmission coefficient decreases with increasing angle of wave attack as is formulated by Van der Meer *et al.* (2003). For rough structures, there is a slight discrepancy between the study data and the rough permeable data of DELOS (2002b). However, based on these two data sets, it is cautious to suggest that oblique wave attack has a negligible influence on the transmission coefficient.

	DELOS rough perm. data	DELOS smooth imperm. data	All three data sets	Study data & DELOS rough	Study data & DELOS smooth
Mean values					
m	-0.0007	-0.0028	0.0002	0.0012	0.0003
a	0.60	0.58	0.58	0.58	0.58
95% Confidence bands					
m_{lower}	-0.0019	-0.0040	-0.0005	0.0007	-0.0005
m_{upper}	0.0006	-0.0016	0.0009	0.0018	0.0012
a_{lower}	0.55	0.53	0.55	0.56	0.55
a_{upper}	0.65	0.62	0.60	0.60	0.60
R^2 [-]	0.04	0.50	0.00	0.06	0.01

Table 4.4: The transmission coefficient K_t with respect to the incident wave direction β_i: Linear regression

4.4 Spectral changes: The percentage of wave energy in the high frequency range ($f \geq 1.5f_p$) of the transmitted spectrum

Qualitative comparison with Van der Meer* et al. *(2005) and DELOS (2002b)

The percentage of energy in the range of high frequencies ($f \geq 1.5f_p$) is shown with respect to the incident wave direction (appendix F) (figure 4.4). The data of DELOS (2002b) is also included for comparison. The relatively narrow scatter of the data of this study lies within the rough permeable data of DELOS (2002b). The average percentage of energy in the range of high frequencies is calculated to be 33%, which corresponds well with the 34% value found by Van der Meer *et al.* (2005). The study data does not compare to the smooth impermeable data of the previous studies, which have higher values.

Qualitative influence of the parameters varied

Similar to the previous analyses, the influence of the permeability of the core, the wave climate and the additional rubble mound were investigated. Again, similar conclusions could be made. There is no significant influence of the permeability of the breakwater core. The fully permeable rough structure behaves no different than the fully impermeable rough structure. There is a slight influence of the wave climate. The percentage wave energy at the range of high frequencies is lower for Test02. This means that the spectral changes are less for a wave climate with relatively longer waves (Test02). This reinforces the fact that low crested breakwaters are more effective in removing energy from wave climates with relatively shorter waves. The additional rubble mound has no influence on the spectral changes.

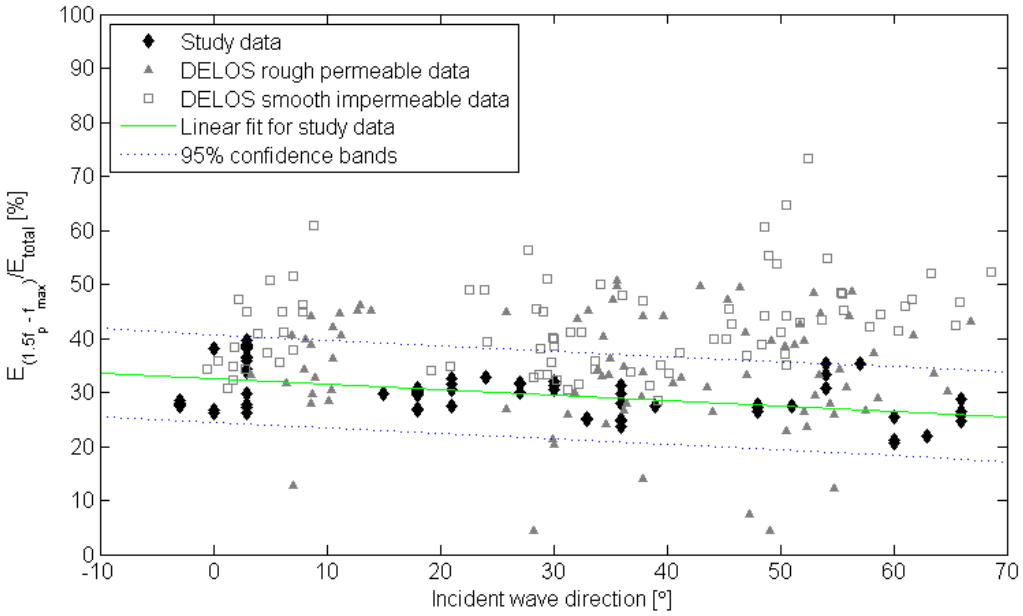

Figure 4.4: Percentage wave energy at the range of high frequencies ($1.5f_p \rightarrow f_{max}$): Linear fit

Quantitative analysis: Linear regressions

As done with the previous analyses, an extensive series of linear regressions is performed. However, as it has already been established that the data of this study do not agree with the smooth impermeable data of DELOS (2002b), the regression analysis will only be performed on the study data, the rough permeable data of DELOS (2002b) and the combined data set (figure F.5) (table 4.5). Again, the linear fit has the form of '$E_{(1.5f_p \rightarrow f_{max})}/E_{total} = m \cdot \beta_i + a$,' where the gradient m is a measure of the influence of oblique attack on the percentage of energy at the range of high frequencies and the constant a is the respective

value for perpendicular wave attack. The study data shows a slight decrease in the considered percentage of energy with increasing wave direction. However, this is only minimal. The gradient m of the rough permeable data of DELOS (2002b) as well as the combined data set both confirm that the spectral change is not dependent on the incident wave direction. This is further supported by the very low R^2 value.

	Study data	DELOS rough perm. data	Study data & DELOS rough
Mean values			
m	-0.10	0.00	-0.02
a	33	34	33
95% Confidence bands			
m_{lower}	-0.14	-0.13	-0.08
m_{upper}	-0.06	0.13	0.05
a_{lower}	31	29	31
a_{upper}	34	40	35
R^2 [-]	0.23	0.00	0.00

Table 4.5: Percentage wave energy at the range of high frequencies ($1.5f_p \rightarrow f_{max}$): Linear fit

4.5 A discussion on the discrepancies between this experiment and that of DELOS (2002b)

When analysing the change in wave direction (section 4.2) and the transmission coefficient (section 4.3), there is a discrepancy between the study data and the rough permeable data of DELOS (2002b). The data of the fully permeable rough structure of this study does not lie within the scatter of the data of the fully permeable rough structure of DELOS (2002b). This is peculiar because the experimental set-up of DELOS (2002b) was followed very closely. Only a few differences can be found.

The waves at the Aalborg University were short crested whereas the waves at the Technical University of Delft were long crested. However, previous studies have shown that there is no significant difference between long crested and short crested waves [Van der Meer *et al.* (2003)]. Specifically for rubble mound structures, short crested waves produce slightly lower values ($1 - 2\%$) for the transmission coefficient. The extent to which this could affect the analysis is minimal.

A second difference with the set-up at the Aalborg University is that the armour layer of the breakwater during this study was fixed. The stones were set in place with Elastocoast. However, the stones were of the same size and narrow grading. Furthermore, the breakwater fulfilled the structural stability requirements so that the fixation of the armour layer should not have affected the transmission.

Another difference lies with the wave basin. The dimensions of the wave basin used during this study are significantly larger. Furthermore, the beach had a gentler slope. Therefore, one may reason that the measuring instruments are less affected by the reflections from the beach and sidewalls. The experimental data should be less affected by the physical constraints of the wave basin. Also, even though the wave generators are not equipped with an active reflection compensator, the re-reflections from the wave board did not cause any problems. It is not clear if the wave generator used by DELOS (2002b) had an active reflection compensator. In short, one could assume that the experimental set-up used for this study produces more stable results than the set-up at the Aalborg University. However, even though the wave basin at the Aalborg University was smaller and did have a steep beach, the wave damping mechanism of the sidewalls was different. The sidewalls were made of crates filled with sea stones with a D_{n50} slightly larger than the armour layer stones. Behind these crates was an empty area. This mechanism is more effective than without having the empty area behind the stones. Considering the difference in the dimensions of the basins, the more effective wave damping sidewall mechanism should not have affected the result of this study very much. On the contrary, the limited dimensions of the set-up of DELOS (2002b) could be a source for the discrepancy between the results of the two studies.

A final difference lies in the length of the physical model. The length of the breakwater is $5m$ for this study. As the width of the wave basin used by DELOS (2002b) was smaller, a breakwater was built over the full width of the basin. This has as consequence that there would be no large scale circulation patterns around the model. Also, the return flow of the water is forced to go over or through the breakwater, which could lead to smaller values measured for the transmission. On the other hand, the finite breakwater will always be partially affected by diffraction, which could increase the measured transmission. In conclusion, the main source for the discrepancy between the two data sets most likely lies with the length of the physical model. As a result, both data sets can still be deemed reliable. Caution should be taken when choosing which results to use; those from the individual or combined data sets. The 95% confidence bands allow for a supplementary safety measure.

Chapter 5

Conclusions

5.1 Conclusions

The importance of oblique wave attack has led to the empirical formulations of Van der Meer *et al.* (2003)(2005), where the behaviour of rough permeable rubble mound structures was found to be significantly different from that of smooth impermeable low crested structures. This behavioural difference, in turn, has led to the research objective of this present study which is to investigate oblique wave transmission through rough impermeable rubble mound submerged breakwaters by means of a 3D physical model.

The framework of the experimental programme of this study allowed four structures to be investigated, ranging from a fully permeable to a fully impermeable rough rubble mound submerged breakwater. The incident angle of wave attack was varied so that its influence on the transmitted wave direction, the transmission coefficient and the transmitted spectrum could be investigated. After validating the acquired data and the spectral analysis software, several conclusions could be formed. The experimental set-up of the DELOS (2002b) was closely followed for this study so that a proper comparison could be made between the results of this study with those formulated by Van der Meer *et al.* (2003)(2005).

After a short general conclusion, more detailed conclusions are formulated concerning the influence of oblique wave attack on the transmitted wave direction, on the transmission coefficient and on the spectral changes of the transmitted spectrum.

General conclusion

This study intentionally uncoupled two parameters, being the permeability of the core and the roughness of the breakwater. Analysing the data of this study shows that the permeability of the core has no influence on the structure's behaviour with respect to the influence of

oblique wave attack. The fully permeable rough rubble mound behaves analogous to the fully impermeable rough rubble mound. Thereafter, when comparing the study data with the data of DELOS (2002b) and the formulations of Van der Meer *et al.* (2003)(2005), many similarities and discrepancies are observed. The data of this study compare best with the data of DELOS (2002b) and the formulations of Van der Meer *et al.* (2003)(2005) for the rough permeable structure. There is little comparison with the smooth impermeable structure. These findings allow one to suggest that the behavioural difference found by Van der Meer *et al.* (2003)(2005) may have its roots in the roughness of the structure instead of the permeability of the core. Therefore, it can be concluded that it is the roughness of the structure rather than the permeability of the core that determines the behaviour of the breakwater with respect to the incident wave direction.

Change in wave direction: the transmitted wave direction β_t with respect to the incident wave direction β_i

Based solely on the data of this study:

- The incident wave direction remains unchanged or increases by a slight 10% after encountering the low crested structure.
- The permeability of the core shows no significant influence on the change in wave direction with oblique wave attack. The permeable rough rubble mound structure shows the same trend as the impermeable rough rubble mound structure. Therefore, the permeability of the core results in no behavioural differences.
- The wave climate has no effect on the correlation between the incident wave direction and the transmitted wave direction. Relatively longer or shorter waves result in the same change in the wave direction.
- The additional rubble mound does not influence the change in wave direction.

These findings differ from those of Van der Meer *et al.* (2003), where its rough permeable rubble mound structure shows a reduction of the incident angle of wave attack. Although its smooth impermeable structure also shows no significant change in wave direction, this is only observed up to an incident wave angle of 45°. At higher incident angles of wave attack, the transmitted wave direction remains at 45°, which contrasts with the findings of this study. Most important, the data of this study originating from the fully permeable rough rubble mound breakwater do not lie within the scatter of the data originating from the previous study for the analogous permeable rough structure.

The data of this study originates from an experimental programme in which few parameters were varied. Moreover, of the few parameters varied, the range of variation was very limited. Therefore, linear regressions were performed for the data of this study, the rough permeable data of DELOS (2002b), the smooth impermeable data of DELOS (2002b) and combinations of the three. This allowed the data to be analysed and compared with that of DELOS (2002b) in an objective manner. In conclusion, it is recommended to use the following formulations with the respective 95% confidence bands of the gradients:

$$\begin{array}{lllll} \text{Rough structures} & \beta_t & = & 0.94\beta_i \pm 0.05\beta_i & \text{for } \beta_i \leq 60^\circ \\ & & & & \\ \text{Smooth structures} & \beta_t & = & 0.94\beta_i \pm 0.05\beta_i & \text{for } \beta_i \leq 45^\circ \\ & \beta_t & = & 45^\circ & \text{for } \beta_i > 45^\circ \end{array} \tag{5.1}$$

It is the roughness of the low crested structure that determines the influence of the incident wave direction on the transmitted wave direction. The behaviour is not influenced by the permeability of the core of the breakwater.

Transmission: The transmission coefficient K_t with respect to the incident wave direction β_i

Based on the data of this study:

- The transmission coefficient remains unchanged or increases slightly with increasing incident angle of wave attack.
- Within the range of the scatter, the permeability of the core has a negligible influence on the transmission coefficient.
- The incident wave climate with the relatively longer waves and lower spectral energy results in relatively higher transmission coefficients. Furthermore, the incident angle of wave attack has a greater influence on the incident wave climate with the shorter waves; the transmission coefficient increases faster with increasing incident wave direction.
- The additional rubble mound leads to overall higher transmission coefficients. It has no significant influence on the rate at which the transmission coefficient increases with increasing angle of wave attack.

These finding differ from the trend found for smooth impermeable breakwaters [Van der Meer *et al.* (2003)], where the transmission coefficient decreases with increasing angle of

wave attack. On the other hand, the data of this study do lie in the scatter of the data originating from the rough permeable rubble mound of the previous study.
After performing linear regressions on the individual data sets as well as the combined sets, it became clear that it is the roughness of the structure that determines the influence of the incident wave direction on the transmission coefficient. Smooth structures are highly influenced by oblique wave attack; the transmission coefficient decreases with increasing angle of wave attack. The transmission coefficient of rough structures, on the other hand, is not dependent on the incident wave direction. Therefore it is recommended to keep using the empirical formulations for the transmission coefficient K_t of Van der Meer *et al.* (2005).

Spectral changes: The percentage of wave energy in the high frequency range ($f \geq 1.5 f_p$) of the transmitted spectrum

The data of this study give the following results:

- The incident wave direction has no significant influence on the percentage of wave energy in the high frequency range of the transmitted spectrum.
- The average percentage of wave energy in the high frequency range of the transmitted spectrum is found to be 33% ($31 - 35\%$).
- The permeability of the core led to no behavioural differences with respect to the percentage of wave energy in the high frequency range of the transmitted spectrum.
- The longer the waves, the less changes are seen in the shape of the transmitted spectrum. This results in slightly lower percentages of wave energy in the high frequency range.
- The additional mound of rubble has no influence on the spectral changes.

These findings compare well to the observations made by Van der Meer *et al.* (2005) for rough permeable rubble mound structures. This further supports that the roughness of the structure is the reason for the behavioural differences found by Van der Meer *et al.* (2005) between smooth impermeable and rough permeable structures.

5.2 Recommendations and future perspectives

The results of this study give a first insight to the reason for the behavioural difference between smooth impermeable and rough permeable low crested structures. However, the findings of both studies are based on relatively small quantities of tests. Furthermore, few

parameters were varied during this study. The discrepancies between this study and the previous one finally lead to several recommendations.

First of all, a better understanding of the directional spectra software DIWASP is essential to gain more freedom during the data processing. The more experience one collects with this software, the more it can be adapted to fit the needs of the specific study. It will allow greater ease and efficiency when analysing the data. Furthermore, research should be put into altering the software so that it becomes more stable and suitable for wave climates with unidirectional long crested waves.

Second of all, it is recommended to obtain more test data by increasing the number of measurements performed. The more an experiment is repeated, the better the spread of the data can be investigated and deemed reliable. Also, when an experiment is rerun several times, possible errors have a higher chance of detection. One may reason that this is not necessary considering that the reproducibility of the tests has been validated in section 3.2.2. However, the scatter of the data was largest for the breakwater orientations of 45° and 60°. Therefore it might be worthwhile to investigate the reproducibility of the experiments under oblique wave angles or to perform numerous experiments so that a reliable selection of data can be acquired.

Third of all, it has been argued that the main source for the discrepancy between the two data sets lies with the length of the physical model. The breakwater of this study was $5m$ whereas the breakwaters used by DELOS (2002b) extended to the basin sidewalls. However, this reasoned suspicion should be investigated to more depth in order to further validate the results.

Another discrepancy between the two data sets lies with the type of waves used. Long crested waves were used in this study whereas short crested waves were used by DELOS (2002b). Even though this discrepancy has been argued to have a minor effect on the results, further confirmation would be cautionary.

The influence of numerous parameters has been identified for perpendicular wave attack. However, is it safe to assume that these parameters will have the same influence under oblique wave attack? More specifically, research on which parameters have an effect on the influence of oblique wave attack is needed. For example, this study seems to indicate that for incident wave climates with relatively shorter waves, the influence of oblique wave attack on the transmission coefficient is heightened. In short, the influence of oblique wave attack may change for different structures due to these secondary effects. Therefore, only when the effect of the different parameters on the influence of oblique wave attack is investigated, can a

better understanding of the overall influence of oblique wave attack on the transmitted wave direction and the transmission coefficient be achieved.

On the one hand, it is essential to acquire insight into the influence of oblique wave attack on the transmitted wave direction and the transmission coefficient. But one should keep in mind that these two effects are only a start to the many other crucial parameters being affected. For example, does the directional spread or the spectral shape change after the breakwater and if so, how does it change with increasing angles of wave attack? Only when the extent to which oblique wave attack affects its surroundings is understood, can the knowledge be used for numerical models and for real design guidelines. As long as these are not available, extensive model research is recommended.

Appendix A

Logbook

Date	Test name [.ASC]	Wave climate [-]	BW core [-]	BW layout [°]	Water depth	Additional rubble mound?
12 Feb 08	film 1	3	a	0	0.302	
12 Feb 08	Test02a0_1	2	a	0	0.302	
12 Feb 08	Test02a0_2	2	a	0	0.302	
13 Feb 08	Test02a0_3	2	a	0	0.301	
13 Feb 08	Test03a0_2	3	a	0	0.301	
13 Feb 08	Test02b0_1	2	b	0	0.301	
13 Feb 08	Test03b0_1	3	b	0	0.301	
13 Feb 08	Test02c0_1	2	c	0	0.301	
13 Feb 08	Test03c0_1	3	c	0	0.301	
14 Feb 08	Test02d0_1	2	d	0	0.300	
14 Feb 08	Test03d0_1	3	d	0	0.300	
14 Feb 08	Test02d30_1	2	d	30	0.300	
14 Feb 08	Test03d30_1	3	d	30	0.300	
14 Feb 08	film 2	3	c	30	0.300	
14 Feb 08	Test02c30_1	2	c	30	0.300	
14 Feb 08	Test03c30_1	3	c	30	0.300	
15 Feb 08	Test02b30_1	2	b	30	0.299	
15 Feb 08	Test03b30_1	3	b	30	0.299	
15 Feb 08	Test02a30_1	2	a	30	0.299	

(Continued on next page)

Date	Test name [.ASC]	Wave climate [-]	BW core [-]	BW layout [°]	Water depth	Additional rubble mound?
15 Feb 08	Test03a30_1	3	a	30	0.299	
18 Feb 08	Test02a30_2	2	a	30	0.312	yes
18 Feb 08	Test03a30_2	3	a	30	0.312	yes
18 Feb 08	film 3	3	a	30	0.312	yes
18 Feb 08	Test02b30_2	2	b	30	0.310	yes
18 Feb 08	Test03b30_2	3	b	30	0.310	yes
18 Feb 08	Test02c30_2	2	c	30	0.310	yes
18 Feb 08	Test03c30_2	3	c	30	0.310	yes
19 Feb 08	Test02d30_2	2	d	30	0.308	yes
19 Feb 08	Test03d30_2	3	d	30	0.308	yes
20 Feb 08	Test02d60_1	2	d	60	0.314	yes
20 Feb 08	Test03d60_1	3	d	60	0.314	yes
20 Feb 08	Test02c60_1	2	c	60	0.314	yes
20 Feb 08	Test03c60_1	3	c	60	0.314	yes
20 Feb 08	Test02b60_1	2	b	60	0.313	yes
20 Feb 08	Test03b60_1	3	b	60	0.313	yes
21 Feb 08	Test02a60_1	2	a	60	0.312	yes
21 Feb 08	Test03a60_1	3	a	60	0.313	yes
21 Feb 08	film 4	3	a	60	0.312	yes
21 Feb 08	Test02a45_1	2	a	45	0.311	yes
21 Feb 08	Test03a45_1	3	a	45	0.311	yes
22 Feb 08	Test02b45_1	2	b	45	0.310	yes
22 Feb 08	film 5	3	b	45	0.310	yes
22 Feb 08	Test03b45_1	3	b	45	0.310	yes
22 Feb 08	Test02c45_1	2	c	45	0.310	yes
22 Feb 08	Test03c45_1	3	c	45	0.310	yes
25 Feb 08	Test02d45_1	2	d	45	0.314	yes
25 Feb 08	Test03d45_1	3	d	45	0.314	yes
25 Feb 08	Test02d15_1	2	d	15	0.314	
25 Feb 08	Test03d15_1	3	d	15	0.314	

(Continued on next page)

Date	Test name [.ASC]	Wave climate [-]	BW core [-]	BW layout [°]	Water depth	Additional rubble mound?
25 Feb 08	Test02c15_1	2	c	15	0.314	
26 Feb 08	Test03c15_1	3	c	15	0.313	
26 Feb 08	film 6	3	c	15	0.313	
26 Feb 08	Test02b15_1	2	b	15	0.313	
26 Feb 08	Test03b15_1	3	b	15	0.313	
26 Feb 08	Test02a15_1	2	a	15	0.313	
26 Feb 08	Test03a15_1	3	a	15	0.313	
27 Feb 08	Test02a15_2	2	a	15	0.312	yes
27 Feb 08	Test03a15_2	3	a	15	0.310	yes
28 Feb 08	Test02b15_2	2	b	15	0.314	yes
28 Feb 08	Test03b15_2	3	b	15	0.314	yes
28 Feb 08	film 7	3	b	15	0.314	yes
28 Feb 08	Test02c15_2	2	c	15	0.313	yes
28 Feb 08	Test03c15_2	3	c	15	0.313	yes
28 Feb 08	Test02d15_2	2	d	15	0.314	yes
28 Feb 08	Test03d15_2	3	d	15	0.314	yes
29 Feb 08	film 8	3	d	0	0.317	yes
29 Feb 08	Test02d0_2	2	d	0	0.314	yes
29 Feb 08	Test03d0_2	3	d	0	0.314	yes
29 Feb 08	Test02c0_2	2	c	0	0.314	yes
29 Feb 08	Test03c0_2	3	c	0	0.314	yes
03 Mar 08	Test02b0_2	2	b	0	0.314	yes
03 Mar 08	Test03b0_2	3	b	0	0.314	yes
03 Mar 08	Test02a0_4	2	a	0	0.313	yes
03 Mar 08	Test03a0_3	3	a	0	0.313	yes
04 Mar 08	Test02a0_5	2	a	0	0.314	
04 Mar 08	Test03a0_4	3	a	0	0.314	
04 Mar 08	Test02b0_3	2	b	0	0.313	
04 Mar 08	film 9	3	b	0	0.313	
04 Mar 08	Test03b0_3	3	b	0	0.316	

(Continued on next page)

Date	Test name [.ASC]	Wave climate [-]	BW core [-]	BW layout [°]	Water depth	Additional rubble mound?
04 Mar 08	Test02c0_3	2	c	0	0.316	
04 Mar 08	Test03c0_3	3	c	0	0.316	
05 Mar 08	Test02d0_3	2	d	0	0.314	
05 Mar 08	Test03d0_3	3	d	0	0.314	
12 Mar 08	film 10	1	d	30	0.312	
13 Mar 08	Test02nb0_1	2	-	-	0.316	no BW
13 Mar 08	Test03nb0_1	3	-	-	0.316	no BW
13 Mar 08	Test0GHM	-	-	-	0.316	no BW; no waves

Table A.1: Logbook

Appendix B

Calibration

Wave	Calibration	Layout [m]			⊥ distance to breakwater [m]				
gauge nr	[m/V]	x	y	z	0°	15°	30°	45°	60°
WG18	0.0242	0.000	0.000	h	2.07	1.99	0.91	1.30	1.02
WG19	0.0244	0.000	0.530	h	2.07	2.13	1.18	1.67	1.48
WG20	0.0236	0.400	0.265	h	1.67	1.67	0.70	1.20	1.05
WG21	0.0251	0.560	-0.230	h	1.51	1.39	0.31	0.74	0.54
WG22	0.0247	0.560	0.760	h	1.51	1.65	0.81	1.44	1.40
WG23	0.0257	0.000	0.000	h	0.60	0.74	0.97	1.00	0.60
WG24	0.0252	0.000	0.560	h	0.60	0.60	0.69	0.60	0.12
WG25	0.0255	0.406	0.280	h	1.01	1.06	1.18	1.08	0.56
WG26	0.0261	0.536	-0.220	h	1.14	1.32	1.54	1.53	1.06
WG27	0.0246	0.536	0.780	h	1.14	1.06	1.04	0.82	0.19

Table B.1: Calibration (h = water depth)

Appendix C

Comparison of EP methods

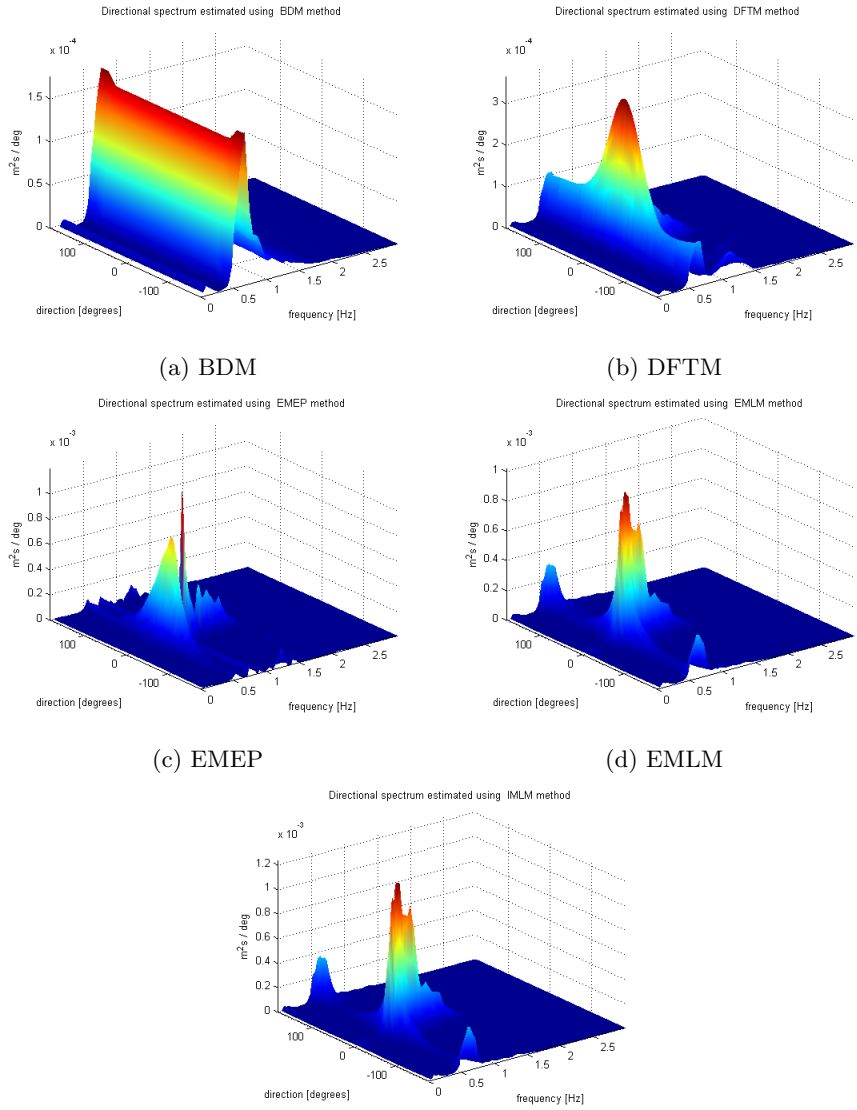

(a) BDM

(b) DFTM

(c) EMEP

(d) EMLM

(e) IMLM

Figure C.1: Test02a0_1: Incident wave climate

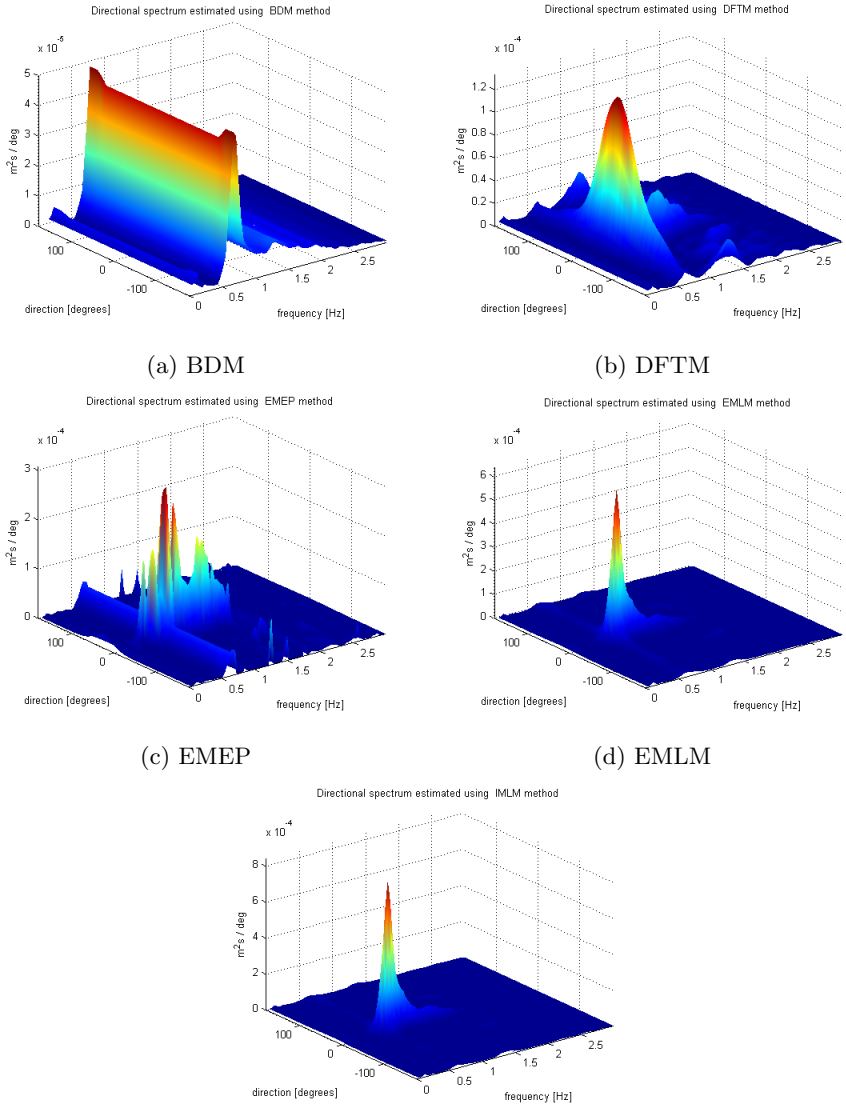

(a) BDM

(b) DFTM

(c) EMEP

(d) EMLM

(e) IMLM

Figure C.2: Test02a0_1: Transmitted wave climate

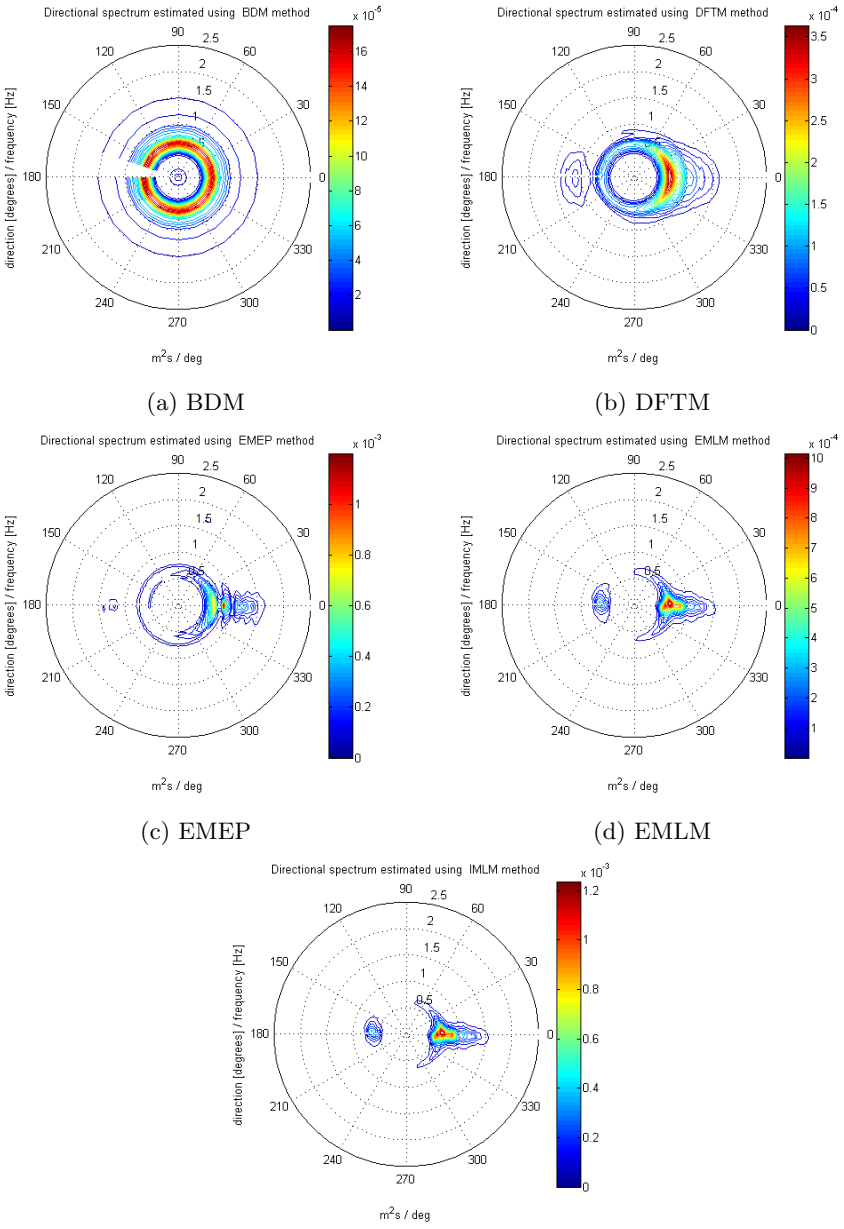

(a) BDM

(b) DFTM

(c) EMEP

(d) EMLM

(e) IMLM

Figure C.3: Test02a0_1: Incident wave climate

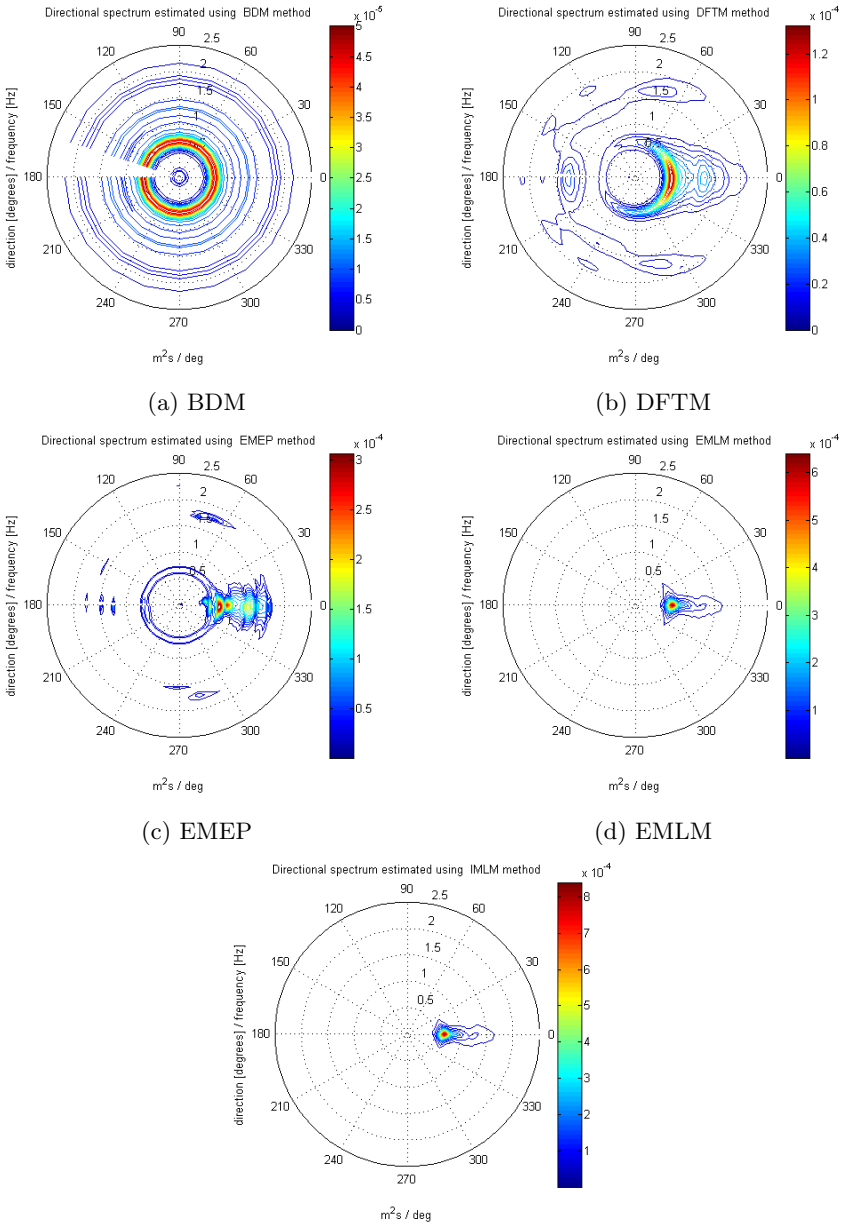

(a) BDM

(b) DFTM

(c) EMEP

(d) EMLM

(e) IMLM

Figure C.4: Test02a0_1: Transmitted wave climate

Appendix D

Change in wave direction

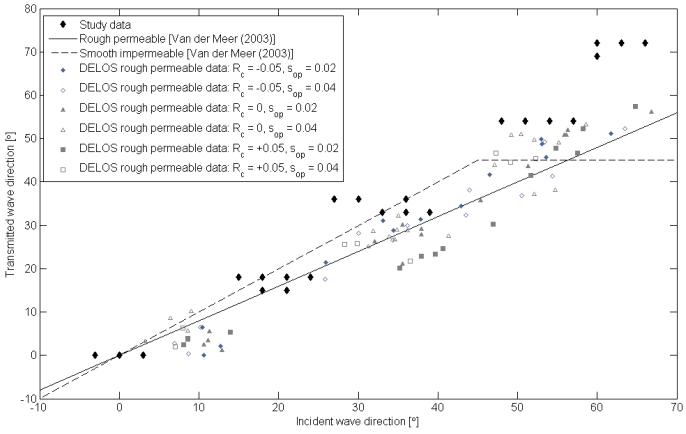

(a) DELOS (2002b) data: Rough permeable breakwater

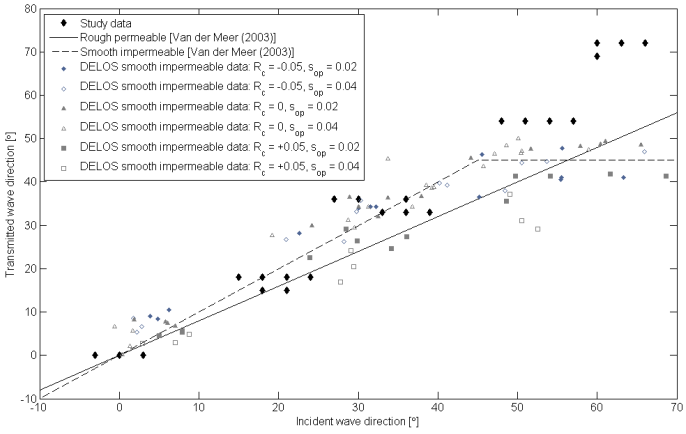

(b) DELOS (2002b) data: Smooth impermeable breakwater

Figure D.1: The transmitted wave direction β_t with respect to the incident wave direction β_i: All study data

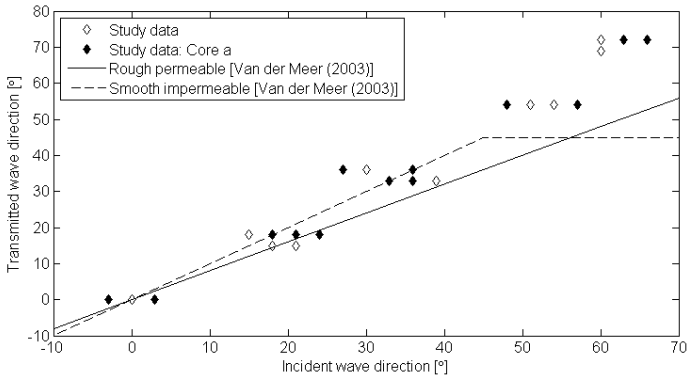

(a) Core a: Fully impermeable

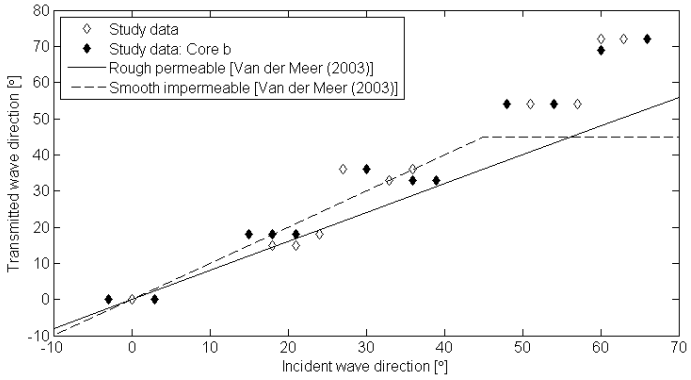

(b) Core b

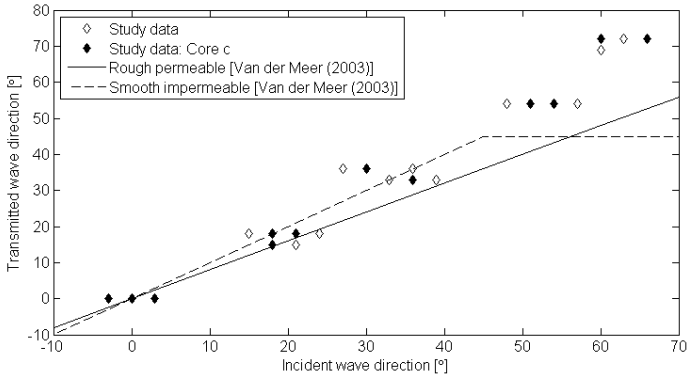

(c) Core c

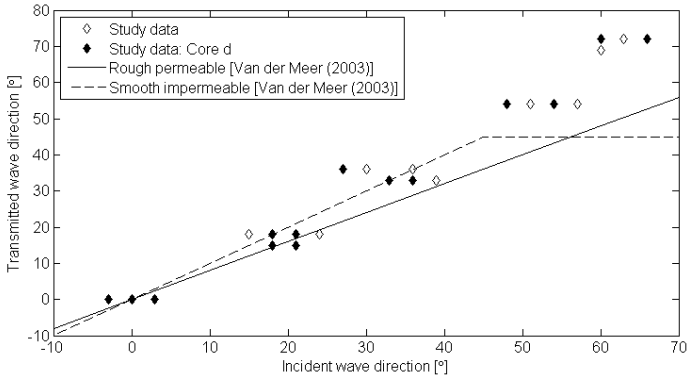

(d) Core d: Fully permeable

Figure D.2: The transmitted wave direction β_t with respect to the incident wave direction β_i: Influence of the core

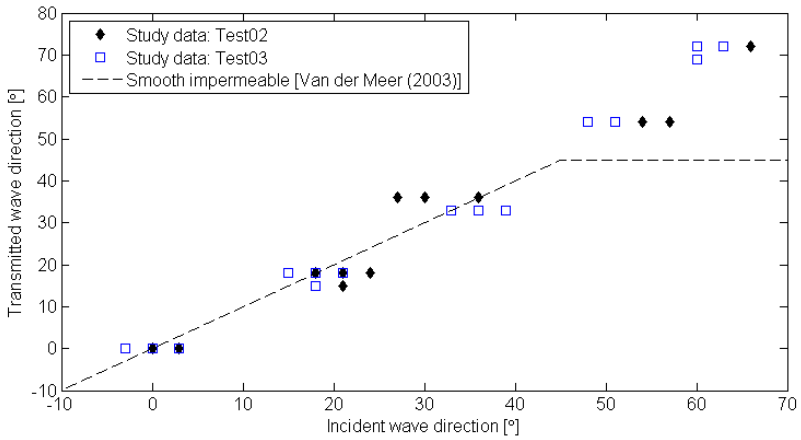

Figure D.3: The transmitted wave direction β_t with respect to the incident wave direction β_i: Influence of the wave climate

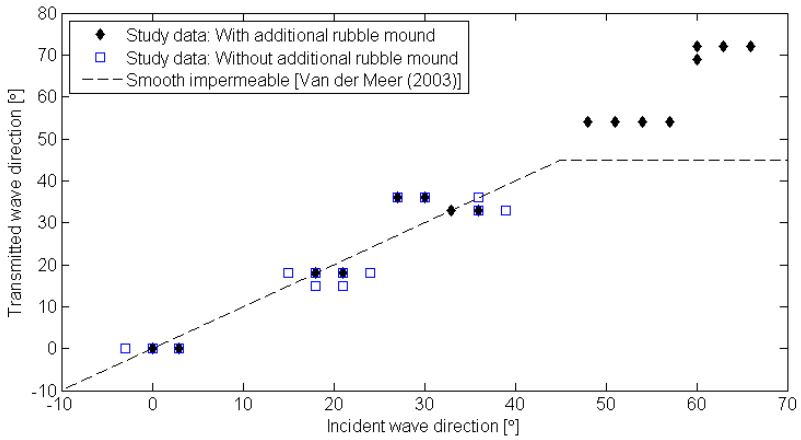

Figure D.4: The transmitted wave direction β_t with respect to the incident wave direction β_i: Influence of the additional rubble mound

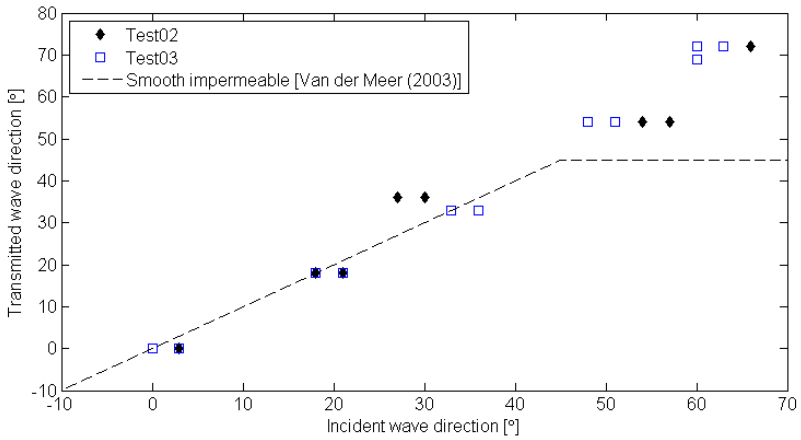

(a) With additional rubble mound

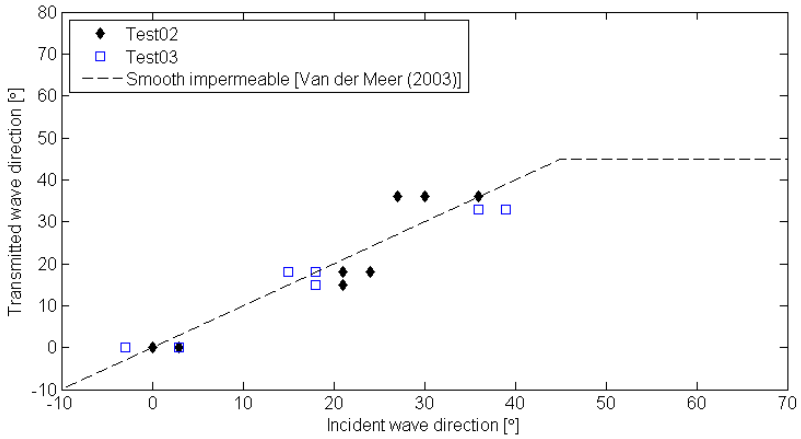

(b) Without additional rubble mound

Figure D.5: The transmitted wave direction β_t with respect to the incident wave direction β_i: Influence of the wave climate and of the additional rubble mound

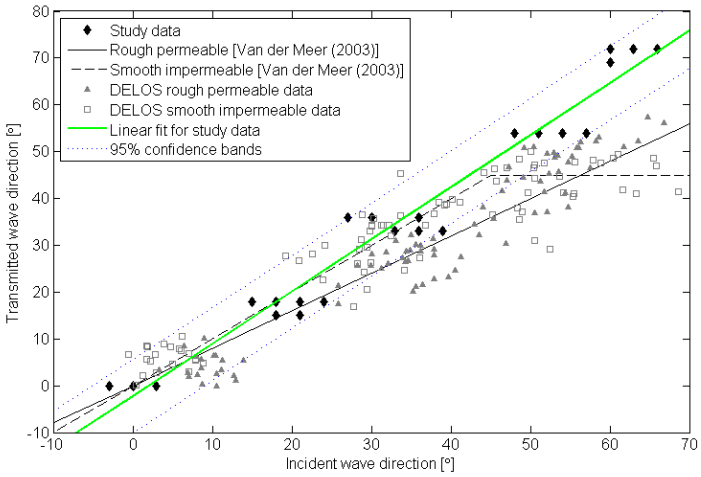

(a) Study data

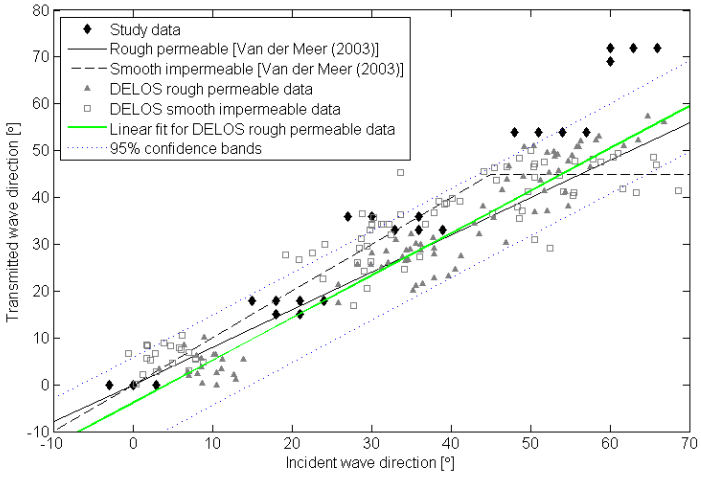

(b) DELOS (2002b) rough permeable data

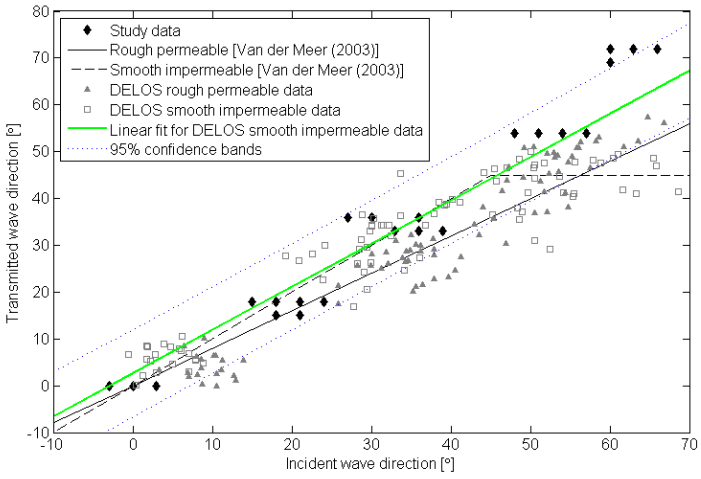

(c) DELOS (2002b) smooth impermeable data

Figure D.6: The transmitted wave direction β_t with respect to the incident wave direction β_i: Linear fits for individual data sets

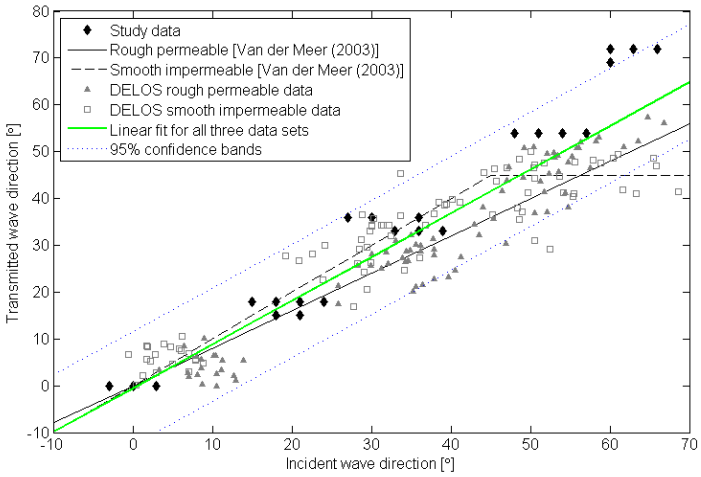

(a) All three data sets

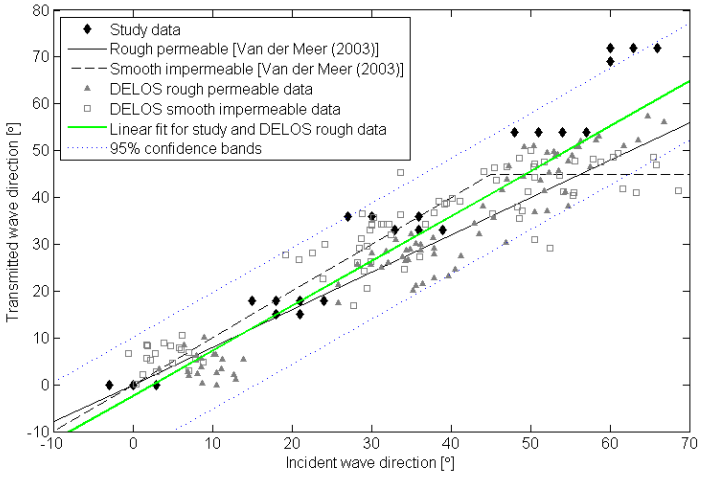

(b) Study and DELOS (2002b) rough permeable data

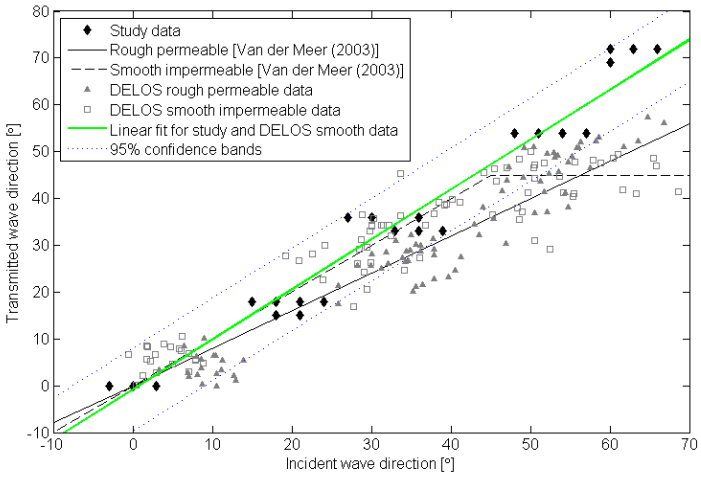

(c) Study and DELOS (2002b) smooth impermeable data

Figure D.7: The transmitted wave direction β_t with respect to the incident wave direction β_i: Linear fits for grouped data sets

Appendix E

The transmission coefficient

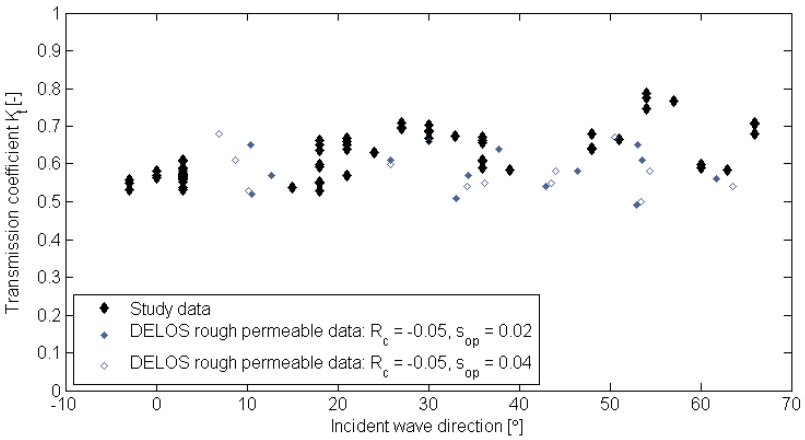

(a) DELOS (2002b) data: Rough permeable breakwater

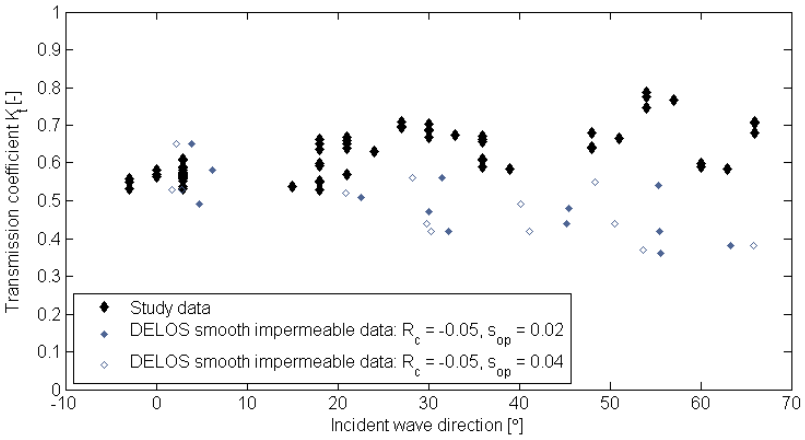

(b) DELOS (2002b) data: Smooth impermeable breakwater

Figure E.1: The transmission coefficient K_t with respect to the incident wave direction β_i: All study data

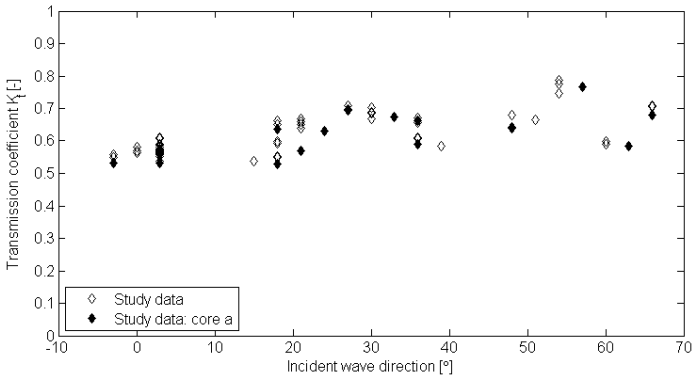

(a) Core a: Fully impermeable

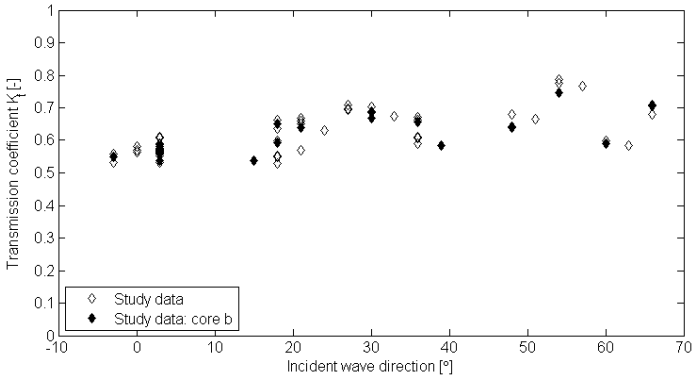

(b) Core b

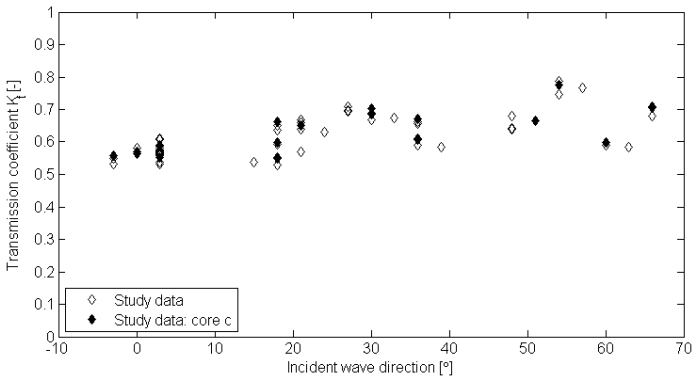

(c) Core c

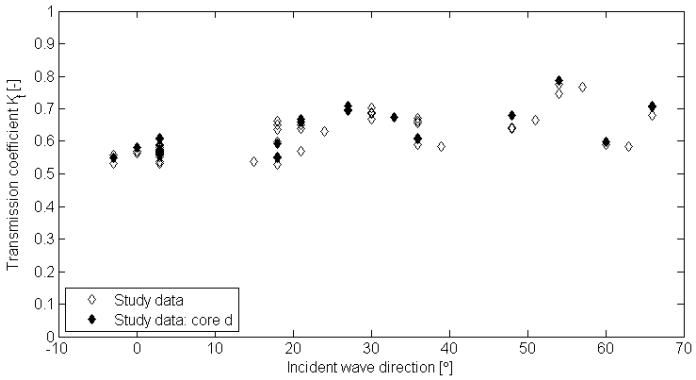

(d) Core d: Fully permeable

Figure E.2: The transmission coefficient K_t with respect to the incident wave direction β_i: Influence of the core

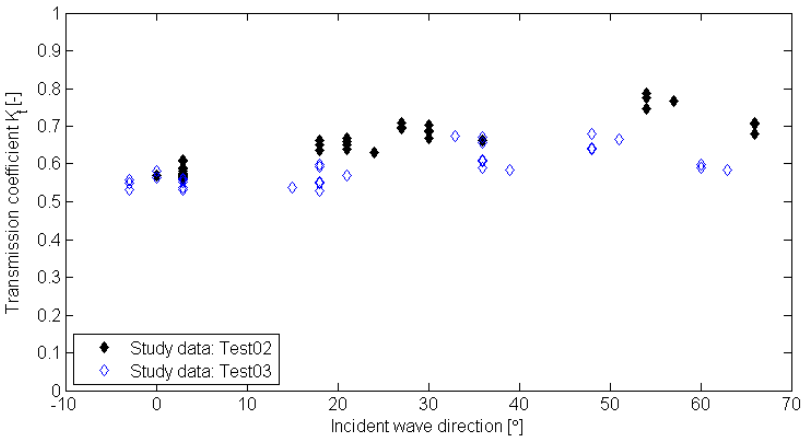

Figure E.3: The transmission coefficient K_t with respect to the incident wave direction β_i: Influence of the wave climate

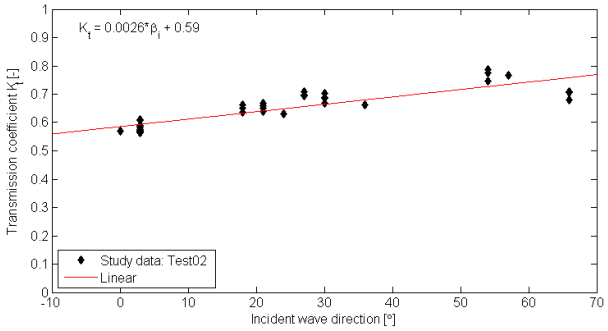

(a) Test02

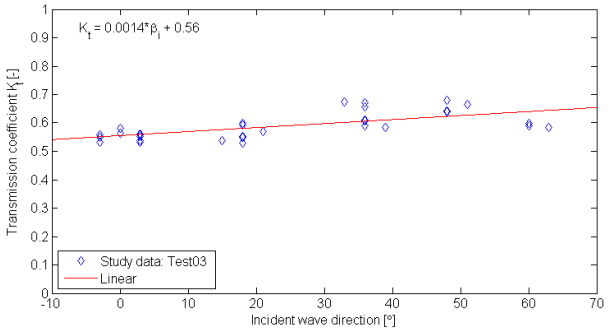

(b) Test03

Figure E.4: The transmission coefficient K_t with respect to the incident wave direction β_i: Influence of the wave climate (Linear fits)

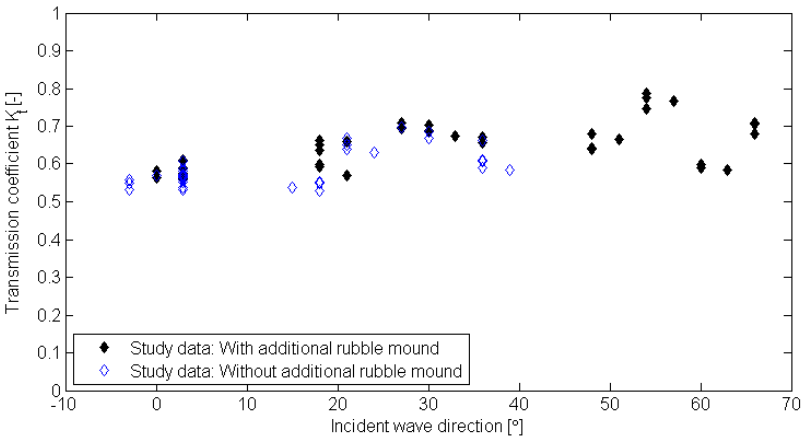

Figure E.5: The transmission coefficient K_t with respect to the incident wave direction β_i: Influence of the additional rubble mound

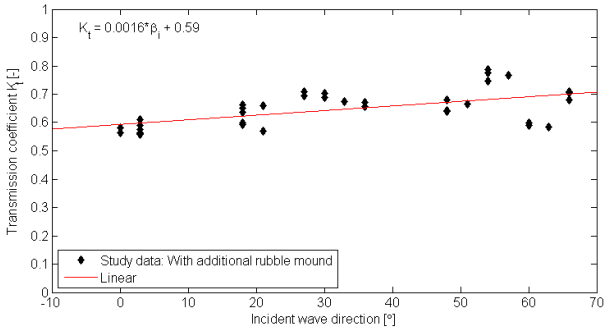

(a) With additional rubble mound

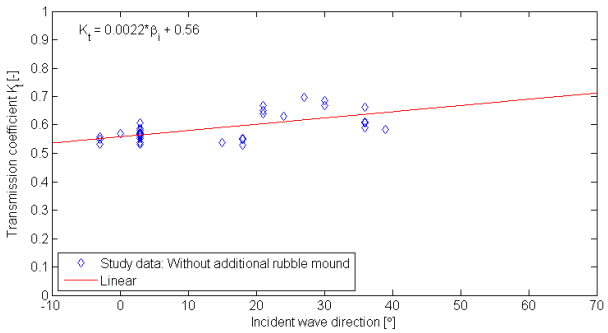

(b) Without additional rubble mound

Figure E.6: The transmission coefficient K_t with respect to the incident wave direction β_i: Influence of the additional rubble mound (Linear fits)

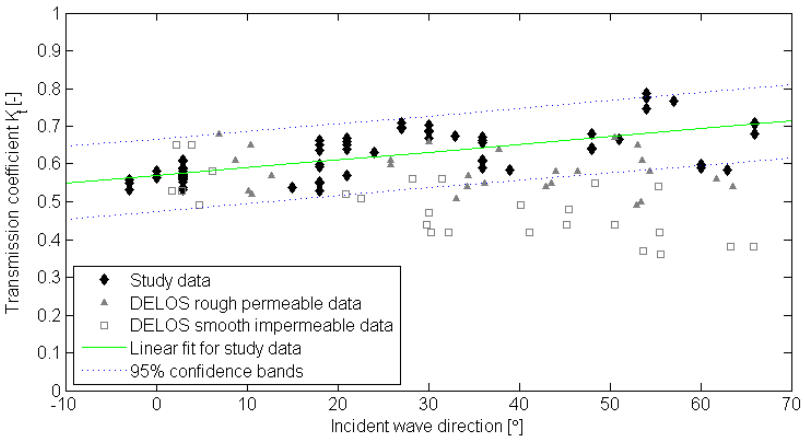

(a) Study data

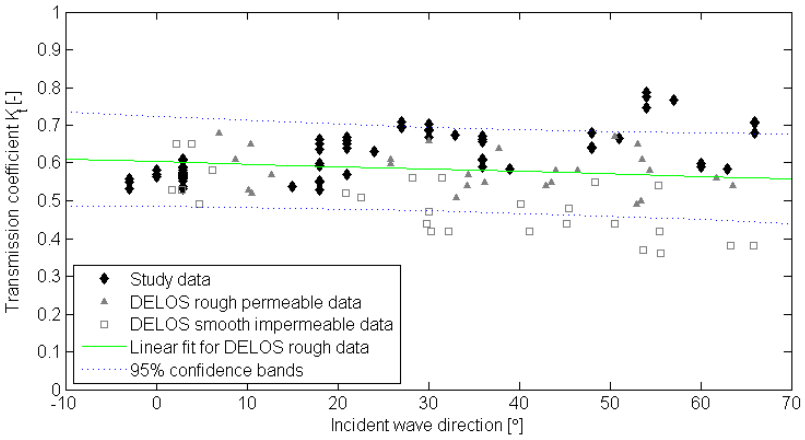

(b) DELOS (2002b) rough permeable data

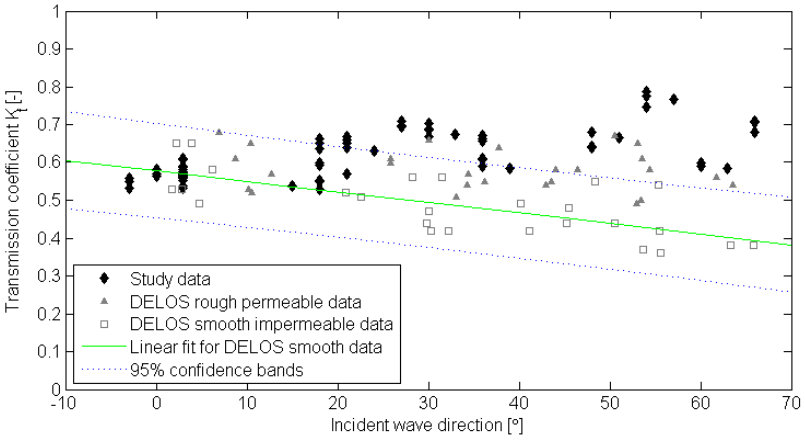

(c) DELOS (2002b) smooth impermeable data

Figure E.7: The transmission coefficient K_t with respect to the incident wave direction β_i: Linear fits for individual data sets

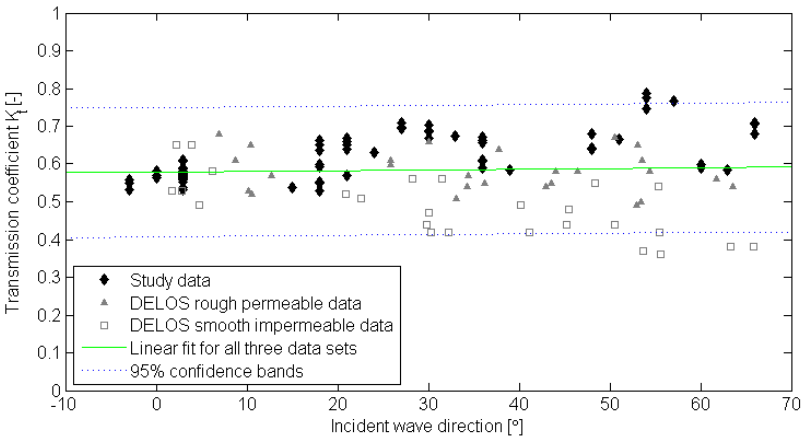

(a) Study data

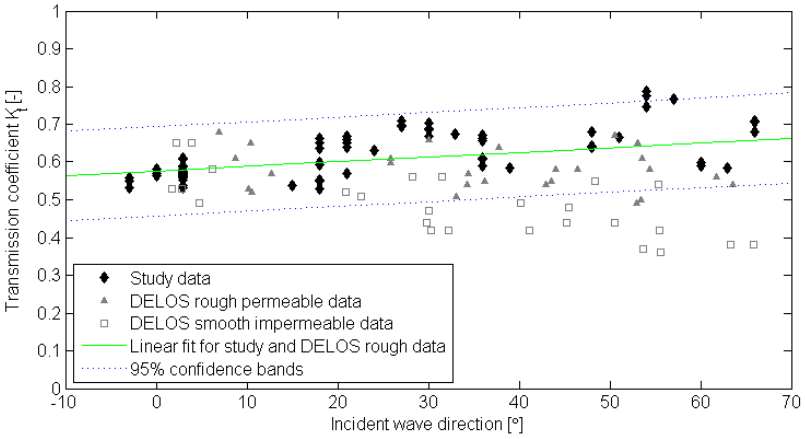

(b) DELOS (2002b) rough permeable data

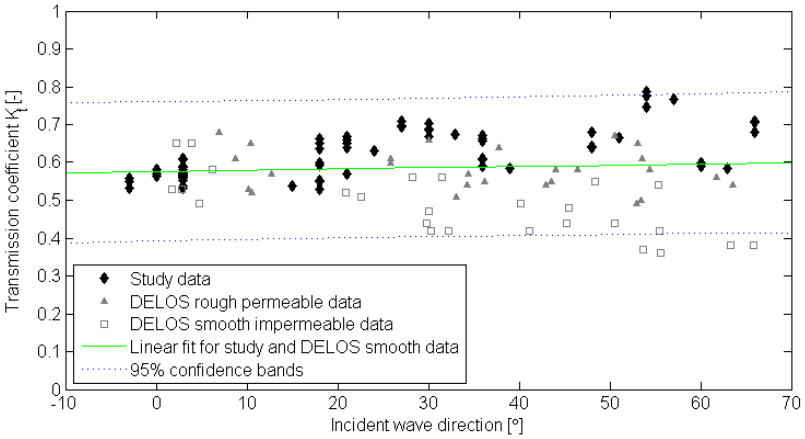

(c) DELOS (2002b) smooth impermeable data

Figure E.8: The transmission coefficient K_t with respect to the incident wave direction β_i: Linear fits for grouped data sets

Appendix F

Spectral Changes

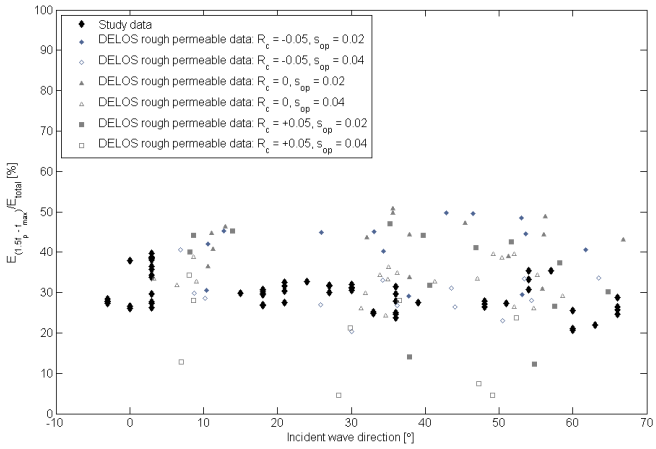

(a) DELOS (2002b) data: Rough permeable breakwater

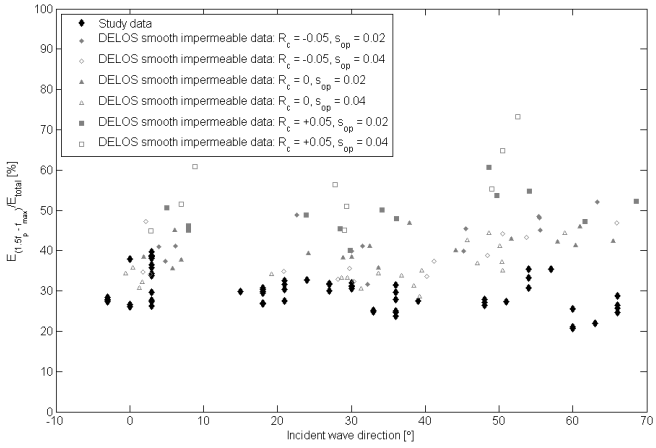

(b) DELOS (2002b) data: Smooth impermeable breakwater

Figure F.1: Percentage wave energy at the range of high frequencies ($1.5f_p \rightarrow f_{max}$): All study data

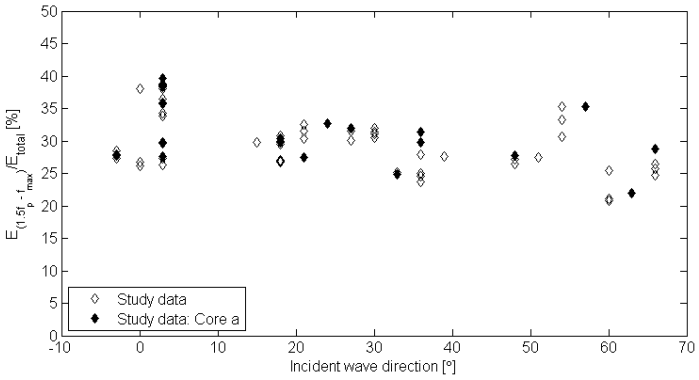

(a) Core a: Fully impermeable

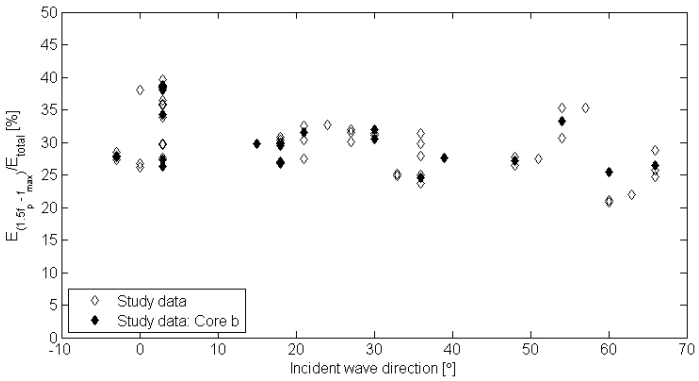

(b) Core b

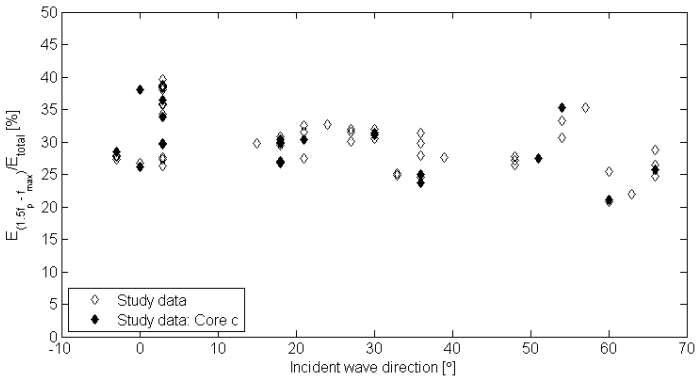

(c) Core c

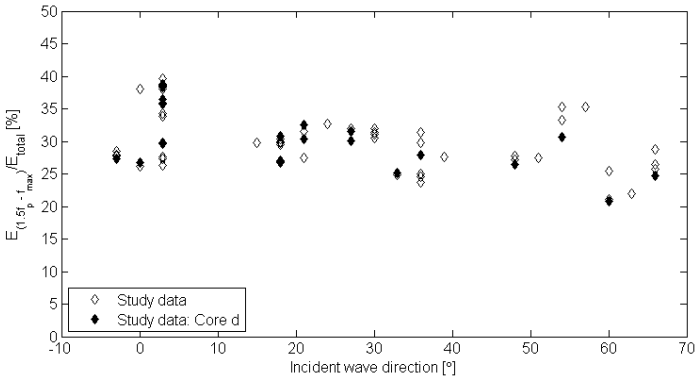

(d) Core d: Fully permeable

Figure F.2: Percentage wave energy at the range of high frequencies ($1.5f_p \rightarrow f_{max}$): Influence of the core

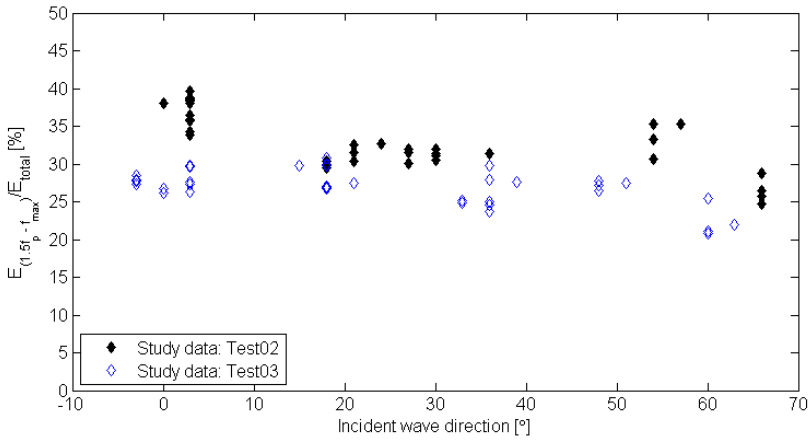

Figure F.3: Percentage wave energy at the range of high frequencies ($1.5f_p \rightarrow f_{max}$): Influence of the wave climate

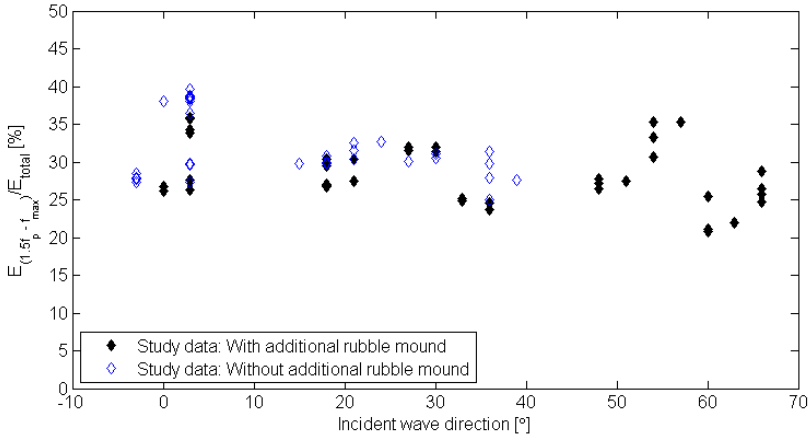

Figure F.4: Percentage wave energy at the range of high frequencies ($1.5f_p \rightarrow f_{max}$): Influence of the additional rubble mound

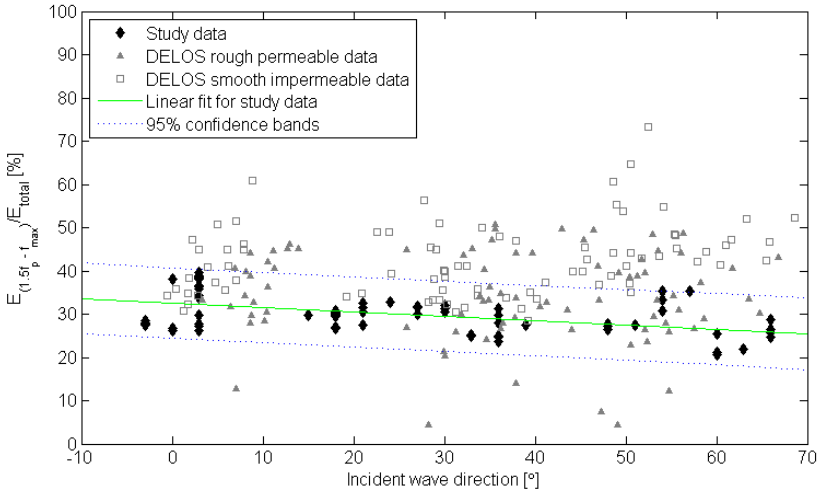

(a) Study data

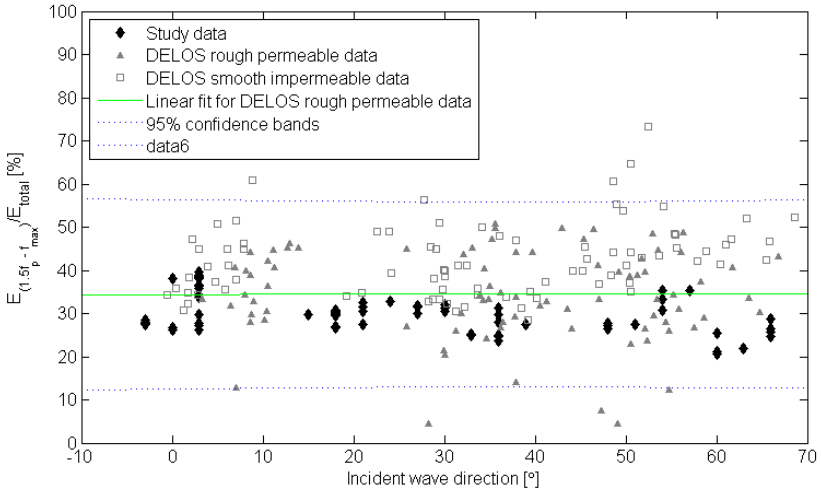

(b) DELOS (2002b) rough permeable data

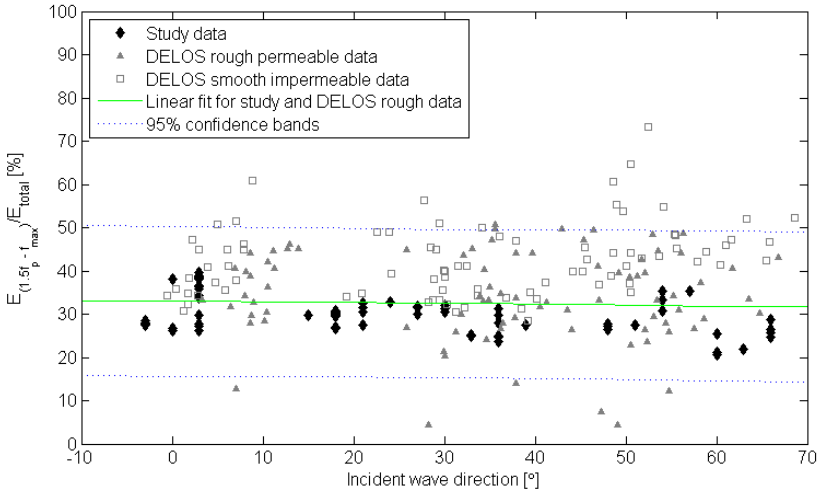

(c) Study and DELOS (2002b) rough permeable data

Figure F.5: Percentage wave energy at the range of high frequencies ($1.5f_p \rightarrow f_{max}$): Linear fits

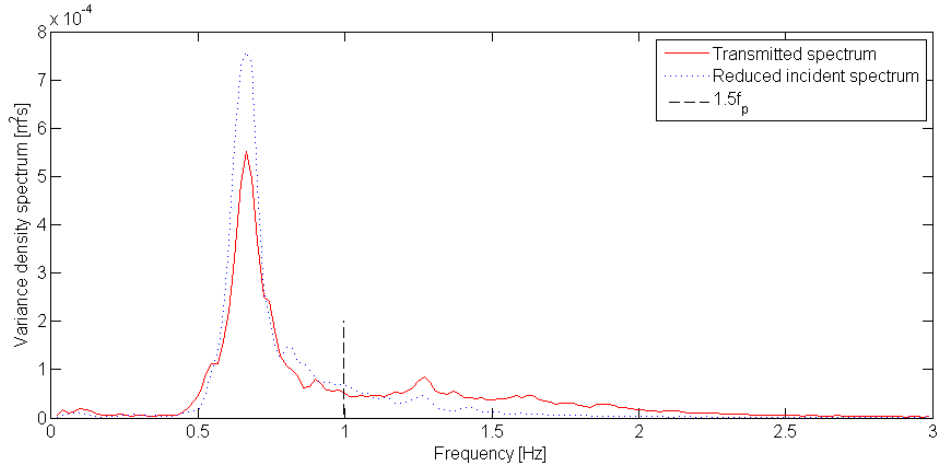

(a) Test02c0_3

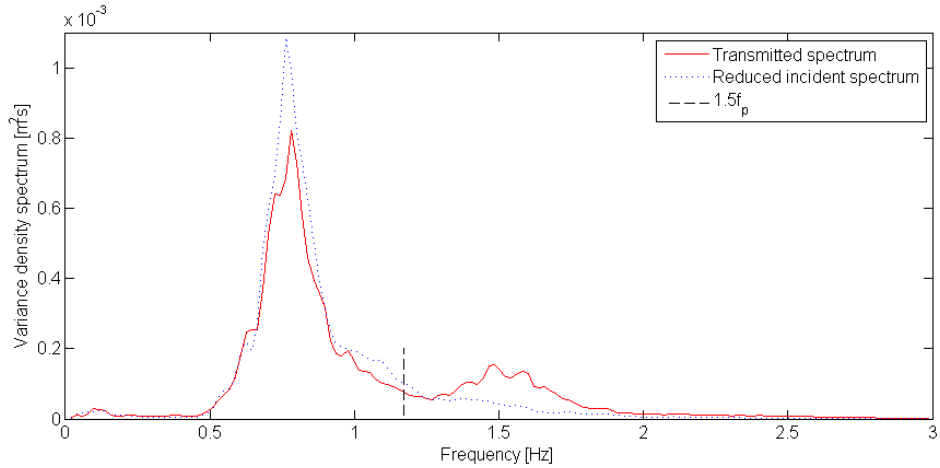

(b) Test03d45_1

Figure F.6: Spectral changes: Two examples (Test02c0_3 and Test03d45_1)

Appendix G

Processed data

Test name	Incident wave climate			Transmitted wave climate		
	H_i $[m]$	β_i $[°]$	$T_{p,i}$ $[s]$	H_t $[m]$	β_t $[°]$	$T_{p,t}$ $[s]$
Test02a0_1	0.0663	3	1.51	0.0404	0	1.51
Test02a0_2	0.0667	3	1.51	0.0405	0	1.51
Test02a0_3	0.0657	3	1.51	0.0400	0	1.51
Test03a0_2	0.0816	-3	1.28	0.0469	0	1.28
Test02b0_1	0.0678	3	1.51	0.0419	0	1.51
Test03b0_1	0.0817	-3	1.28	0.0485	0	1.28
Test02c0_1	0.0742	0	1.51	0.0456	0	1.51
Test03c0_1	0.0817	-3	1.28	0.0494	0	1.28
Test02d0_1	0.0697	3	1.51	0.0428	0	1.51
Test03d0_1	0.0835	-3	1.28	0.0496	0	1.35
Test02d30_1	0.0719	27	1.51	0.0541	36	1.51
Test03d30_1	0.0864	36	1.35	0.0567	33	1.35
Test02c30_1	0.0706	30	1.51	0.0522	36	1.51
Test03c30_1	0.0851	36	1.28	0.0560	33	1.35
Test02b30_1	0.0703	30	1.51	0.0508	36	1.51
Test03b30_1	0.0865	39	1.35	0.0545	33	1.35
Test02a30_1	0.0696	36	1.51	0.0499	36	1.51
Test03a30_1	0.0868	36	1.35	0.0552	33	1.35
Test02a30_2	0.0728	27	1.51	0.0546	36	1.51
Test03a30_2	0.0844	33	1.35	0.0615	33	1.28
Test02b30_2	0.0712	30	1.51	0.0530	36	1.51

(Continued on next page)

Test	Incident wave climate			Transmitted wave climate		
name	H_i $[m]$	β_i $[°]$	$T_{p,i}$ $[s]$	H_t $[m]$	β_t $[°]$	$T_{p,t}$ $[s]$
Test03b30_2	0.0849	36	1.35	0.0600	33	1.28
Test02c30_2	0.0716	30	1.51	0.0544	36	1.51
Test03c30_2	0.0854	36	1.35	0.0619	33	1.28
Test02d30_2	0.0724	27	1.51	0.0553	36	1.51
Test03d30_2	0.0872	33	1.35	0.0635	33	1.28
Test02d60_1	0.0730	66	1.42	0.0557	72	1.51
Test03d60_1	0.0904	60	1.28	0.0585	72	1.28
Test02c60_1	0.0719	66	1.42	0.0549	72	1.51
Test03c60_1	0.0905	60	1.28	0.0586	72	1.28
Test02b60_1	0.0717	66	1.42	0.0549	72	1.51
Test03b60_1	0.0899	60	1.35	0.0574	69	1.35
Test02a60_1	0.0732	66	1.51	0.0537	72	1.51
Test03a60_1	0.0908	63	1.28	0.0573	72	1.28
Test02a45_1	0.0671	57	1.51	0.0555	54	1.51
Test03a45_1	0.0890	48	1.28	0.0615	54	1.28
Test02b45_1	0.0691	54	1.51	0.0557	54	1.51
Test03b45_1	0.0878	48	1.28	0.0610	54	1.28
Test02c45_1	0.0668	54	1.51	0.0559	54	1.51
Test03c45_1	0.0867	51	1.28	0.0624	54	1.28
Test02d45_1	0.0693	54	1.42	0.0589	54	1.51
Test03d45_1	0.0876	48	1.28	0.0644	54	1.28
Test02d15_1	0.0708	21	1.51	0.0511	15	1.51
Test03d15_1	0.0898	18	1.35	0.0534	15	1.35
Test02c15_1	0.0723	21	1.51	0.0508	18	1.51
Test03c15_1	0.0896	18	1.35	0.0534	15	1.35
Test02b15_1	0.0722	21	1.51	0.0500	18	1.51
Test03b15_1	0.0891	15	1.35	0.0518	18	1.35
Test02a15_1	0.0714	24	1.51	0.0486	18	1.51
Test03a15_1	0.0897	18	1.35	0.0513	18	1.35
Test02a15_2	0.0705	18	1.51	0.0484	18	1.51
Test03a15_2	0.0843	21	1.35	0.0520	18	1.35

(Continued on next page)

Test	Incident wave climate			Transmitted wave climate		
name	H_i $[m]$	β_i $[°]$	$T_{p,i}$ $[s]$	H_t $[m]$	β_t $[°]$	$T_{p,t}$ $[s]$
Test02b15_2	0.0713	18	1.51	0.0501	18	1.51
Test03b15_2	0.0869	18	1.35	0.0556	18	1.35
Test02c15_2	0.0708	18	1.51	0.0507	18	1.51
Test03c15_2	0.0871	18	1.35	0.0562	18	1.35
Test02d15_2	0.0722	21	1.51	0.0514	18	1.51
Test03d15_2	0.0882	18	1.35	0.0565	18	1.35
Test02d0_2	0.0726	3	1.51	0.0478	0	1.51
Test03d0_2	0.0877	0	1.28	0.0550	0	1.35
Test02c0_2	0.0741	3	1.51	0.0472	0	1.51
Test03c0_2	0.0865	0	1.28	0.0528	0	1.35
Test02b0_2	0.0742	3	1.51	0.0461	0	1.51
Test03b0_2	0.0861	3	1.28	0.0519	0	1.35
Test02a0_4	0.0735	3	1.51	0.0448	0	1.51
Test03a0_3	0.0867	3	1.28	0.0526	0	1.35
Test02a0_5	0.0734	3	1.51	0.0449	0	1.51
Test03a0_4	0.0859	3	1.28	0.0492	0	1.35
Test02b0_3	0.0719	3	1.51	0.0452	0	1.51
Test03b0_3	0.0884	3	1.22	0.0514	0	1.35
Test02c0_3	0.0742	3	1.51	0.0470	0	1.51
Test03c0_3	0.0877	3	1.28	0.0522	0	1.35
Test02d0_3	0.0738	3	1.51	0.0484	0	1.51
Test03d0_3	0.0887	3	1.28	0.0533	0	1.35
Test02nb0_1	0.0704	0	1.51	0.0759	0	1.51
Test03nb0_1	0.0908	0	1.28	0.0969	0	1.28

Table G.1: Processed data

Appendix H

Summary in Dutch

H.1 Introductie

Golfbrekers zijn bekend voor hun kruin die ver boven het waterniveau uitsteekt. In veel gevallen is echter een aanzienlijke hoeveelheid golfoverslag aanvaardbaar, waardoor het gebruik van golfbrekers met lage kruin is toegenomen. Hun gedrag wordt gedomineerd door deze golfoverslag en hun kruin kan zowel boven als onder het wateroppervlak gelegen zijn. In het laatste geval spreekt men van onderwatergolfbrekers.

Onderwatergolfbrekers hebben enkele uitgesproken voordelen. Er is geen visuele hinder zodat het landschap behouden wordt. Bovendien blijft water- en sedimenttransport over de golfbreker mogelijk. Dit bevordert de kwaliteit van kust en milieu aan de lijzijde van de golfbreker. Tegelijkertijd biedt de golfbreker er beschutting.

Het primair doel van golfbrekers is kustverdediging of bescherming van een haveningang. De werking berust op breking, reflectie en dissipatie van de inkomende golven en de energie die ze dragen. De transmissie van energie is daarom een belangrijke variabele om de condities aan de lijzijde te bepalen. Ook kennis van het energiespectrum aan de lijzijde is gewenst, bijvoorbeeld voor morfologische veranderingen op lange termijn. Modelleren van de interactie tussen de golf en de golfbreker blijkt zeer complex. In de praktijk wordt dit verder bemoeilijkt door de vele soorten golfbrekers. Ruwe steenslag golfbrekers, gladde asfalt golfbrekers, strandhoofden, caisson golfbrekers en golfbrekers met betonnen deklagen zijn maar een paar voorbeelden. Classificatie gebeurt onder andere volgens ruwheid en doorlatendheid. Onderzoek heeft geleid tot empirische formules, elk met beperkte geldigheid.

De laatste tien jaar is er veel onderzoek gedaan waarbij het probleem vereenvoudigd wordt tot twee dimensies. Hierbij wordt verondersteld dat de golf loodrecht op de golfbreker invalt. Veelal is die aanname gerechtvaardigd, zoals bij golfbrekers evenwijdig aan de kust.

Meer algemeen gebeurt de golfinval onder een willekeurige hoek of uit verschillende richtingen. Golfbrekers ter bescherming van havens staan bijvoorbeeld typisch niet loodrecht op de golfrichting. Het tweedimensionale model gaat in dat geval niet meer op. Kennis van de invloed van schuine golfinval op de transmissie en het energiespectrum is dan gewenst bij het ontwerp van de golfbreker.

Het Europese project DELOS (Environmental Design of Low Crested Coastal Defence Structures) heeft de invloed van schuine golf aanval onderzocht in het laboratorium van de Aalburg Universiteit in Denemarken. In totaal zijn er 168 testen uitgevoerd in een kortkammige-golfbassin. Het onderzoek is gebaseerd op twee laagkruinige structuren: de gladde ondoorlatende en de ruwe doorlatende golfbreker. De invloed op de richtingverandering van de golf, de transmissie en de spectrale veranderingen waren onderzocht. De data werden vervolgens bestudeerd door Van der Meer *et al.* (2005) er de bevindingen zijn kort toegelicht:

De richtingverandering van de golf

Voor ruwe doorlatende golfbrekers is de hoek van de golf ten opzichte van de normaalas 20% kleiner na breking dan ervoor [Van der Meer *et al.* (2003)] (figuur H.1a):

$$\text{Ruwe doorlatende golfbrekers} \qquad \beta_t = 0.8\beta_i \tag{H.1}$$

In het geval van gladde ondoorlatende golfbrekers ondergaan golven met invalshoeken kleiner dan 45° geen richtingverandering. Voor grotere invalshoeken blijft de richting van de uitgaande golf constant op 45° [Van der Meer *et al.* (2003)] (figuur H.1b):

$$\text{Gladde ondoorlatende golfbrekers} \qquad \begin{aligned} \beta_t &= \beta_i \quad \text{voor } \beta_i \leq 45° \\ \beta_t &= 45° \quad \text{voor } \beta_i > 45° \end{aligned} \tag{H.2}$$

Een intern rapport van DELOS (2002b) ('Transmission Internal Report') maakt een gelijkaardige analyse, de bekomen coëfficiënten zijn echter licht verschillend:

$$\text{Gladde ondoorlatende golfbrekers} \qquad \begin{aligned} \beta_t &= 0.9\beta_i \quad \text{voor } \beta_i < 50° \\ \beta_t &= 45° \quad \text{voor } \beta_i \geq 50° \end{aligned} \tag{H.3}$$

Deze resultaten gelden enkel voor een relatieve kruinhoogte met $R_c/H_i > -1$. Bij dieper gelegen golfbrekers of kleiner kruinhoogtes zullen de golven weinig invloed van de golfbreker ondervinden.

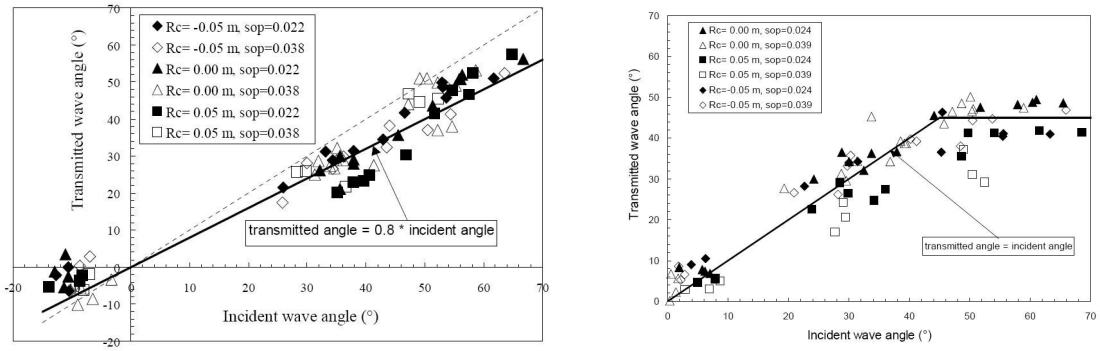

(a) Ruw doorlatend (b) Glad ondoorlatend

Figure H.1: De richtingverandering van de golf [Van der Meer *et al.* (2003)]

Transmissie

Volgens Van der Meer *et al.* (2003) heeft de invalshoek geen significante invloed op de transmissiecoëfficiënt bij ruwe doorlatende golfbrekers. De transmissie van gladde ondoorlatende golfbrekers daarentegen vertoond wel een hoekafhankelijkheid: een grotere invalshoek resulteert in een kleinere transmissiecoëfficiënt. Er is geen onderscheid tussen de transmissie van langkammige en kortkammige golven voor gladde ondoorlatende golfbrekers, bij ruwe doorlatende golfbrekers geven kortkammige golven aanleiding tot $1-2\%$ lagere transmissiecoëfficiënten.

Spectrale veranderingen

Men kan het energiespectrum aan de lijzijde van de golfbreker benaderen door dat van de inkomende golf te verschalen volgens de transmissiecoëfficiënt. Meer algemeen zal niet enkel de totale energie, maar ook de vorm van het spectrum wijzigen. Van der Meer *et al.* (2000) concludeert dat de piekperiode niet verandert. Er is wel een shift van de energie naar hogere frequenties. Ruwweg 60% van de energie ligt in het frequentie gebied $f < 1.5f_p$, waar de overige 40% in het hoge frequentie gebied $1.5f_p < f < 3.5f_p$ ligt. De invaslhoek vertoont geen significante invloed. Deze resultaten gelden enkel voor onderwatergolfbrekers.

H.2 Doelstelling

Volgens Van der Meer *et al.* (2005) is er een groot verschil in gedrag tussen de ruwe doorlatende en de gladde ondoorlatende golfbreker wat betreft de invloed van de invalshoek van de golf op de richtingverandering van de golf, de transmissie en de spectrale veranderingen. De doelstelling van deze studie is om meer inzicht te krijgen in de oorzaken van dit verschillende

gedrag. Daartoe wordt schuine golfinval aan ruwe onderwatergolfbrekers bestudeerd, waarbij de doorlatendheid gevariëerd kan worden van volledig ondoorlatend tot volledig doorlatend. Dit gebeurt aan de hand van een 3D schaal model.

H.3 Experimentele opstelling

De driedimensionale experimenten zijn uitgevoerd in het Laboratorium voor Vloeistofmechanica van de vakgroep Civiele Techniek en Geowetenschappen aan de Technische Universiteit van Delft. De gebruikte opstelling is gelijkaardig aan die van DELOS (2002b) zodat de data vergelijkbaar zijn. Het golfbassin heeft een maximum diepte van $0.60m$ en horizontale afmetingen van $28.60m$ x $16.60m$. Omdat dit bassin groter is dan bij DELOS (2002b), kan dezelfde schaal 1 : 20 gebruikt worden als in DELOS (2002b). Een algemeen overzicht van de opstelling is weergegeven in figuur H.2. Een golfgenerator wekt golven op, die gebroken worden aan het schaalmodel. Vijf meetpunten voor en na de golfbreker laten toe de respectievelijke energiespectra te bepalen. Steenslag en een strand bepalen de randen van het bassin.

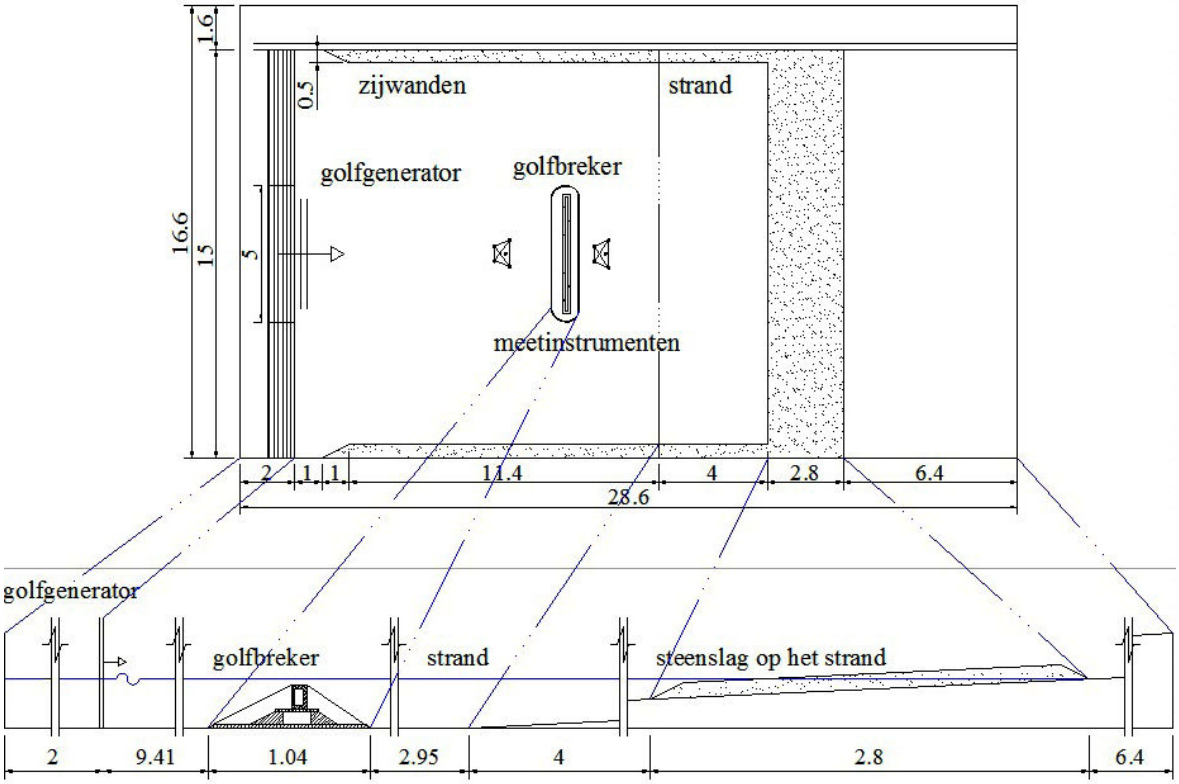

Figure H.2: Overzicht van het golfbassin [Dimensies in meters]

Het strand en de zijwanden

Het experiment mag niet beïnvloed worden door de fysische beperkingen van het bassin. Het is dus belangrijk dat de golven niet reflecteren aan de wanden en het strand. Om de golven aan de zijwanden te dempen, is een schuin oplopende laag steenslag aangebracht aan de wanden. Om dezelfde reden heeft ook het strand een licht oplopende helling van 1 : 30. Hogerop het strand is er een bijkomende steenslag voorzien voor verdere demping. Het geheel van deze maatregelen laat toe reflectie van golven te minimaliseren.

Golfopwekking

Er staan drie hydraulische golfgeneratoren naast elkaar, elk met een lengte van vijf meter. De drie machines zijn onderling gesynchroniseerd, zodat langkammige onregelmatige golven opgewekt kunnen worden. In de experimenten worden er twee golfcondities met een JONSWAP-spectrum opgewekt (table H.1). De eerste golfconditie bestaat uit relatief lange golven met relatief lage energie. De tweede golfconditie heeft hogere, kortere golven.

Test naam	$H_i[m]$	$T_p[s]$	$s_{op}[-]$	$E[N/m]$
Test02	0.07	1.5	0.020	3
Test03	0.09	1.3	0.034	5

Table H.1: Beoogde golfkcondities

De golfmachines zijn niet uitgerust met een actieve reflectie compensator. Dit wil zeggen dat de gereflecteerde golven van de golfbreker niet actief gedempd worden door de machine, maar wel weer gereflecteerd. Dit kan het experiment in negatieve zin beïnvloeden. Ten eerste kan het inkomende golfspectrum meer energie bezitten dan verwacht. In dat geval zal de significante golfhoogte hoger zijn. Gezien de lage waterdiepte heeft dit als bijkomend gevolg dat hoge golven vroegtijdig breken door interactie met reflecties van de golfbreker. Dit verstoort het spectrum ter hoogte van de golfbreker nog meer. Verder is er de kans op vorming van een laagfrequente staande golf. Indien er bovendien resonantie optreedt, dan zullen de groeiende golfhoogtes resulteren in een instabiel golfconditie. Aangezien de golfbreker maximaal een derde van de breedte van het bassin inneemt, is de kans op staande golven tussen de golfbreker en de golfmachine erg klein.

Het schaalmodel

Om het verschil tussen gladde ondoorlatende en ruwe doorlatende golfbrekers te analyseren, wordt de doorlatendheid van een ruwe golfbreker gevariëerd. Op die manier kunnen de invloeden van ruwheid en doorlatendheid ontkoppeld worden. Op figuur H.3a is de opbouw van het schaalmodel weergegeven. Het bestaat hoofdzakelijk uit een variabele kern en een vaste beschermlaag van steenslag. Om een constante ruwheid te bekomen, werd de steenslag onderling vastgelijmd met Elastocoast. Dat is een polyurethaan bindmiddel dat de stenen vastlijmt zonder de doorlatendheid van de laag als geheel te veranderen. De kern van de golfbreker is gemaakt van een ondoorlatende houten balk die beschikbaar is in drie hoogtes zodat in totaal vier verschillende structuren getest kunnen worden; variërend van een volledig doorlatend (d) tot een volledig ondoorlatend (a) ruwe golfbreker (figuur H.3b). De bekledingsstenen in de variabele kern van de golfbreker zijn niet vastgelijmd maar komen telkens uit dezelfde selectie stenen en worden op een willekeurige manier geplaatst. De stenen zijn oorspronkelijk van Noorwegen en hebben een nauwe gradatie en een D_{n50} van $0.033m$. Dit heeft als gevolg dat de bekledingslaag zeer doorlatend is.

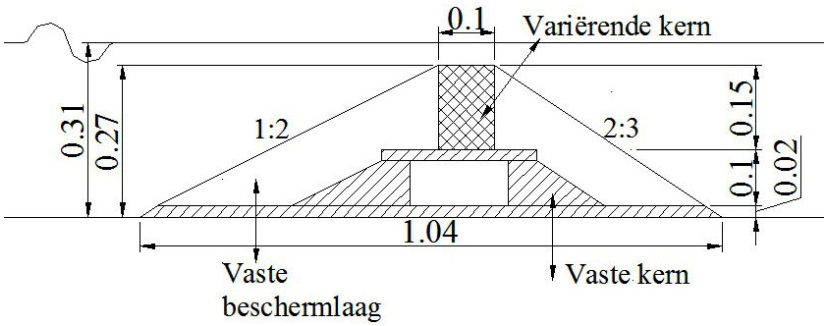

(a) Algemene doorsnede

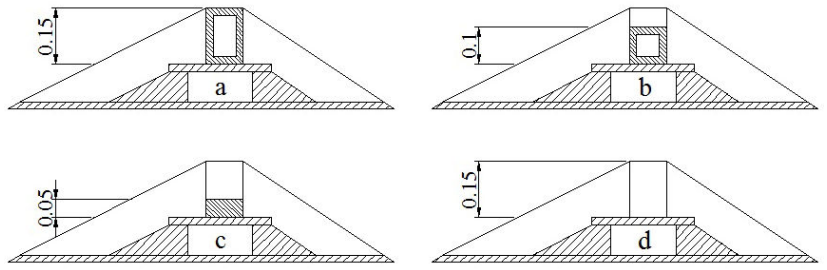

(b) Variërende kern

Figure H.3: De doorsnede van de golfbreker

De golfbreker heeft een totale lengte van $5m$, maar wordt in twee delen gemaakt zodat de constructie veilig en eenvoudig gedraaid kan worden tijdens het experiment. Tijdens de verschillende testen wordt de hoekinval gevariëerd van 0° tot 60° in stappen van 15°. Het

is niet de bedoeling de invloed van diffractie te observeren tijdens het experiment. Daarom plaatsen we bij erg scherpe hoeken een bijkomende ruwe doorlatende steenslag golfbreker naast het model. Deze bijkomende golfbreker onderdrukt ook grootschalige stromingen in het bassin.

Meetinstrumenten

Twee groepen van vijf golfhoogtemeters worden gebruikt om de energiespectra van inkomende en uitgaande golven te bepalen. Elk groep van vijf instrumenten worden in een kruisconfiguratie geplaatst zodat richtingsgevoelige energiespectra berekend kunnen worden. De instrumenten worden bevestigd aan een kader om hun onderlinge posities constant te houden tijdens de experimenten. Daarnaast dienen de meters regelmatig gekalibreerd te worden. Tenslotte is de positie van de instrumenten zo dat ongewenste effecten als reflecties en diffractie tot een minimum herleid worden.

Data-acquisitie

De signalen worden simultaan van de golfhoogtemeters naar de computer gestuurd. Het programma DasyLab slaat de data op met een sampling frequentie van $100Hz$ in een ASCI datafile. Om de datafiles enerzijds numeriek handelbaar te houden en anderzijds aliasing te vermijden, werden de data uiteindelijk omgezet naar een frequentie van $20Hz$.

Experimentele programma

De kern van de golfbreker, de hoek van aanval van de golven, de golfconditie en het gebruik van bijkomende steenslag golfbreker zijn allemaal onafhankelijke variabelen waarvan de invloed onderzocht moet worden. Dit resulteert in 77 testen. De eerste test is drie keer uitgevoerd om de reproduceerbaarheid van de testen te bewijzen. Elke andere test is slechts een keer uitgevoerd. Twee testen zijn uitgevoerd zonder de golfbreker in het bassin om de twee groepen van meetinstrumenten te vergelijken met elkaar. De testen met invalshoeken van $45°$ en $60°$ werden niet zonder de bijkomende steenslag golfbreker uitgevoerd, omdat de secundaire effecten te groot waren. Verder is een laatste test zonder golven uitgevoerd om de gevoeligheid van de meetinstrumenten te bekijken.

H.4 Dataverwerking

H.4.1 Software voor spectrale analyse

De DIrectional WAve SPectra toolbox versie 1.3 (DIWASP) wordt gebruikt voor de spectrale analyse van de data. Daarvoor worden de algoritmen van Hashimoto (1997) en Pawka (1983) toegepast. Dit vrije software pakket is ontwikkeld door Johnson (2007) aan de Universiteit van West Australië, Perth en wordt tegenwoordig beheerd en verdeeld door MetOcean Solutions Ltd, Nieuw Zeeland.
De structuur van DIWASP is relatief simpel. Aan de hand van de gemeten data, de layout van de meetinstrumenten en de gekozen algoritmes, worden de gewenste karakteristieken berekend. Standaard datatypes die het kan verwerken zijn oppervlaktehoogtes, drukken of stroomsnelheden. Na het specificeren van de inputparameters, worden eerst de cross power spectral densities van de discrete tijdssignalen berekend. Daarna wordt de data omgevormd naar een drie dimensionaal variance density spectrum, afhankelijk van de gekozen schattingsmethode. Daarmee worden de significante golfhoogte, de piekperiode en de golfrichting berekend.

Schattingsmethodes

DIWASP maakt het mogelijk verschillende schattingsmethodes te gebruiken om de variance spectral densities te bepalen:

- DFTM: Direct Fourier Transform Method
- EMLM: Extended Maximum Likelihood Method
- IMLM: Iterated Maximum Likelihood Method
- EMEP: Extended Maximum Entropy Principle
- BDM: Bayesian Direct Method

Aangezien een gedetailleerde analyse van de verschillende methoden buiten het kader van deze studie valt, wordt de nodige kennis gezocht in vroegere studies. De data analyse van de transmissie experimenten van DELOS (2002b) is niet uitgevoerd met het programma DIWASP maar een andere variant. Zanuttigh & Lamberti (2002) hebben wel DIWASP gebruikt tijdens een ander onderdeel van het DELOS project over drie dimensionale hydrodynamisch onderzoek met een vergelijkbare opstelling as die van de transmissie testen. Hieruit is nuttige informatie te verkrijgen.

De DFTM methode is de snelste, meest stabiele methode. Het levert een goed initieel overzicht van de spectrale vorm. De nadelen zijn de lager directionele nauwkeurigheid en het feit dat het soms negatieve energie verdelingen levert. De EMLM methode werkt goed met reeksen meetinstrumenten. De IMLM methode is een variant van de EMLM methode waarbij het resultaat verbeterd wordt via iteratie. Ook reguliere signalen kunnen hiermee verwerkt worden waar de andere methoden in deze situatie niet convergeren. De EMEP methode werkt het best voor configuraties met drie meetinstrumenten. Bovendien wordt rekening gehouden met fouten in de ruwe data. Nadeel is dat hoge en lage frequenties tot sterk oplopende rekentijden kunnen leiden. De meest numeriek intensieve methode is de BDM methode, die enkel toepasbaar is voor vier of meer meetinstrumenten configuraties.
DIWASP en andere directionele golf spectra programma's verwerken de data in de veronderstelling dat de golven kortkammig zijn en een hoge directionele spreiding bezitten. In de praktijk vertoont de golfconditie ook meestal een dergelijk gedrag. De golfmachines van dit experiment wekken echter langkammige golven op met een nauwe directionele spreiding. Daarom wordt aan de hand van twee testen gecontroleerd of de software de correcte spectra genereerd. In een eerste test verwerken we de data van de eerste meting met de verschillende schattingsmethodes. Daaruit blijkt dat IMLM en EMLM de beste resultaten leveren. Als tweede test analyseren we een met de computer gesimuleerd tijdsignaal met gekende spectrale en directionele verdeling. Ook hieruit blijkt dat IMLM en EMLM goede resultaten geven (zie tabel H.2).

EP methode	Frequentie spectra	Directionele spreiding	β	H_s	T_p
DFTM	$+$	$--$	$-$	$+$	$+$
EMLM	$++$	$++$	$+$	$++$	$+$
IMLM	$++$	$++$	$+$	$++$	$+$
EMEP	$--$	$+$	$-$	$--$	$-$
BDM	$-$	$-$	$+$	$-$	$+$

Table H.2: Een kwalitatieve vergelijking tussen de verschillende schattingsmethoden

Naast de keuze van de schattingsmethode moet het aantal frequentiebins en directionele bins voor de berekening gekozen worden. Deze keuze vergt een optimalisatie tussen resolutie, rekenkracht en nauwkeurigheid. Op basis van dezelfde twee testen concluderen we dat het beste resultaat bereikt wordt met 512 frequentiebins van $0.04Hz$, 120 directionele bins van $3°$ en vijf iteraties. Op die manier bekomen we voor een gesimuleerd tijdsignaal met een sig-

nificante golfhoogte van $0.070m$, een richting van $0°$ en een periode van $1.50s$ respectievelijke waarden van $0.070m$, $0°$ en $1.51s$.

H.4.2 Mogelijke foutenbronnen

Er zijn veel mogelijke foutenbronnen eigen aan het experiment, die de resultaten kunnen beïnvloeden. Deze moeten gevonden en gevalideerd worden om de betrouwbaarheid van de resultaten te bepalen.

- Er moet voldoende lang gesampled worden opdat de inkomende golfconditie het doelkimaat zo goed mogelijk zou benaderen. Elke test duurde minimaal $50min$, wat overeenkomt met ongeveer 2400 golven. Dit is ruim voldoende rekening houdend met de algemene richtlijn van 1000 golven.

- Om de reproduceerbaarheid van de testen te controleren is de eerste test drie keer uitgevoerd (Test02a0_1, Test02a0_2 en Test02a0_3). De resultaten komen goed overeen.

- De nauwkeurigheid van de golfhoogtemeters is voldoende groot voor deze studie. Verder wijken de individuele kalibraties weinig af van de gemiddelde factoren.

- Er zijn twee testen uitgevoerd zonder golfbreker om de twee groepen van meetinstrumenten onderling te kalibreren. De gevonden transmissie coëfficiënt is 1.08 in plaats van de theoretische 1.00. Om de reden voor deze overschatting van 8% te achterhalen, is het frequentiespectrum van elk meetinstrument apart berekend. Hierbij blijkt dat er effectief 12% meer energie aanwezig is ter hoogte van de tweede groep instrumenten. Dit wijst op een lange staande golf in het golfbassin. Die heeft geen invloed op de resultaten, indien de transmissiecoëfficiënt gereduceerd wordt met 8%.

- Een meetfout van de waterdiepte heeft geen significante invloed op de resultaten van DIWASP.

- De grootste meetfout ligt in het positioneren van de golfbreker en de twee groepen van meetinstrumenten. Dit heeft gezamenlijk een hoekfout van $\pm 2.2°$. Die heeft geen invloed op de andere parameters zoals de significante golfhoogte.

- De relatieve positie van de golfhoogtemeters onderling heeft wel een belangrijke invloed op de uitkomsten van DIWASP. Dit kan leiden tot hoekfouten van $\pm 3°$ en fouten op de significante golfhoogte van $\pm 0.0005m$. Aangezien de golfhoogtemeters bevestigd zijn aan een kader, kan het meten van de relatieve posities echter zeer nauwkeurig gebeuren. Grote deviaties zullen dus niet optreden.

- Diffractie en grootschalige stromingen zijn bij scherpe invalshoeken duidelijk waar te nemen. De extra steenslag golfbreker vermindert deze effecten substantieel.

H.5 Resultaten

Van der Meer *et al.* (2005) heeft een groot verschil in gedrag tussen de ruwe doorlatende en de gladde ondoorlatende golfbreker gevonden wat betreft de invloed van de invalshoek van de golf op de richtingverandering van de golf, de transmissie en de spectrale veranderingen. Door de doorlatendheid van de ruwe golfbreker te variëren in deze studie, is het mogelijk de invloeden van ruwheid en doorlatendheid te ontkoppelen. Door de data als een geheel te analyseren en daarna te vergelijken met de data van DELOS (2002b) en de bevindingen van Van der Meer *et al.* (2000) (2003), is het mogelijk inzicht te verkrijgen omtrent de reden voor het verschil in gedrag.

De transmissiecoëfficiënt K_t ten opzichte van de relatieve kruinhoogte R_c/H_i

Bij het plotten van de transmissie coëfficiënt K_t ten opzichte van de relatieve kruinhoogte R_c/H_i, merkt men op dat de transmissiecoëfficiënten hoger liggen verwacht [d'Angremond *et al.* (1996)]. Indien de 8% overschatting van de transmissiecoëfficiënt in rekening wordt gebracht, liggen de data wel binnen het verwachte interval [d'Angremond & van Roode F.C. (2001)].

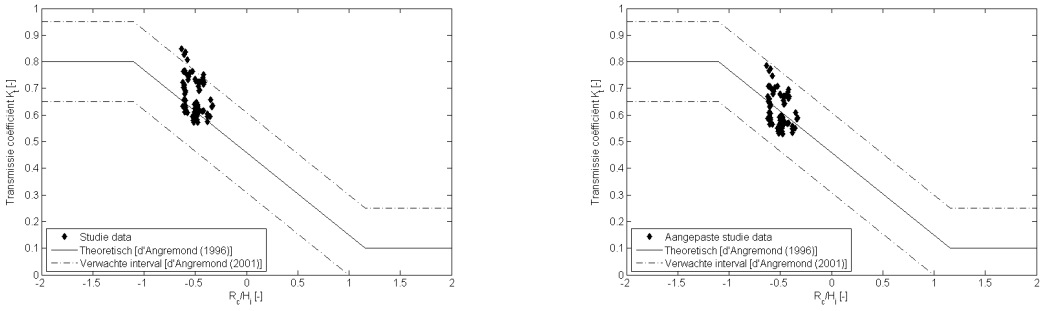

(a) Data van de studie onveranderd (b) Aangepaste data van de studie

Figure H.4: De transmissie coëfficiënt K_t ten opzichte van de relatieve kruin hoogte R_c/H_i

De richtingverandering van de golf: De uitvalshoek β_t ten opzichte van de invalshoek β_i

Op basis van de data van deze studie concludeert men hetvolgende:

- De golfrichting verandert nauwelijks of neemt licht toe (10%) na transmissie.

- De doorlatendheid van de kern van de golfbreker heeft geen significante invloed op de richtingverandering van de golf. De volledig doorlatende ruwe structuur vertoont hetzelfde gedrag als de volledig ondoorlatende ruwe structuur.
- De golfconditie heeft geen effect op de invloed op de golfrichting aan de lijzijde van de golfbreker. Relatief lange en korte golven geven dezelfde richtingverandering.
- Het toevoegen van de bijkomende steenslag golfbreker heeft geen effect op de golf richtingverandering.

Deze resultaten komen niet volledig overeen met Van der Meer *et al.* (2003), waar er bij een ruwe doorlatende golfbreker een vermindering van de hoek waargenomen wordt (figuur H.5). Na vergelijking met een gladde ondoorlatende golfbreker, merkt men een gelijkaardig gedrag op tot een invalshoek van 45°. Bij grotere hoeken verschillen de data. Tenslotte ligt de data van deze studie voor de volledig doorlatend ruwe golfbreker niet in de spreiding van de overeenkomstige data van DELOS (2002b).

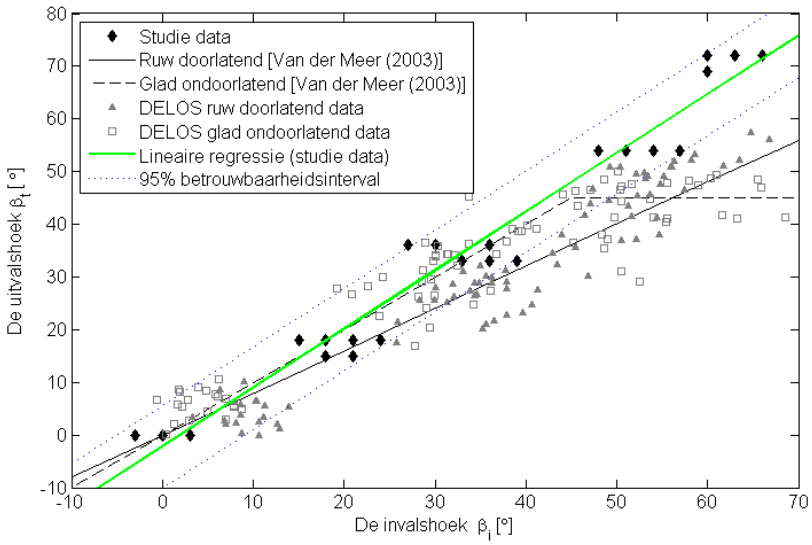

Figure H.5: De uitvalshoek β_t ten opzichte van de invalshoek β_i: Lineaire regressie

De data van deze studie zijn afkomstig van een experiment dat weinig parameters varieert. Om dus een objectieve vergelijking te maken met DELOS (2002b) zijn lineaire regressies uitgevoerd op de datasets van DELOS (2002b) enerzijds, en de combinatie van DELOS (2002b) en de eigen data anderzijds. Uit de data van DELOS (2002b) bekomen we een verband tussen invals- en uitvalshoek van 0.9, zowel voor ruwe doorlatende golfbrekers als voor gladde ondoorlatende golfbreker. Dit verschilt licht van de waarden gerapporteerd in Van der Meer *et al.* (2003), die respectievelijk 0.8 en 1 bedragen. Na lineaire regressies op de gecombineerde

data verkrijgen we volgende waardes, waarbij het 95% betrouwbaarheidsinterval aangegeven is (figuur H.5):

$$\begin{array}{lrcll} \text{Ruwe golfbrekers} & \beta_t & = & 0.94\beta_i \pm 0.05\beta_i & \text{voor } \beta_i \leq 60^\circ \\ & & & & \\ \text{Gladde golfbrekers} & \beta_t & = & 0.94\beta_i \pm 0.05\beta_i & \text{voor } \beta_i \leq 45^\circ \\ & \beta_t & = & 45^\circ & \text{voor } \beta_i > 45^\circ \end{array} \tag{H.4}$$

Samenvattend, heeft de doorlatendheid van de kern geen invloed op het gedrag van de golfbreker met betrekking tot de richtingverandering van de golf. De ruwe doorlatende golfbreker gedraagt zich zoals de ruwe ondoorlatende golfbreker van deze studie. Verder komen de bevindingen van deze studie overeen met de bevindingen op de ruwe doorlatende golfbreker en niet met de gladde ondoorlatende golfbreker van Van der Meer *et al.* (2003). Hieruit blijkt dat het eerder de ruwheid dan de doorlatendheid van de golfbreker is die de richtingverandering van de golf bepaalt.

De transmissie coëfficiënt K_t ten opzichte van de invalshoek β_i

De data van deze studie laat het volgende concluderen:

- De transmissie coëfficiënt blijft onveranderd met toenemende invalshoek.
- Binnen de spreiding van de data, heeft de kern van de golfbreker geen invloed op de transmissiecoëfficiënt.
- De golfconditie met de relatief lange golven en lage spectrale energie geeft hogere transmissiecoëfficiënten dan de golfconditie met de relatief korte golven en hoge spectrale energie. Dit bevestigd de algemene aanname dat onderwatergolfbrekers kortere golven meer beïnvloeden.
- Het toevoegen van het bijkomende steenslag golfbreker heeft geen invloed op de resultaten.

De gemeten data ligt in de spreiding van de data voor ruwe doorlatende golfbrekers van DELOS (2002b) (figuur H.6). Uitvoeren van lineaire regressie toont aan dat de data van deze studie overeenkomt met de bevindingen van Van der Meer *et al.* (2003) voor de ruwe doorlatende golfbreker. De data verschillen echter van de bevindingen van Van der Meer *et al.* (2003) voor de gladde ondoorlatende golfbreker. Ook hier merkt men dus dat de ruwheid en niet de doorlatendheid van de golfbreker bepalend is voor het gedrag van de golfbreker.

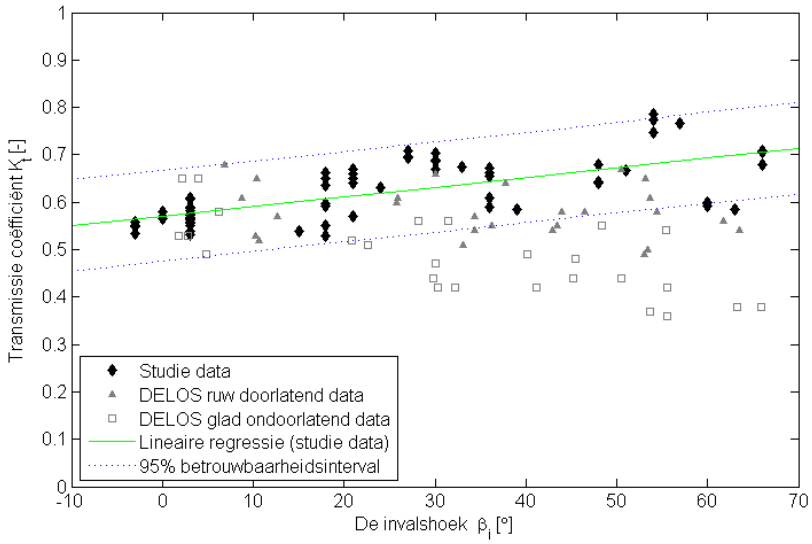

Figure H.6: De transmissie coëfficiënt K_t ten opzichte van de invalshoek β_i: Lineaire regressie

De spectrale veranderingen: Het percentage golfenergie in het hoge frequentie bereik ($f \geq 1.5 f_p$) van het spectrum aan de lijzijde van de golfbreker

Uitgaande van de data van deze studie volgen deze conclusies:

- Het gemiddelde percentage golfenergie in het hoge frequentie bereik is 33% ($31 - 35\%$).
- De golfrichting van de inkomende golf heeft geen significante invloed op het percentage golfenergie in het hoge frequentie bereik van het spectrum aan de lijzijde van de golfbreker.
- Variatie van de kern van de golfbreker heeft niet geleid tot verschillen in gedrag betreffende het percentage golfenergie.
- De relatief lange golven hebben lagere percentages golfenergie in het hoge frequentie bereik. Dit wil zeggen dat het spectrum minder veranderingen ondergaat bij het transmissie. Dit komt overeen met het feit dat de invloed van een onderwater op een golfconditie met relatief lange golven kleiner is.
- De bijkomende steenslag golfbreker heeft geen invloed op de spectrale veranderingen.

Deze bevindingen zijn zeer gelijkaardig aan de bevindingen van Van der Meer *et al.* (2005) voor ruwe doorlatende golfbrekers. Dit steunt nogmaals het vermoeden dat het de ruwheid eerder dan de doorlatendheid van de golfbreker is die het gedrag van de golfbreker sterk beïnvloed.

H.6 Conclusies

Vier structuren zijn onderzocht; variërend van een volledig doorlatende tot een volledig ondoorlatende ruwe golfbreker. Hierbij is geen invloed gevonden op het gedrag van deze structuren op de richtingverandering van de golf, de transmissiecoëfficiënt en de spectrale verandering ten opzichte van de invalshoek van de golf. Door de data te vergelijken met de data van DELOS (2002b), blijkt vooral de ruwheid van doorslaggevend belang te zijn. Men concludeert de invloed van schuine hoekinval op het algemeen gedrag van een golfbreker voornamelijk afhangt van zijn ruwheid.

Bibliography

Battjes, J. A. 2000. *Korte Golven CTwa4320; Collegehandleiding.* Faculteit Civiele Techniek en Geowetenschappen, Technische Universiteit Delft.

Briganti, R., Van der Meer, J. W., Buccino, M., & Calabrese, M. 2003. Wave transmission behind low crested structures. *Proceedings Coastal Structures 2003.*

Briggs, M. J., Thompson, E. F., & Vincent, C. L. 1995. Wave diffraction around breakwater. *Journal of Waterway, Port, Coastal, and Ocean Engineering.*

Buccino, M., & Calabrese, M. 2007. Conceptual approach for prediction of wave transmission at low-crested breakwaters. *Journal of Waterway, Port, Coastal, and Ocean Engineering.*

Calabrese, M., Vicinanza, D., & Buccino, M. 2002. Large-scale experiments on the behaviour of low crested and submerged breakwaters in presence of broken waves. *Proceedings 28th International Conference on Coastal Engineering.*

CERC. 1984. *Shore Protection Manual.* Coastal Engineering Research Center, US Army Corps Of Engineers. US government Printing Office, Washington D. C.

d'Angremond, K., & van Roode F.C. 2001. *Breakwaters and closure dams.* Delft University Press, The Netherlands.

d'Angremond, K., Van der Meer, J. W., & de Jong, R. J. 1996. Wave transmission at low crested structures. *Proceedings 25th International Conference on Coastal Engineering.*

DELOS. 2002a. *Structural design report for LCS: Final report.* http:// www.delos.unibo.it/ Docs/ Deliverables/ D52.pdf. EU Fith Framework Programme 1998-2002 (Contract EVK3-CT-2000-00041).

DELOS. 2002b. *Wave basin transmission tests: Internal report.* http:// www.delos.unibo.it/ Docs/ Deliverables/ D31.pdf. EU Fifth Framework Programme 1998-2002 (Contract EVK3-CT-2000-00041).

EurOtop. 2007. *Wave overtopping of sea defences and related structures: Assessment manual.* http:// www.overtopping-manual.com.

Garcia, N., Lara, J.L., & Losada, I.J. 2004. 2-D numerical analysis of near-field flow at low-crested permeable breakwaters. *Journal of Coastal Engineering 51.*

Gironella, F. X., Sànchez-Arcilla, A., Briganti, R., Sierra, J. P., & Moreno, L. 2002. Submerged detached breakwaters: Towards a functional design. *Proceedings 28th International Conference on Coastal Engineering.*

Hashimoto, N. 1997. Analysis of the directional wave spectrum from field data. *In:* Liu, P. L. F. (ed), *Advances in Coastal and Ocean Engineering.* World Scientific Publishing Co. Pte. Ltd., Singapore.

Hirose, N., Watanuki, A., & Saito, M. 2002. New type units for artificial reef development of ecofriendly artificial reefs and the effectiveness thereof. *Proceedings 30th International Navigation Congress, PIANC.*

Holthuijsen, L. H. 2007. *Waves in Oceanic and Coastal Waters.* Cambridge University Press, New York.

Hughes, S. A. 1993. *Physical Models and Laboratory Techniques in Coastal Engineering.* World Scientific Publishing Co. Pte. Ltd., Singapore.

Johnson, D. 2007. *DIWASP: DIrectional WAve SPectra toolbox version 1.3.* http:// www.metocean.co.nz/ software. MetOcean Solutions Ltd., New Zealand.

Kramer, M., Zanuttigh, B., Van der Meer, J. W., Vidal, C., & Gironella, F. X. 2005. Laboratory experiments on low-crested breakwaters. *Journal of Coastal Engineering 52.*

Massel, S. R. 1996. *Ocean surface waves: Their physics and prediction.* World Scientific Publishing Co. Pte. Ltd., Singapore.

McIver, P. 2005. Diffraction of water waves by a segmented permeable breakwater. *Journal of Waterway, Port, Coastal, and Ocean Engineering.*

Melito, I., & Melby, J. A. 2001. Wave runup, transmission, and reflection for structures armoured with Core-Loc. *Journal of Coastal Engineering 45.*

Pawka, S. S. 1983. Island shadows in wave directional spectra. *Journal of Geophysical Research.*

Seabrook, S. R., & Hall, K. R. 1998. Wave transmission at submerged rubble mound breakwaters. *Proceedings 26th International Conference on Coastal Engineering.*

Tirindelli, M., & Lamberti, A. 2002. *Wave action on rubble mound breakwaters: The problem of scale effects.* http:// www.delos.unibo.it/ Docs/ Deliverables/ D43.pdf. EU Fifth Framework Programme 1998-2002 (Contract EVK3-CT-2000-00041).

Van der Meer, J. W., Regeling, H. J., & de Waal, J. P. 2000. Wave transmission: Spectral changes and its effects on run up and overtopping. *Proceedings 27th International Conference on Coastal Engineering.*

Van der Meer, J. W., Wang, B., Wolters, A., Zanuttigh, B., & Kramer, M. 2003. Oblique wave transmission over low-crested structures. *Proceedings Coastal Structures 2003.*

Van der Meer, J. W., Briganti, R., Zanuttigh, B., & Wang, B. 2005. Wave transmission and reflection at low-crested structures: Design formulae, oblique wave attack and spectral change. *Journal of Coastal Engineering 52.*

Van Dongeren, A. 2007. Deltares specialist morphology and waves. Personal contact.

Vidal, C., Losada, M. A., Medina, R., Mansard, E. P. D., & Gomez-Pina, G. 1992. A universal analysis for the stability of both low-crested and submerged breakwaters. *Proceedings 23rd International Conference on Coastal Engineering.*

Wang, B., Otta, A. K., & Chadwick, A. J. 2006. Transmission of obliquely incident waves at low-crested breakwaters: Theoretical interpretations of experimental observations. *Journal of Coastal Engineering 54.*

Zanuttigh, B., & Lamberti, A. 2002. *Wave basin hydrodynamic tests: Internal report.* http:// www.delos.unibo.it/ Docs/ Deliverables/ D31.pdf. EU Fifth Framework Programme 1998-2002 (Contract EVK3-CT-2000-00041).